CENTER FOR DEVICES AND RADIOLOGICAL HEALTH, FOOD AND DRUG ADMINISTRATION: Report of Measurements and Assessment for Potential Electromagnetic Interference Effects on Personal Medical Electronic Devices (PMEDs) from Exposure to Emissions from the L-3 ProVision® 2 Millimeter Wave Advanced Imaging Technology (AIT-2) Security System
December 22nd, 2016

Table of Contents

1. Executive Summary

This document contains information about research, testing, and risk assessment for prevalent active medical devices that could be screened at a security checkpoint using the L-3 ProVision® 2 Advanced Imaging Technology (AIT-2) system. The AIT-2 uses non-ionizing millimeter wave (mmW) radiation for the security screening. Under Inter Agency Agreement (IAA) number HSTSFT15XCTO045 with the Department of Homeland Security (DHS), Transportation and Security Administration (TSA) the Center for Devices and Radiological Health (CDRH) at the Food and Drug Administration (FDA) performed emissions measurements and assessed the risk of exposure to the AIT-2 emissions with a sample of currently marketed, ambulatory active medical devices that are referred in the report as personal medical electronic devices (PMEDs). Over 50 sample PMEDs were tested including: pacemakers, neuro-stimulators, implantable cardioverter defibrillators, insulin pumps and transcutaneous electrical nerve stimulators. The work also included an assessment of human exposure to the AIT-2 mmW emissions.

Emissions and exposure measurements were performed at several locations in and around the AIT-2. The locations were carefully chosen to provide information to assess risks related to exposure to the AIT-2 emissions for people (e.g., passengers, security personnel) and their implanted or body-worn PMEDs. Estimates of the exposure time were developed based on AIT-2 emissions measurements and geometric considerations, and the estimates were used to perform exposure testing of the selected PMEDs. A mmW simulation system was built to mimic the AIT-2 emissions and the expected PMED exposures with intent to develop an AIT-2 independent test method that could be used by the PMED manufacturers and others. The emissions measurements were also used to assess the potential human exposure during the brief screening procedure. In addition, per a suggestion from TSA personnel an inexpensive mmW detection instrument was designed and tested to measure the AIT-2 emissions.

Findings from the tests with the sample PMEDs indicate that no effects were observed for any of the sample PMEDs exposed to the mmW emissions from the AIT-2. The results were used to assess the risks for electromagnetic interference (EMI) to the PMEDs that might harm the medical device user (patient). The results of the risk assessment indicate the risks for users of these types of medical devices should be very low. In addition, a transcutaneous electrical nerve stimulator (TENS) under a low battery voltage condition was found to be effected by emissions from the AIT-2 uninterruptible power supply (UPS) that is mounted just outside the AIT-2 exit. While the low battery voltage condition is potentially possible, the instructions recommend against such use. At full battery voltage, the TENS exhibited much smaller effects which were not reproducible on another TENS unit (with the same model) during exposure to the emissions from the UPS. These effects were deemed very low risk. Other sample devices tested at the UPS location showed no effects.

In addition, based on the emissions measurements, the findings of the assessment for human exposure indicated that the mmW energy levels emitted by the L-3 AIT-2 and the resulting exposure at the location tested were many times less than the safe exposure levels as referenced from international standards and guidelines such as the Institute of Electrical and Electronic Engineers (IEEE) C95.1 [1] and International Commission on Non-Ionizing Radiation Protection (ICNIRP) [2] guidelines.

2. Introduction

This report presents the findings of the Center for Devices and Radiological Health (CDRH) of the Food and Drug Administration (FDA) performed for the Department of Homeland Security (DHS), Science and Technology Directorate under the Inter Agency Agreement (IAA) number HSTSFT15XCTO045. The findings cover CDRH research, measurements, and testing that examined the risks of electromagnetic interference (EMI) on active medical devices (hereafter called personal electronic medical devices or PMEDs) exposed to the emissions from the L-3 ProVision® 2 Advanced Imaging Technology (AIT-2) security screening system. The AIT-2 utilizes non-ionizing, millimeter wave (mmW) emissions for the security screening. For the purposes of this report the security screening system under test will be referred to as the AIT-2. Sample PMEDs evaluated in this study were selected based on the prevalence of the active devices, expected exposure to the AIT-2 screening system (e.g., implanted device), potential susceptibility to electromagnetic interference (EMI), and potential hazards and risks that could result from EMI.

The report is organized to present the following information: a brief introduction and background information about the AIT-2, an estimation of PMED exposure times to the AIT-2 mmW emissions, discussion of methods used to measure the electromagnetic emissions from the AIT-2 and the measurement results, assessment of human exposure to the AIT-2 mmW emissions, discussion of methods and materials used to test PMEDs in the AIT-2, information about the CDRH designed AIT-2 mmW simulator system, a summary of the findings of the PMED testing in the AIT-2 and the AIT-2 mmW simulator, and a brief risk assessment. Detailed discussions and test data are located in the respective appendix.

A qualitative assessment of the public exposure was performed per a DHS request to examine the exposure of security screening subjects to the non-ionizing electromagnetic energy emitted by the mmW AIT-2 using both CDRH measurements and other information. Electric field levels at worst case locations inside the AIT-2 security system were measured to be on the order of 1.5 V/m in the intended (in-band) mmW frequency range. Taking into consideration the short duration of exposure, and the very low levels of emissions from the mmW AIT-2, the electromagnetic energy levels were determined to be millions of times less than the limits in the IEEE C95.1 [1] standards and guidelines from International Commission on Non-Ionizing

Radiation Protection (ICNIRP) [2]. Based on a request from TSA, the CDRH developed a method that enables the assessment of the safety of the AIT-2 to evaluate the safety of the in-band mmW emissions from the AIT-2. Technical details about it are not presented in this report due to TSA's filing of a patent application.

The novel mmW simulator system was developed by engineers in CDRH to emulate the mmW emissions from the AIT-2. The simulator allowed for a controlled testing environment for the PMEDs enabling careful study with predictable and reproducible electric field strengths and exposure durations that were designed to be well above the expected worst case exposure scenario in the AIT-2.

Test methods were developed for each PMED type, tailored to its configuration, accessories, and programming. For the mmW simulator, the PMED exposure test was performed at a fixed distance and was set to produce an exposure several times greater than the expected mmW exposure received from the AIT-2 so that any effects on the PMED could be studied. For the AIT-2, testing methods were developed considering the following factors: the in band and out of band emission measurement results in and around the AIT-2, and device exposure locations and elevations that span the possibilities for subjects and the sample PMEDs. Monitoring of the PMEDs was based on consensus standards for electromagnetic compatibility (EMC) testing for active medical devices intended to minimize perturbations of the exposure and spurious signals or artifacts.

The laboratory testing performed with the mmW emissions of the AIT-2 and the mmW simulator showed no effects on the sample PMEDs. High priority ambulatory, PMEDs were selected for this study based on history of electromagnetic compatibility concerns and risks, priority of device function, and concerns for potential EMI. Those PMED samples consisted of fourteen implantable pacemakers, fifteen implantable cardioverter defibrillators (ICDs), eleven implantable neuro-stimulators, and nine insulin pumps and four transcutaneous electrical nerve stimulators (TENS). Arrangements were made with several medical device manufactures to borrow selected devices and provide expertise in their function and testing. The medical device manufacturers' representatives visited the test site during testing providing PMED programming and set-up expertise and guidance.

The risks for active medical devices when exposed to mmW emissions from the AIT-2 were analyzed using the methods in the ISO 14971 standard [3]. Following the basic process given in this standard the probability of EMI occurrence and the severity of harm were analyzed. Based on the test observations and findings, the likelihood of effects on PMEDs and the risk of EMI when exposed to the mmW emissions of this particular AIT-2 appear to be very low. Thus, from the findings to date, EMI would appear to be rare for the PMEDs tested. Caution should be taken in understanding the scope of these findings. While the expected likelihood of PMED

effects from exposure to the mmW emissions of the AIT-2 appears to be rare, these findings might not be applicable for every model and type of PMEDs that could be exposed to the mmW emissions of the AIT-2. However, the low level of mmW exposure from the AIT-2 suggests it would likely not cause effects on the vast majority of PMEDs.

A hot spot of spurious electromagnetic emission was discovered within a few centimeters of the front panel of the UPS (uninterruptible power supply) of the AIT-2. One TENS device that was operating under a low battery voltage, which is a condition not recommended for use in this devices' labeling. For this device the low battery voltage status was indicated by a dim light on the TENS and it showed signs of EMI when it was placed within 2 cm of the front panel of the UPS (uninterruptible power supply) of the AIT-2. When the experiment was performed with the appropriate full battery voltage only a very subtle EMI effect was noted. This subtle effect was not reproducible on a newer TENS unit of the same model. Based on the risk assessment methodology in the ISO 14971 standard [3], which considers the probability of occurrence and clinical significance of the observed EMI, the risk for the use of the TENS device was classified as low to very low. All other PMEDs tested at the location proximal to the front panel of the UPS of the AIT-2 showed no effects.

It should be noted that the medical devices used in this study cover a limited portion of the entire device population and extrapolation of the findings to the vast range of devices and users could be misleading.

3. Background Information about the AIT-2 (Task 1 Report)

Per task 1 of the TSA/FDA IAA, the FDA CDRH has thoroughly reviewed the AIT-2 information provided by TSA and the open/closed calibration document provided by L3. The CDRH used this information in performing tests and assessing risks for certain personal medical electronic devices (PMEDs) exposed to the AIT-2.

The CDs (Compact Discs) received from TSA included the following information. Basic technical specifications and geometric dimensions of the transmitting and receiving antennas were provided. The technical specifications of the antennas consisted of their polarization and beam-width.

TSA also provided the CKC Laboratories Report No. 92757-31A entitled "Radio Frequency Addendum Exposure Report to 92757-31". This report [4] indicates that the emissions from the AIT have a power density of 1.6×10^{-4} mW/cm^2 in the mmW operating frequency range of 24.25 GHz to 30 GHz at a distance of 3.5 cm. However, there is no mention of reference points for the 3.5 cm distance measurement. The report states that this power density level is below the US [5] and Canadian [6] limits for human exposure (referenced as 1 mW/cm^2).

The document received from L-3 contains instructions to run the AIT-2 in advanced mode. The advanced mode enables emission measurements while the masts are fixed stationary at the middle of their arc path. The document also contains timing diagrams that show the duty cycle of the emitted pulse signal, and the pulse width, which help confirm that the AIT-2 emits the same waveform as the first generation L-3 ProVision® Advanced Imaging Technology (AIT-1).

The CDs from TSA also contained an AIT-2 operator manual which describes the standard operating procedures, basic troubleshooting, cleaning, and maintenance procedures. The TSA provided the checkpoint design guide that shows the typical layout of a security screening check point area, which consists of AIT, X-Ray device, Walk Through Metal Detectors, etc. Finally, the TSA provided information about the typical location of security personnel operating the AIT-2 scanner and passengers who are scanned.

4. Pulse Exposure Time Considerations

The mmW exposure times of a PMED occupying a 10 cm by 10 cm area were estimated in order to aid in determining the risks for EMI in the AIT-2. The 6 locations shown in figure 1 were chosen to do emissions measurements in and around the AIT-2. Please see section 5 of this

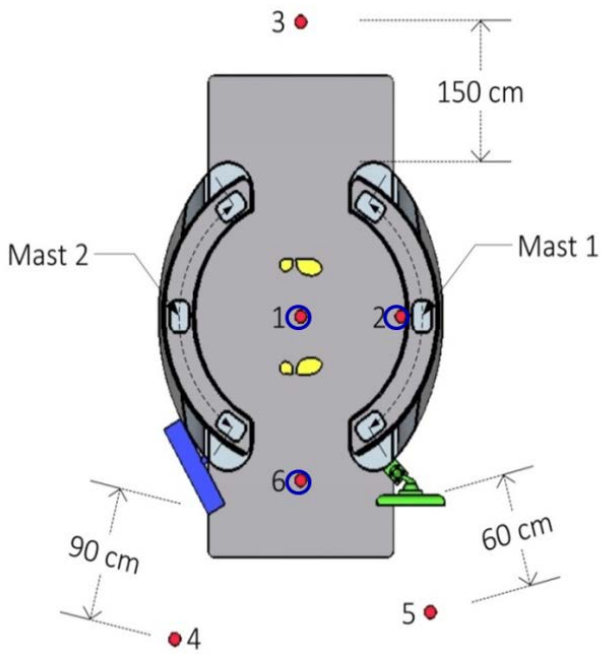

Figure 1: This is a top down view of the AIT-2. The exposure times were calculated for location 1 (center of the AIT-2), location 2 (inner wall of the AIT-2) and location 6 (at the exit gate of the AIT-2) shown using red dots encircled with blue rings. These three locations were chosen for exposure time calculation because they are the closest to the masts which emit the mmW radiation.

report for details about the emissions measurements. Out of these 6 locations, three locations (location 1, 2, and 6) were chosen for mmW exposure time calculations because they are closest to the masts containing the mmW radiating antennas of the AIT-2, and hence these three locations were expected to receive the strongest mmW emission levels.

Based on the mmW emissions characteristics and dimensions of the AIT-2, the number of pulses that are received at a PMED of dimension 10 cm by 10 cm was estimated at location 1, location 2, and location 6. The results of the calculations are summarized in table 1, which presents the worst case exposure time estimates for a typical PMED. The total number of pulses that are emitted from a single mast of the AIT-2 during a scan is 171,584. Appendix D provides more details about the pulse exposure assessment summarized in table 1.

Location	Number of antennas from mast 1 that irradiate the 10 cm by 10 cm PMED	Arc length travelled by mast 1 while it is irradiating the PMED	Number of pulses received from mast 1 during 1 scan	Duration of mmW chirp received from mast 1 during 1 scan	Duration of mmW chirp received from mast 2 during 1 scan
1	92	1.23 meters	41,216	0.23 s	0.23 s
2	14	32 cm	1,792	10 ms (mast closer to location 2)	< 0.86 s (mast further from location 2)
6	< 170	< 1.23 m	< 76,160	< 0.43 s	< 0.43 s

Table 1: This summarizes the mmW exposure time calculations. These apply to a 10 cm by 10 cm PMED situated at 1 meter height above the ground, which is the height that would have the worst case exposure time as the height of the mast is roughly 2 meters. The results for location 6 are based on a conservative upper bound estimate. The PMED at location 2 is situated asymmetrically between the two masts, and thus the exposure time for this device depends on the mast that is considered. Location 1, 2, and 6 are shown in figure 1.

5. Emission Measurements

The electromagnetic emissions from the AIT-2 can be classified into two types: mmW emissions that are the intentional emissions or “in-band”, and the spurious or unintended “out-of-band” emissions. Both types of emissions have the potential to affect the PMEDs via electromagnetic disturbance (EMD) and cause EMI to the PMED. The in-band mmW and out-of-band emission measurements are further discussed in appendix E and appendix F respectively.
Understanding the spatial distributions of the in-band and the out-of-band emissions fields helps in the assessment of potential risks to the PMEDs and humans exposed to the fields. A high resolution and uniform spatial sampling of the electromagnetic fields in and around the AIT-2 was not possible given the limitations of the AIT-2 project and resources. Instead, attention was focused on 24 representative measurement points in and around the AIT-2 that were distributed

three dimensionally. These 24 emission measurement points were distributed at 4 distinct heights and 6 distinct locations. The rationale for picking these locations and heights are summarized in table 2 and table 3. Please see appendix C for more details. Figure 2 shows the 6 locations in and around the AIT-2, and the 4 heights with respect to the AIT-2.

Location #	Description	Rationale
1	Center of the AIT-2	Passengers stand here for about 3 seconds for security screening.
2	3 cm away from the AIT-2 mast	Portions of the passenger's body might reach here during the scan which lasts for about 1.5 seconds. The in-band emissions have maximum field strength at this location.
3	1.5 meters away from the entrance of the AIT-2	Passengers typically might stand here for several seconds waiting to be scanned.
4	90 cm away from the UPS	This represents the location with a worst case emission exposure during secondary screening of the passengers, (due to its relative proximity to the UPS and the masts). The secondary screen generally takes place approximately 90 cm to 3 meters from the exit of the AIT-2.
5	60 cm away from the monitor	Security personnel location to observe passenger and watch the AIT-2 computer monitor
6	Between the UPS and the monitor at the AIT-2 exit	Chosen to better understand the spatial variation of the fields between locations 1, 4, and 5

Table 2: Summary of the 6 locations where the in-band and out-of-band emission measurements were performed. The locations are based on information from TSA regarding the Standard Operating Procedure of the TSA. Please see appendix B for details about the information received from TSA.

Height	Rationale
1.7 m	PMEDs in or on the head
1.3 m	PMEDs implanted or worn slightly below shoulder height
1 m	PMEDs implanted or worn at waist height
0.25 m	PMEDs, such as insulin pumps, placed just above ankles

Table 3: Rationales for the 4 heights, where the in-band and out-of-band emission measurements were performed, based on anthropomorphic data for an average human [7].

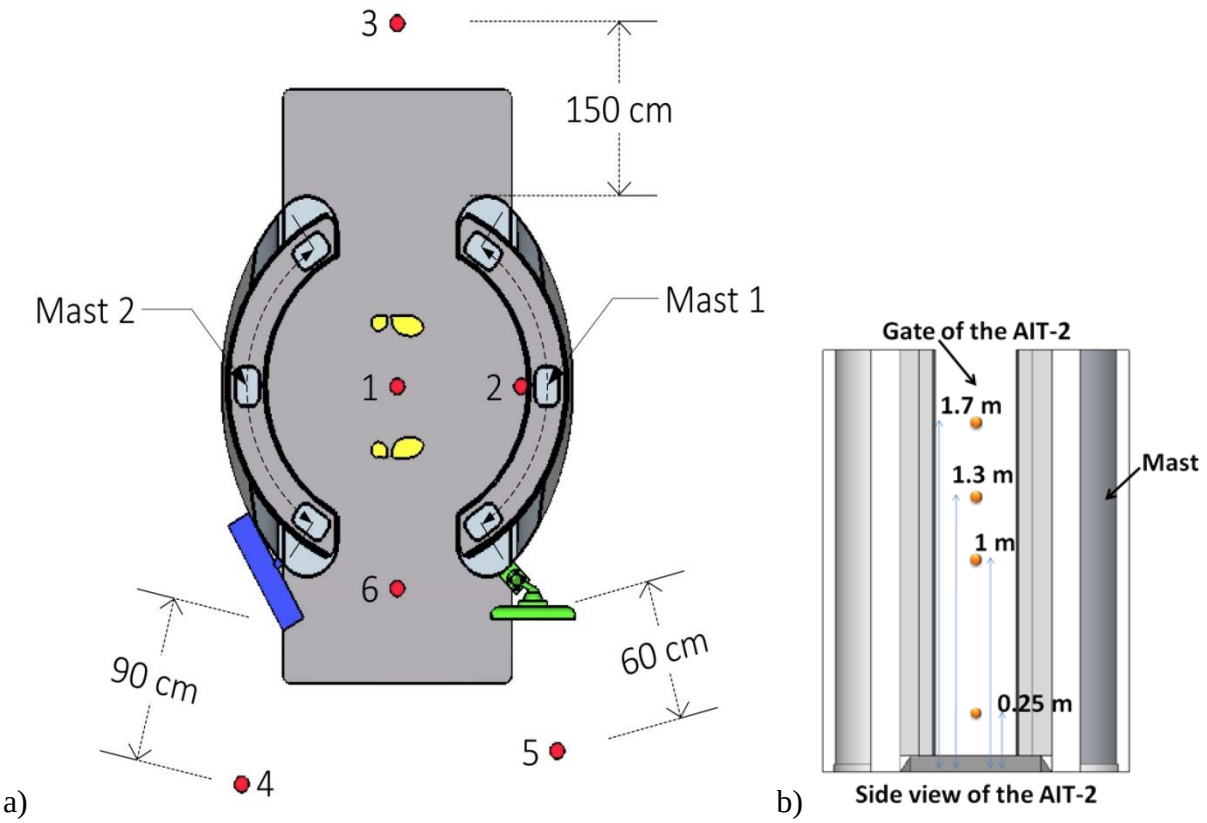

Figure 2: These two schematics define the 24 emission measurement points distributed at 6 locations and 4 heights. a) This is the top view of the AIT-2, depicting the six locations in and around the AIT-2 chosen to perform the in-band and out-of- band emission measurements. The UPS is shown to the left of location 6 in blue, and the AIT-2 computer monitor is shown to the right of location 6 in green. b) This is the side view of the AIT-2 looking through the gate of the AIT-2. These four heights were chosen to perform the emission measurements at the six locations shown in part a.

5.1. Summary of In Band Emission Measurements

A detection system was assembled at the CDRH to measure the in-band emissions (i.e. 24.25 GHz to 30 GHz) from the AIT-2. Individual pulses of mmW energy were measured using an envelope detection system. Figure 3 illustrates this envelope detection system. The envelope detector was fed by an antenna connected to a low noise amplifier (LNA). The antenna was either a WR34 horn antenna or an open ended waveguide. For distances closer than 44 cm from the radiating antennas of the AIT-2, an open ended waveguide was used as the receiving antenna. This is because these close distances are in the near field of the horn antenna and the aperture of the receiving antenna should be as small as possible. Using this detection system, the captured pulses were analyzed using the detector diode conversion factor for power in vs. output voltage. This allowed calculation of the power density and electric field at the aperture of the antennas as a function of frequency.

The design and calibration of the in-band emission detection system is discussed in detail in appendix E. The detection system was used to measure the peak electric field strength of the

mmW emission at the 24 measurement points in and around the AIT-2 whose 6 distinct locations and 4 distinct heights are shown in figure 2.

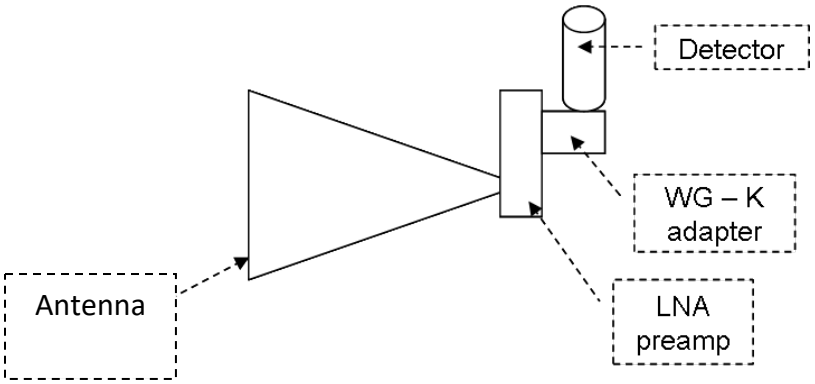

Figure 3: Schematics of the envelope detector system for measuring emissions from the mmW AIT-2.

Figure 4 shows the experimental set up that was used to measure the in-band emission at one of the measurement points using a WR34 horn antenna. Among the 24 measurement points, the highest peak electric field was measured to be 1.5 V/m at location 2 (refer to figure 2). The safety of human exposure to these mmW AIT-2 emissions is assessed in section 6.

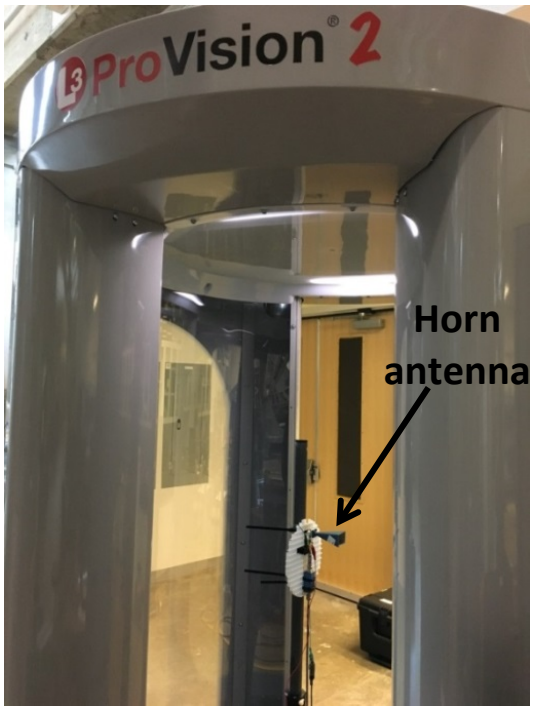

Figure 4: The in-band emissions from the AIT-2 were measured using a WR34 horn antenna for the measurement points that are at least 44 cm away from the radiating antennas on the AIT-2's mast. An open ended wave guide was used to measure the in-band emissions at distances that are smaller than 44 cm to the radiating antennas.

5.2. Summary of Out of Band Emission Measurements

Measurements were performed to investigate the AIT-2 for any non-primary emissions or out-of-band (unintended) spurious emissions. This was done using a set of electric field measurement instruments that can measure frequencies ranging from 100 kHz to 60 GHz, and a set of magnetic field instruments that can measure frequencies ranging from 1 Hz to 1 GHz. An example of an experimental set up to measure the spurious emissions using one of the field instruments is shown in figure 5. These measurements were done because PMEDs can be susceptible to electromagnetic emission in these lower frequency ranges which is why for the most part EMC testing for PMEDs is conducted in these lower frequency ranges. Electric and magnetic field survey instruments were used to measure the emitted field strengths at the 24 measurement points defined in figure 2. The values obtained at these 24 measurement points were compared with background field levels that were measured at the CDRH laboratory before the AIT-2 was installed. The comparison showed that the background ambient electromagnetic "noise" was insignificant and did not affect the AIT-2 emissions measurements at the 24 measurement points in and around the AIT-2. Our measurements agree reasonably well with those performed by the AIT-2 manufacturer to certify compliance with FCC rules [8]. However the AIT-2 manufacturer's measurements were done at greater distances from the AIT-2 and direct comparisons are very difficult to make.

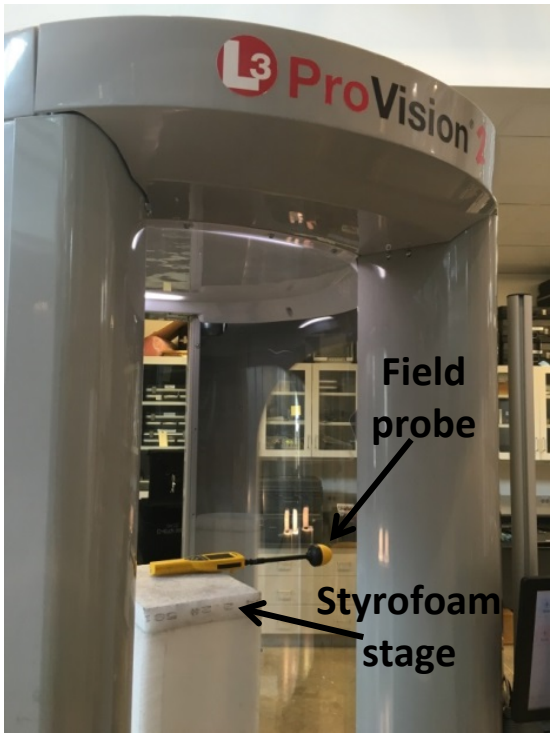

Figure 5: An example of a field probe at one of the 24 emission measurement points to assess the spurious emission levels from the AIT-2.

Findings from our measurements indicate that all peak electric fields measured at the 24 locations were less than 1.7 V/m for frequencies ranging from 100 kHz to 60 GHz. Similarly, the maximum magnetic field at the 24 locations was 0.828 A/m for frequencies ranging from 1 Hz to 1 GHz. The electromagnetic field strengths at these 24 measurement points can depend on AC power line quality or other sources of electromagnetic emissions located in proximity. Thus, while these measurements represent reasonable findings at a point in time and space for the AIT-2 system, there are environmental factors around a deployment outside the emissions from the AIT-2 that could alter PMED exposure in the security checkpoint area.

As a point of reference, the international standard for EMC immunity testing of most non-implanted medical electrical equipment is the IEC 60601-1-2 standard [9] includes radiated immunity testing between 80 MHz and 2.7 GHz at the 3 V/m level (for professional healthcare facility environment) and at 10 V/m (for home healthcare environment) with specified modulations. At lower frequencies, immunity testing is performed via direct injection of voltages into the medical device from 150 kHz to 80 MHz using 3 V rms. Testing for immunity to magnetic fields is limited in these standards to the AC power line frequencies of 50/60 Hz at 3 A/m. However, certain particular implantable active medical device standards recommend testing up to 30 MHz with up to 150 A/m, though this is not a strict requirement and varies by the device type. Implantable medical devices are tested for EMC at various levels and for specific emitters such as external defibrillators. Such testing is done at generally more intense exposures in these frequency ranges. None of the present medical device standards include testing in the range of the mmW AIT-2 primary frequency range between 24.25 GHz and 30 GHz.

These out-of-band emission measurements may not reflect the highest level emitted by the AIT-2 because of temporal changes to the emissions. These measurements indicate the tested AIT-2 does not seem to emit very large spurious electric or magnetic fields at the 24 emission measurement points. Further details about the instrumentation and the out-of-band emission measurements performed are found in appendix F.

After characterizing the out-of-band emission from the AIT-2 at the selected 24 emission measurement points, a second approach was taken to scan the entire vicinity of the AIT-2 for any hot spots of spurious emission that stand out from the background noise level. Each of the field survey instrument probes were moved around slowly close to the AIT-2. A spurious emission hot spot was discovered at the front panel of the UPS using an electric field probe shown in figure 6. Electric field strengths as strong as 100 V/m were measured in front of the front panel of the UPS. These electric fields decayed to the background noise level within just about 15 cm from the front panel of the UPS. Please see appendix F for detailed discussion of the fields measured in front of this spurious emission hot spot at the UPS.

To summarize, a hot spot of spurious emission was found at the front panel of the UPS of the AIT-2. The electric field around the hot spot can be as high as 100 V/m though this field decayed to background noise level within 15 cm distance from the front panel of the UPS. The associated magnetic field can be as high as 0.08 A/m. These spurious emissions were seen at frequencies roughly ranging from 10 MHz to 30 MHz. These field strengths are orders of magnitude higher than the background noise at these frequencies. The discovery of a spurious emission hot spot at the front panel of the UPS of the AIT-2 prompted the decision to do PMED testing right next to the front panel of the UPS of the AIT-2. The locations where the PMED testing was done are discussed in section 7.

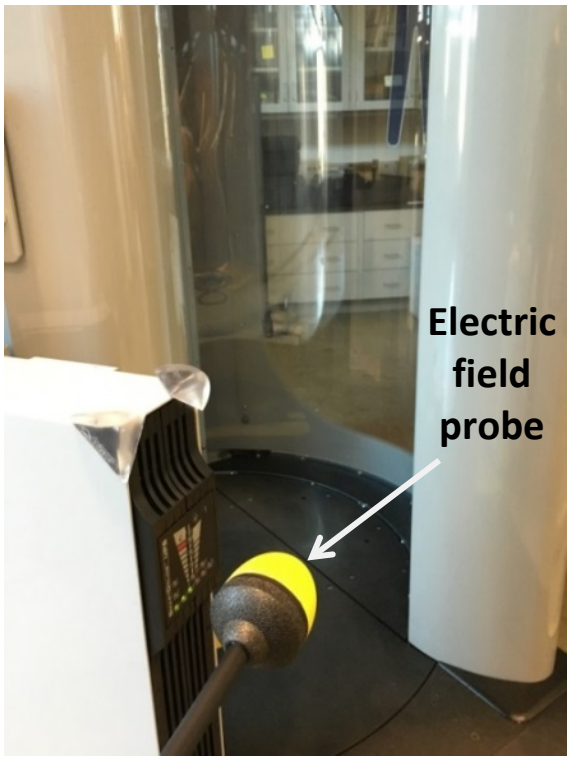

Figure 6: A spurious emission hot spot was discovered at the front panel of the UPS of the AIT-2. The measured electric field was as high as 100 V/m there, and it decayed to background noise level within 15 cm distance from the front panel of the UPS.

5.3. Summary of Leakage Current Measurements

CDRH measured leakage currents according to IEC 60601-1 standard [10]. The CDRH test results along with the maximum values allowed by the standard are summarized in the table below. In all cases, the measured values were lower than the limits specified by the standard. More detail regarding the leakage current testing is available in appendix G.

Measurement Type	IEC 60601-1 Limits	Maximum Measurements	
		Normal Polarity	Reversed Polarity
Earth Leakage Current	5 mA	4.31 mA	4.51 mA
Maximum Surface to Ground Leakage Current	100 µA	1 µA	1.1 µA
Maximum Surface to Surface Leakage Current	100 µA	2.0 µA	2.2 µA

Table 4: Leakage Current Measurements for the AIT-2 show that the leakage currents are below the limits for the IEC 60601-1 standard.

6. Human Exposure Assessment

The mmW emissions from the AIT-2 antenna arrays (masts) were measured within the AIT-2 at locations 1 and 2. This was done to analyze the levels of exposures of personnel. The exposure of a person occurs for only a brief period, which is less than 1.5 seconds, as the AIT-2 masts sweep around the center of the scanner.

The peak electric field strengths (E-field) were measured at each of the 24 measurement points shown in figure 2. The highest peak electric field was measured to be 1.5 V/m at the AIT-2's inner wall (i.e. location 2) during the in-band emission measurement; see appendix E for more details. The conservative upper bound for the energy density at the AIT-2's inner wall was calculated to be $4x10^{-3}$ J/m^2. However, the exposures that are very close to the internal AIT-2 wall expose very small areas of a person's body at any instant. In contrast, lower levels of whole body exposures occur for a person standing at the center of the AIT-2 (location 1). The AIT-2 scan exposes persons at location 1 to peak E-fields of 0.065 V/m for the duration of the scan, which from the first scan line to the last is about 1.324 seconds. The energy density of the whole body averaged exposure in the center of the scanner is 1×10^{-5} J/m^2.

For the frequency range of the mmW AIT-2, the IEEE C95.1-2005 [1] standard for the general public is 10 W/m^2 averaged over the whole body for a period of 6.25 minutes at 24 GHz and 5 minutes at 30 GHz respectively. That is equivalent to 3750 J/m^2 at 24 GHz. Allowable occupational exposures in the mmW frequency range have limits that are much higher (100 W/m^2) and are averaged over a period of approximately 40 seconds.

The International Commission on Non-Ionizing Radiation Protection (ICNIRP) guidelines published in 1998 [2], and endorsed by the European Union, are somewhat different from the IEEE C95.1 limits. They specify 10 W/m^2 (the same as IEEE) but averaged over any period of

$68/(f^{1.05})$ minutes (where f is in GHz). For 24 GHz this averaging period is 2.4 minutes while at 30 GHz it is 1.9 minutes. This is in contrast to the IEEE averaging time of 6.25 minutes at 24 GHz. This limits the energy density at 24 GHz to 1440 J/ m^2 which is less than the IEEE limit of 3750 J/m^2. The smaller averaging area of the body for the ICNIRP standard is not relevant to the AIT-2 since a single scan covers the whole body equally with no "hot spot" that needs to be averaged.

To place the AIT-2 exposures in context we can compare that allowable exposure of the ICNIRP standard limit of 1440 J/m^2 and the IEEE limit of 3750 J/m^2 with the AIT-2 exposure levels of $1x10^{-5}$ J/m^2. This gives the AIT-2 a safety margin of 128 million and for the ICNIRP standard 49 million.

7. Medical Device Testing Methodology

In addition to measuring and analyzing the emissions from the AIT-2, a two prong approach was taken to perform PMED testing in the AIT-2 system and PMED testing in a mmW hardware simulation system of the AIT-2. The mmW simulation system was developed by CDRH to create an alternative to performing tests with the mmW AIT-2 that is repeatable and reproducible for a wide range of PMEDs. A simulation of the human body called the torso simulator was created based on previous work as a platform on which to expose the PMEDs or devices under test (DUTs) with minimum effects on the exposure and device function. The development of the torso simulator and the mmW simulator are briefly discussed below. In addition, the procedures used for PMED testing in the AIT-2 and in the mmW simulator are summarized.

7.1. Methods and Materials for Testing PMEDs with the AIT-2

The CDRH developed and used a torso simulator to test implantable and body worn PMEDs. The torso simulator for implantable PMEDs consisted of saline tank filled with saline prepared in accordance with the appropriate standards [11, 12]. For the simulator configuration the leads of the implantable devices were loaded inside the saline in accordance with the requirements of the appropriate testing standards [11, 12]. The header of the Implantable Pulse Generator (IPG) is theoretically the most susceptible part of the implantable PMEDs to mmW radiation because there are short, electrically unshielded wires located here that lead into the pulse generator enclosure. Therefore, the IPG was placed in free space (air) outside the torso simulator's saline tank to maximize the exposure to mmW radiation. The conducting surface of the IPG was connected to the saline using a conducting wire in order to complete the circuit. The saline tank was covered with a commercially available mmW absorber that simulates the absorption of mmW radiation by the skin of a human body.

Figure 7: This shows the setup of an implantable PMED on a torso simulator inside the AIT-2. The electrical wires coming out of the torso simulator inside the AIT-2 were protected from the mmW emissions by a hollow tube that was covered by a mmW absorber.

The torso simulator for body worn PMEDs (i.e. insulin pumps and TENS) was simply a cavity covered with the mmW absorber, and the body worn PMEDs were placed outside the mmW absorber. A special approach was used to monitor the function of the insulin pump device because these devices deliver insulin rather than electrical stimulation as pacemakers and ICDs do. For the insulin pump devices, their output activity was monitored using a 10 turn, 5 cm diameter loop antenna behind the mmW absorbing material. This technique was supplemented with a technique that involved using a displacement meter to measure the movement of the cylinder delivering insulin in the insulin pump.

Figure 7 shows the setup of an implantable PMED on the torso simulator that was being situated inside the AIT-2. PMED monitoring cables were fed out of the AIT-2 unit through a hollow fiber glass tubing oriented parallel to the floor (perpendicular to the radiated electric field) and wrapped with a mmW absorber to protect the cables from any mmW interference. Please see appendix I for detailed discussion about the development of the torso simulator.

The electrical output of the PMEDs was monitored before, during, and after exposure for changes to the output while exposed. Observations were focused to look for any effects particularly indications of malfunction, degradation of performance, or deviation beyond the

tolerances indicated in the individual device specifications. The monitoring circuitry for implantable devices was designed and arranged to minimize influence on testing such as perturbations of the exposure electric fields or pick-up of spurious emissions.

7.2. PMED Test Procedure Using the AIT-2

The in-band and out-of-band emission measurement results were used to select 5 PMED testing points in and around the AIT-2. The selected PMED testing points are summarized in table 4 along with the rationale for the selection. Please see appendix C for detailed discussion of the rationale.

PMED testing point	PMEDs tested	Rationale
Location 1, height = 1.3 m	All PMEDs	There was a 0.23 seconds long exposure time to about 0.075 V/m peak electric field strength.
Location 1, height = 0.25 m	1 insulin pump type per manufacturer	There was about 0.23 seconds long exposure time to about 0.075 V/m electric field strength. Insulin pumps worn on ankles or lower leg areas may have slightly different (smaller) exposure times compared to those at heights between 0.3 m and 1.7 m.
Location 2, height = 1.3 m	1 PMED per device category per manufacturer	The maximum peak electric field strength (i.e. 1.5 V/m) was measured here despite the relatively short exposure time (i.e. 10 ms).
Location 2, height = 0.25 m	1 insulin pump type per manufacturer	The maximum peak electric field strength (i.e. 1.5 V/m) was measured here despite the relatively short exposure time (i.e. about 10 ms). Insulin pumps worn on ankles or lower leg areas may have slightly different (smaller) exposure times compared to those at heights between 0.3 m and 1.7 m.
UPS front panel, height = 75 cm	1 PMED per device category per manufacturer	There is a hot spot of spurious emission that can have electric fields as high as 100 V/m by the front panel of the UPS.

Table 4: Rationales for the five PMED test points selected based on in-band and out-of-band emission data, and exposure time calculations.

The following steps summarize the commonalities of the testing procedures used to test all of the PMED categories (DUT) in the AIT-2. Please see appendix H for detailed test protocols tailored for each PMED category.

1. Program the DUT to applicable settings, and activate it.
2. Power and calibrate the AIT-2.
3. Place the DUT on the torso simulator and place these at the test location.
4. Conduct five AIT-2 scans during a 30 seconds time period.
5. Record the DUT output and observe for any changes or effects during exposure.
6. Analyze DUT recordings.
7. Repeat the test for new test location and height for select group of PMED samples.

7.3. AIT-2 mmW Simulator System

In order to create a more controlled, less costly yet reproducible exposure system in pursuit of evaluating potential worst case PMED effects, a novel mmW simulator was created in the CDRH laboratory to mimic the exposure of emissions from the mmW AIT-2 system. The mmW simulator consisted of a system of signal generation fed into a waveguide horn antenna to expose the PMEDs. This mmW simulator generated waveforms similar to the ones from the AIT-2, and it allowed exposure above the field strengths and the exposure times expected in the mmW AIT-2 to simulate worst case conditions. The PMED was placed on mmW absorbing material covering the torso simulator at a separation distance of 47 cm from the transmitting horn of the mmW simulator. This is illustrated in figure 8 and figure 9. Please see appendix M for more details about the design of the mmW simulator.

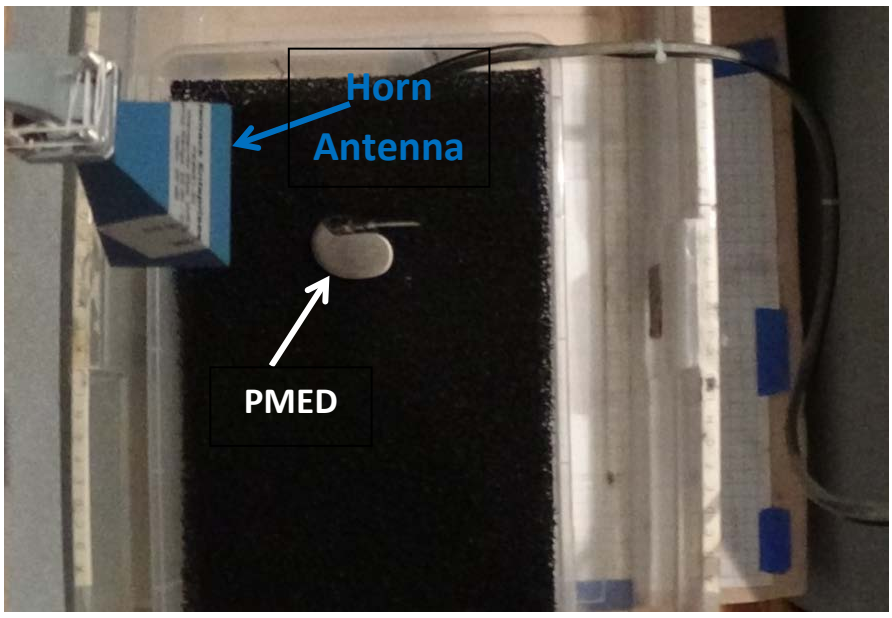

Figure 8: This shows the horn antenna of the mmW simulator that was situated 47 cm above the PMEDs under test.

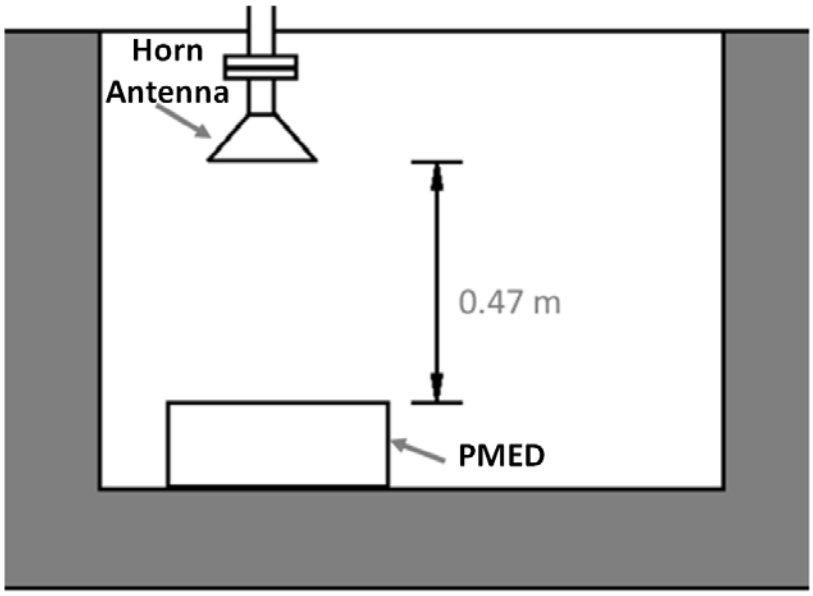

Figure 9: This is a schematic of the PMED test setup inside the mmW simulator. The horn antenna of the mmW simulator and the PMED are shown with a vertical separation of 0.47 m.

7.4. PMED Test Procedure Using the AIT-2 mmW Simulator System

The following steps summarize the commonalities of the testing procedures used to test all of the PMED categories (DUT) in the mmW simulator system. The PMED samples that were chosen for additional testing at different locations and / or heights in the AIT-2 were chosen for testing in the mmW simulator as well. Please see appendix N for detailed test protocols tailored for each PMED category.

1. Program the DUT to applicable settings, and activate it.
2. Verify the mmW simulator equipment setup and operation.
3. Place the DUT and leads at the proper location and orientation.
4. Initiate test sequence which involves 30 seconds long exposure.
5. Record the DUT output and observe for any changes or effects during exposure.
6. Analyze DUT recordings.

The mmW AIT-2 exposure simulations used the following output parameters.

- Chirp frequency range: 24.25 GHz - 30 GHz.
- Primary modulation: 8.08 μs pulse width with a 70% duty cycle.
- Simulated vertical exposure time to the mast during a single vertical scan line emission:
    i) 1.49 ms to simulate the condition at the center of the AIT-2 (location 1), and
    ii) 0.22 ms to simulate the condition at the inner wall of the AIT-2 (location 2).
- Total exposure time: 30 seconds.
- Antenna field polarization with respect to the DUT: horizontal and vertical.

• Peak exposure E-field strength:

i) ~ 0.075 V/m to simulate E-field (electric field) at the center of the AIT-2 (location 1),
ii) ~ 0.75 V/m to simulate 10 times the E-field at the center of the AIT-2 (location 1),
iii) ~ 1.5 V/m to simulate the E-field at the inner wall of the AIT-2 (location 2), and
iv) ~ 15 V/m to simulate 10 times the E-field at the inner wall of the AIT-2 (location 2).

The appropriate combination of E-field strength (~ 0.075 V/m, ~ 0.75 V/m, ~ 1.5 V/m, ~ 15 V/m) and vertical exposure time parameters (1.49 ms, 0.22 ms) were used to simulate typical field strength and 10 times the field strength conditions at location 1 and location 2. In general, the mmW simulator simulated the worst case total exposure time condition that would happen if a stationary AIT-2 mast were to irradiate the PMED with consecutive burst of vertical scan lines for 30 seconds.

8. Summary of Findings for PMED Testing with the AIT-2

This section summarizes results of testing conducted on over 50 PMEDs in the AIT-2. The PMEDs included 14 implantable pacemakers (A1-A14), 15 ICDs (B1-B15), 11 implantable neuro-stimulators (C1-C11), 9 insulin pumps (D1-D9), and 4 TENS (E1-E4). The PMED testing in the AIT-2 was mainly done at location 1, where the passengers stand to get scanned. One PMED type per manufacturer was selected for additional testing at all the PMED testing locations specified in table 4. The following PMEDs were the ones chosen for additional testing at multiple locations in the AIT-2: 5 implantable pacemakers (A1-A5), 4 ICDs (B1-B4), 2 neuro-stimulators (C1-C2), 3 insulin pumps (D1-D3), and 1 TENS (E1).

All of the PMEDs were tested with horizontal and vertical orientation. The cardiac devices were tested with and without a simulated cardiac signal being injected into the saline of the torso simulator. The pacemakers were tested with a unipolar and bipolar lead configuration. The mode of the cardiac devices was chosen to be DDD as long as the mode is available. Neuro-stimulators C1, and C2 were tested using their magnet mode which enables the device to be turned off and / or mode switched. The rest of the neuro-stimulators (i.e. C3 to C11) do not have magnet mode, which enables turning off the device, and hence they were also tested after turning them off using the clinician programmer. Please see appendix J to find more details about the PMED test settings.

Tables 5-8 show a summary of the tests done on implantable pacemakers, ICDs, neuro-stimulators, and insulin pumps. There was no effect of EMI seen in these devices. Please see appendix K for detailed presentation of the PMED test results in and around the AIT-2.

Device	Location	Height	Test Mode	Lead Configuration	Cardiac Signal	Orientation	Observed Reaction
A1	1 2 UPS	1.3 m 1.3 m 0.75 m	DDD	Unipolar / Bipolar	On / Off	Horizontal / Vertical	None
A2	1 2 UPS	1.3 m 1.3 m 0.75 m	DDD	Unipolar / Bipolar	On /Off	Horizontal / Vertical	None
A3	1 2 UPS	1.3 m 1.3 m 0.75 m	DDD	Unipolar / Bipolar	On / Off	Horizontal / Vertical	None
A4	1 2 UPS	1.3 m 1.3 m 0.75 m	DDD	Unipolar / Bipolar	On / Off	Horizontal / Vertical	None
A5	1 2 UPS	1.3 m 1.3 m 0.75 m	DDD	Unipolar / Bipolar	On / Off	Horizontal / Vertical	None
A6	1	1.3 m	DDD	Unipolar / Bipolar	On / Off	Horizontal / Vertical	None
A7	1	1.3 m	DDD	Unipolar / Bipolar	On / Off	Horizontal / Vertical	None
A8	1	1.3 m	DDD	Unipolar / Bipolar	On / Off	Horizontal / Vertical	None
A9	1	1.3 m	VVI	Unipolar / Bipolar	On / Off	Horizontal / Vertical	None
A10	1	1.3 m	VVI	Unipolar / Bipolar	On / Off	Horizontal / Vertical	None
A11	1	1.3 m	DDD	Unipolar / Bipolar	On / Off	Horizontal / Vertical	None
A12	1	1.3 m	DDD	Unipolar / Bipolar	On / Off	Horizontal / Vertical	None
A13	1	1.3 m	DDD	Bipolar (works only with bipolar pacing)	On / Off	Horizontal / Vertical	None
A14	1	1.3 m	DDD	Unipolar / Bipolar	On / Off	Horizontal / Vertical	None

Table 5: Summarized test data of sample Implantable Pacemakers. Pacemakers A1, A2, A3, A4, and A5 were selected for additional testing.

Device	Location	Height	Test Mode	Lead Configuration	Cardiac Signal	Orientation	Observed Reaction
B1	1 2 UPS	1.3 m 1.3 m 0.75 m	DDD	Bipolar	On / Off	Horizontal / Vertical	None
B2	1 2 UPS	1.3 m 1.3 m 0.75 m	DDD	Bipolar	On / Off	Horizontal / Vertical	None
B3	1 2 UPS	1.3 m 1.3 m 0.75 m	DDD	Bipolar	On / Off	Horizontal / Vertical	None
B4	1 2 UPS	1.3 m 1.3 m 0.75 m	VVI	Bipolar	On / Off	Horizontal / Vertical	None
B5	1	1.3 m	DDD	Bipolar	On / Off	Horizontal / Vertical	None
B6	1	1.3 m	DDD	Bipolar	On / Off	Horizontal / Vertical	None
B7	1	1.3 m	DDD	Bipolar	On / Off	Horizontal / Vertical	None
B8	1	1.3 m	VDD	Bipolar	On / Off	Horizontal / Vertical	None
B9	1	1.3 m	VVI	Bipolar	On / Off	Horizontal / Vertical	None
B10	1	1.3 m	DDD	Bipolar	On / Off	Horizontal / Vertical	None
B11	1	1.3 m	DDD	Bipolar	On / Off	Horizontal / Vertical	None
B12	1	1.3 m	DDD	Bipolar	On / Off	Horizontal / Vertical	None
B13	1	1.3 m	DDD	Bipolar	On / Off	Horizontal / Vertical	None
B14	1	1.3 m	VVI	Bipolar	On / Off	Horizontal / Vertical	None
B15	1	1.3 m	VVI	Bipolar	On / Off	Horizontal / Vertical	None

Table 6: Summarized test data of sample Implantable Cardioverter Defibrillators. ICDs B1, B2, B3, and B4 were selected for additional testing.

Device	Location	Height	Test Mode	Orientation	Observed Reaction
C1	1 2 UPS	1.3 m 1.3 m 0.75 m	Normal / Magnet	Horizontal / Vertical	None
C2	1 2 UPS	1.3 m 1.3 m 0.75 m	Normal / Magnet	Horizontal / Vertical	None
C3	1	1.3 m	Normal / Off	Horizontal / Vertical	None
C4	1	1.3 m	Normal / Off	Horizontal / Vertical	None
C5	1	1.3 m	Normal / Off	Horizontal / Vertical	None
C6	1	1.3 m	Normal / Off	Horizontal / Vertical	None
C7	1	1.3 m	Normal / Off	Horizontal / Vertical	None
C8	1	1.3 m	Normal / Off	Horizontal / Vertical	None
C9	1	1.3 m	Normal / Off	Horizontal / Vertical	None
C10	1	1.3 m	Normal / Off	Horizontal / Vertical	None
C11	1	1.3 m	Normal / Off	Horizontal / Vertical	None

Table 7: Summarized test data of sample Implantable Neuro-stimulators. Neuro-stimulators C1, and C2 were selected for additional testing.

Insulin pump D2 is a special insulin pump designed solely to test the communication between the insulin pump and the Glucose Sensor Transmitter (GST). It communicates with a special GST which operates at a 2 Hz rate. Insulin pumps D1, D5, D6, D7, and D8 are regular insulin pumps that communicate with a regular GST once every five minutes, making it harder to discover the effect of electromagnetic interference on the communication scheme. Insulin pump D3, D4, and D9 are regular insulin pumps that do not have the capability to communicate with a GST. D2 does not have a reservoir for insulin delivery, and it was only tested with the "PING at 2 Hz" mode, which is an idle mode. Most of the insulin pumps were tested while delivering just 1 unit of bolus. However, D3 was tested while delivering 16 units of bolus because its cylinder does not move in small enough increments to make accurate measurements of the cylinder's displacement. Please see appendix J to find more details about the PMED test settings.

Device	Location	Height	Test Mode	Orientation	Observed Reaction
D1	1 2 UPS	0.25 m /1.3 m 0.75 m	1 Unit of Bolus / Alarm / Idle	Horizontal / Vertical	None
D2	1 2 UPS	0.25 m /1.3 m 0.75 m	PING at 2Hz	Horizontal / Vertical	None
D3	1 2 UPS	0.25 m /1.3 m 0.75 m	16 Units of Bolus / Alarm / Idle	Horizontal / Vertical	None
D4	1	1.3 m	1 Unit of Bolus / Alarm / Idle	Horizontal / Vertical	None
D5	1	1.3 m	1 Unit of Bolus / Alarm / Idle	Horizontal / Vertical	None
D6	1	1.3 m	1 Unit of Bolus / Alarm / Idle	Horizontal / Vertical	None
D7	1	1.3 m	1 Unit of Bolus / Alarm / Idle	Horizontal / Vertical	None
D8	1	1.3 m	1 Unit of Bolus / Alarm / Idle	Horizontal / Vertical	None
D9	1	1.3 m	1 Unit of Bolus / Alarm / Idle	Horizontal / Vertical	None

Table 8: Summarized test data of sample Insulin Pumps. D1, D2, and D3 were selected for additional testing.

Table 9 shows that the E1 TENS device was affected by electromagnetic interference (EMI) within 2 cm of the front panel of the UPS only under a special circumstance. This special circumstance was created when the E1 was operated under a low battery voltage (i.e. < 6 V) condition. The TENS device expects a full battery voltage (i.e. 9 V) to operate normally. The

Device	Location	Height	Test Mode	Orientation	Observed Reaction
E1	1 2 UPS	1.3 m 1.3 m 0.75 m	Normal	Horizontal / Vertical	None at location 1 and location 2. Sporadic subtle EMI that was mainly seen under limited circumstances immediately next to the UPS front panel
E2	1	1.3 m	Normal / Modulated Burst	Horizontal / Vertical	None
E3	1	1.3 m	Normal / Modulated / Burst	Horizontal / Vertical	None
E4	1	1.3 m	Normal / Modulated / Burst	Horizontal / Vertical	None

Table 9: Summarized test data of sample Transcutaneous Electrical Nerve Stimulators (TENS). E1 was selected for additional testing.

user manual of the TENS device explicitly asks the user to change the battery if the “on and yellow light are dim”, which were triggered when the low battery voltage was used. We repeated the experiment with a new TENS device which is called E1.2 from now on. E1.2 has the same model name as E1 but different serial number. The EMI was reproduced when the E1.2 TENS was operated under a low battery voltage condition, and placed within 2 cm of the front panel of the UPS.

Finally, the experiment was performed using the proper full battery voltage condition for both TENS (i.e. E1 and E2). The E1 TENS showed a very subtle EMI type effect when it was placed within 0 cm (i.e., touching) of the front panel of the UPS despite the use of the full battery voltage. However, this was not reproduced with the E1.2 TENS, which showed no EMI effects around the UPS front panel; E1.2 has the same model name as E1 except for a different serial

number. Please look at appendix L for more detailed discussions about the additional TENS device testing near the UPS of the AIT-2.

9. Summary of Findings for PMED Testing with the AIT-2 mmW Simulator

The sample PMEDs selected for additional testing at multiple locations in the AIT-2 were also tested using the mmW simulator. The PMEDs were tested under four different conditions that exposed the PMED to worst case mmW exposure conditions in the AIT-2. Tables 10-14 show that none of the PMEDs showed EMI when tested inside the mmW simulator. Please see appendix O for more detailed test results.

Device	Condition Simulated	Test Mode	Lead Configuration	Cardiac Signal	Orientation	Observed Reaction
A1	Electric field at location 1; 10 times the electric field at location 1; Electric field at location 2; 10 times the electric field at location 2	DDD	Unipolar / Bipolar	On / Off	Horizontal / Vertical	None
A2	Electric field at location 1; 10 times the electric field at location 1; Electric field at location 2; 10 times the electric field at location 2	DDD	Unipolar / Bipolar	On / Off	Horizontal / Vertical	None
A3	Electric field at location 1; 10 times the electric field at location 1; Electric field at location 2;	DDD	Unipolar / Bipolar	On / Off	Horizontal / Vertical	None

Device	Condition Simulated	Test Mode	Lead Configuration	Cardiac Signal	Orientation	Observed Reaction
	10 times the electric field at location 2					
A4	Electric field at location 1; 10 times the electric field at location 1; Electric field at location 2; 10 times the electric field at location 2	DDD	Unipolar / Bipolar	On / Off	Horizontal / Vertical	None
A5	Electric field at location 1; 10 times the electric field at location 1; Electric field at location 2; 10 times the electric field at location 2	DDD	Unipolar / Bipolar	On / Off	Horizontal / Vertical	None

Table 10: Summarized test data of sample Implantable Pacemakers tested in the mmW simulator.

Device	Location	Test Mode	Lead Configuration	Cardiac Signal	Orientation	Observed Reaction
B1	Electric field at location 1; 10 times the electric field at location 1; Electric field at location 2; 10 times the electric field at location 2	DDD	Bipolar	On / Off	Horizontal / Vertical	None
B2	Electric field at location 1; 10 times the electric field at location 1; Electric field at location 2; 10 times the electric field at location 2	DDD	Bipolar	On / Off	Horizontal / Vertical	None
B3	Electric field at location 1; 10 times the electric field at location 1; Electric field at location 2; 10 times the electric field at location 2	DDD	Bipolar	On / Off	Horizontal / Vertical	None
B4	Electric field at location 1; 10 times the electric field at location 1; Electric field at location 2; 10 times the electric field at location 2	VVI	Bipolar	On / Off	Horizontal / Vertical	None

Table 11: Summarized test data of sample Implantable Cardioverter Defibrillators tested in the mmW simulator.

Device	Location	Test Mode	Orientation	Observed Reaction
C1	Electric field at location 1; 10 times the electric field at location 1; Electric field at location 2; 10 times the electric field at location 2	Normal / Magnet	Horizontal / Vertical	None
C2	Electric field at location 1; 10 times the electric field at location 1; Electric field at location 2; 10 times the electric field at location 2	Normal / Magnet	Horizontal / Vertical	None

Table 12: Summarized test data of sample Implantable Neuro-stimulators tested in the mmW simulator.

Device	Location	Test Mode	Orientation	Observed Reaction
D1	Electric field at location 1; 10 times the electric field at location 1; Electric field at location 2; 10 times the electric field at location 2	1U Bolus / Alarm / Idle	Horizontal / Vertical	None
D2	Electric field at location 1; 10 times the electric field at location 1; Electric field at location 2; 10 times the electric field at location 2	PING at 2Hz	Horizontal / Vertical	None
D3	Electric field at location 1; 10 times the electric field at location 1; Electric field at location 2; 10 times the electric field at location 2	16U Bolus / Alarm / Idle	Horizontal / Vertical	None

Table 13: Summarized test data of sample Insulin Pumps tested in the mmW simulator.

Device	Location	Test Mode	Orientation	Observed Reaction
E1	Electric field at location 1; 10 times the electric field at location 1; Electric field at location 2; 10 times the electric field at location 2	Normal	Horizontal / Vertical	None

Table 14: Summarized test data of sample Transcutaneous Electrical Nerve Stimulators (TENS) tested in the mmW simulator.

10. Risk Analysis

A key task under the IAA is to assess the risks for users of the high priority PMEDs for exposure to the emissions from the mmW AIT-2. The process called out in the ISO 14971 standard [3] standard was used to analyze these risks. This standard entails a risk analysis process for medical devices which includes: determining the device intended use and identification of characteristics related to the safety of the medical device, identification of the hazards, and estimation of the risks for each hazardous situation. If it is determined that the risks are unacceptable, then risk control measures must be implemented. Samples of medical devices most likely to be exposed to electromagnetic fields from the mmW AIT-2 were analyzed using this process. Table 15 describes the sample devices used in this study and their intended use.

Device Category	Number of Devices Tested	Major Category of Intended Use
Pacemakers	14	Life sustaining / supporting
ICDs	15	Life sustaining / supporting
Neuro-stimulators	11	Therapeutic
Insulin pumps	9	Life sustaining / supporting
TENS	4	Therapeutic

Table 15: Device category and intended use of the PMEDs tested in the AIT-2.

The hazards for pacemakers, ICDs and neuro-stimulators include pulse inhibition, pulse rate change, programming change, and false shock (for ICDs). For insulin pumps, the hazards include failure of insulin delivery, false alarm, and program change. Based on work by Hayes et al. [13] with implantable cardiac pacemakers and ICDs, the hazards were categorized into three different classes based on the severity of harm: clinically significant (Class I), probably clinically significant (Class II), and probably not clinically significant (Class III). The risks of the hazards associated with each device category were estimated based on their probability of occurrence and severity of harm. Because there were no effects observed with exposure to the mmW emissions of the AIT-2, the general risks for the sample devices were categorized as very low. This finding

applies to the sample PMEDs that were tested. Extrapolation of these findings to other medical device types might be misleading.

The above conclusions are based on the results of PMED tests that showed no effects. There was a TENS device (E1) that showed an EMI effect when it was tested within 2 cm of the front panel of the UPS of the AIT-2, and when the TENS was under a low battery voltage condition, which is not recommended by the TENS manufacturer's labeling. This experiment was reproduced using a newer TENS device (E1.2), which has the same model name as E1 but a different serial number, when E1.2 was operating under a low battery voltage. The E1 TENS device showed a very subtle EMI when it was tested within 0 cm (i.e. touching) of the UPS front panel while the E1 TENS was operating under the proper full battery condition. However, this experiment could not be reproduced with the E1.2 TENS device operating under the proper full battery condition. The E1.2 TENS showed no EMI around the UPS when it was operating under the full battery voltage. Please see section 8 or appendix L for more detailed discussion of the testing of the TENS device next to the front panel of the UPS of the AIT-2.

The following is an assessment of the risk of the TENS devices based on ISO 14971 standard [3]. The EMI can affect the output of the TENS (i.e. both E1 and E1.2) when the following three circumstances happen simultaneously: i) the TENS device is operating under a low battery voltage that is not recommended for use by the manufacturer's labeling; ii) the user does not stop using the TENS device according to the instructions in the manual, when the on and yellow light become dim because of the low battery voltage conditions; iii) the user puts the TENS device within 2 cm of the front panel of AIT-2's UPS, almost touching the surface of the UPS. The simultaneous occurrence of these three circumstances can lead to a hazardous situation involving EMI induced change in the output signal of the TENS device. According to annex E of [3], the underlying hazards that lead to this hazardous situation can be classified as a use error operational hazard (which leads to circumstances i & ii above) and an electromagnetic energy hazard (which leads to circumstance iii). The probability of occurrence of each of the three circumstances is relatively low. Therefore, the probability of simultaneous occurrence of all of the three statistically independent circumstances (which can lead to EMI induced change in the output signal of the TENS) is very low.

When only condition iii occurred (i.e. without simultaneous occurrence of conditions i and ii), the EMI subtly affected the E1 TENS but not the E1.2 TENS. Once again, the probability of occurrence of condition iii (which can lead to sporadic (i.e. unreproducible) EMI induced change in the output signal of the TENS) itself is relatively low.

If the EMI induced change in the output signal of the TENS device is harmful, the probability of the occurrence of such harm is very low. Moreover, TENS devices are not life sustaining, and the severity of the harm (i.e. over or under stimulation) by EMI induced change in the output

signal of the TENS device is generally expected to be low. Based on the assessment of the probability of the harm and the severity of the harm, the risk associated with the use of the TENS (i.e. both E1 and E1.2) around the AIT-2 is low to very low [3].

11. Conclusion

CDRH performed laboratory testing using several sample personal medical electronic devices (PMEDs) with the millimeter wave (mmW) exposure simulator and the AIT-2 and performed a risk assessment for potential electromagnetic interference (EMI) effects. No effects were observed for all PMEDs exposed to the mmW emissions of the AIT-2.

One transcutaneous electrical nerve stimulator (TENS) device showed an EMI effect within 2 cm of the front panel of the UPS of the AIT-2, when the TENS was operating under a low battery voltage condition, which is not recommended by the TENS manufacturer's labeling. The TENS showed a subtle EMI when it was touching the front panel of the UPS of the AIT-2 while operating under the full battery voltage condition; however, this result could not be reproduced with a newer TENS unit with the same model name. Based on the assessment of the severity of the harm (i.e. over or under stimulation) and the probability of the harm, the risk associated with the use of the TENS device around the AIT-2 is low to very low [3]. All other PMEDs (except for the above mentioned TENS device) tested next to the front panel of the UPS of the AIT-2 did not show any EMI effects.

Most concerns about EMI that are associated with active medical devices tend to focus on exposure to radio frequency emissions below a few gigahertz (GHz) which are more common in the environment (e.g., broadcast commercial radio and TV, cellular telephones). Generally, medical devices tend to be more susceptible to emissions that contain carrier frequencies or modulations within the band pass of the medical device. For example, a cardiac pacemaker generally senses the cardiac electrical activity between 0.5 Hz up to perhaps several Hz and in some cases sensing capabilities may go to a few kilohertz (kHz) to effectively capture the rhythm of the heart. Other types of devices such as insulin pumps have different characteristics and functions that change the potential susceptibilities.

Based on the work performed on a sample of over 50 different PMEDs from 5 different types of devices, it appears the risks are very low for the non-ionizing mmW and out-of-band emissions from AIT-2 to disrupt the function of the PMEDs that we evaluated in this study. The medical device types that were tested comprise a significant portion of the types of PMEDs that are in use today with historical concern for EMI. The work described in this report is directly applicable only to those devices tested and analyzed for EMC from exposure to the AIT-2. However, based on the low exposure to extremely high frequency mmW emissions it seems highly unlikely that other similar PMEDs would be affected by the in-band mmW emissions of the AIT-2. This is

due to physics and electrical engineering factors and the typical electronic components found in many ambulatory, active medical devices that result in very low susceptibility to the AIT-2 mmW emissions. The field strengths of out of band emissions are low, relative to other common electromagnetic environments routinely encountered by PMEDs. Therefore, it seems unlikely that other similar PMEDs would be affected by these emissions of the AIT-2. It should be noted that our results cannot be applied to other AIT-2 systems.

Human exposures to millimeter wave emissions from the AIT-2 were also evaluated. Considering the short duration of exposure, and the very low levels of mmW emissions from the AIT-2, the measured mmW energy levels were determined to be 128 million times less than the limits in the IEEE C95.1 [1] standards and 49 million times less than the limits in the International Commission on Non-Ionizing Radiation Protection (ICNIRP) [2]. Based on request from the TSA, the CDRH developed a method that enables the assessment of the safety of the AIT-2 based on these standards. This method is being filed by TSA for a patent. Therefore technical details about it are not presented in this report. An overview and details of its design and performance are contained in a technical report previously submitted to the following key personnel associated with this IAA: David Hobbs, William Garrett, William Washington of TSA, and Lee Spanier of the Transportation Security Laboratory.

12. References

1. IEEE Std C95.1-2005: IEEE Standard for Safety Levels with Respect to Human Exposure to Radio Frequency Electromagnetic Fields, 3 kHz to 300 GHz. Institute of Electrical and Electronics Engineers, 19 April 2006.

2. ICNIRP Guidelines for Limiting Exposure to Time-Varying Electric, Magnetic, and Electromagnetic Fields (up to 300 GHz). Health Physics 74 (4):494-522, 1998.

3. BS EN ISO 14971:2012: Medical devices — Application of risk management to medical devices. BSI, 2012.

4. CKC Laboratories, Inc. Report No. 92757-31A, Radio Frequency Addendum Exposure Report to 92757-31. CKC Laboratories, Inc., October 30, 2012.

5. Title 47 CFR, Part 1.1310, Radiofrequency Radiation Exposure Limits.

6. Industry Canada RSS-102, Issue 4, Radio Frequency (RF) Exposure Compliance of Radiocommunication Apparatus (All Frequency Bands). Industry Canada, March 2010 (including update December, 2010).

7. ISO/TR 7250-2:2010(E): Basic Human Body Measurements for Technological Design. ISO, 2010.

8. CKC Laboratories, Inc. Test Report for ProVision 2, PV-2. Tested to the Following Standards: FCC Part 15 Subpart B Sections 15.107 and 15.109. Report No.: 92821-13. CKC Laboratories, Inc., August 23, 2012.

9. IEC 60601-1-2: Edition 4.0, 2014-02: Medical Electrical Equipment – Part 1-2: General Requirements for Basic Safety and Essential Performance – Collateral Standard: Electromagnetic Disturbances – Requirements and Tests. International Electrotechnical Commission, 2014.

10. IEC 60601-1, Edition 3.1, 2012-08, Medical Electrical Equipment – Part 1: General Requirements for Basic Safety and Essential Performance. International Electrotechnical Commission, 2012.

11. ANSI/AAMI/ISO 14117:2012, Active Implantable Medical Devices ---Electromagnetic Compatibility --- EMC Test Protocols for Implantable Cardiac Pacemakers, Implantable Cardioverter Defibrillators, and Cardiac Resynchronization Devices. AAMI, 2012.

12. ANSI/AAMI/ISO 14708-3:2008/(R) 2011, Implants for Surgery --- Active Implantable Medical Devices --- Part 3: Implantable Neurostimulators. AAMI, 2009.

13. Hayes D, Wang P, Reynolds D, et al. Interference with Cardiac Pacemakers by Cellular Telephones. New England Journal of Medicine; 21:1473-1479, 1997.

14. K. T. Selvan. Simple Formulas for the Gain and Far-Field of Open-Ended Rectangular Waveguides. IEE, IEE Proceedings Online No. 19981552, 1998.

15. IEC 60601-2-24: Edition 2.0, 2012-10, Particular Requirements for the Basic Safety and Essential Performance of Infusion Pumps and Controllers. International Electrotechnical Commission, 2012.

16. ANSI/AAMI NS4:2013, Transcutaneous Electrical Nerve Stimulators. AAMI, 2013.

17. DHS/ST/TSL-12/118 Compilation of Emission Safety Reports on the L3 Communications, Inc. ProVision 100 Active Millimeter Wave Advanced Imaging Technology (AIT) System, Version 2. DHS, 2012.

13. List of Appendices

Appendix A: Glossary of acronyms and terms
Appendix B: Background information about the AIT-2
Appendix C: AIT-2 test locations and heights
Appendix D: Detailed pulse exposure time considerations
Appendix E: AIT-2 primary frequency band emission measurements
Appendix F: AIT-2 lower frequency band emission measurements
Appendix G: Results of leakage current testing
Appendix H: Procedures for testing medical devices with the AIT-2
Appendix I: Torso simulator
Appendix J: PMED device under test settings
Appendix K: Findings for PMED testing with the AIT-2
Appendix L: Testing of TENS near the UPS of the AIT-2
Appendix M: AIT-2 mmW Simulator
Appendix N: Procedures for testing PMEDs with the AIT-2 mmW simulator
Appendix O: Findings for PMED testing with the AIT-2 mmW simulator
Appendix P: Video of the PMED testing

Appendix A

Glossary of acronyms and terms

A	Ampere
A/m	Ampere per meter
AAI	This is a cardiac device mode that stands for Atrial pacing Atrial sensing and Inhibition by sensing
AC	Alternating current
AIT	Advanced Imaging Technology, which is an L-3 security scanning system.
AIT-2	Advanced Imaging Technology – 2, which is second generation of the L-3 security scanning system.
AWG	Arbitrary waveform generator
BNC cable	"Bayonet Neill-Concelman" radio frequency connector cable
CDRH	Center for Devices and Radiological Health
CFR	Code of Federal Regulations
cm	Centimeter
CW	Continuous wave
dB	Decibel
dBi	This emphasizes that the gain of the antenna is compared to an isotropic antenna in dB
dBm	Decibel milliwatts
DDD	This is a cardiac device mode that stands for Dual pacing Dual sensing and Dual response to sensing
DHS	Department of Homeland Security
DUT	Device under test
E	Electric field strength
E-field	Electric field
EMC	Electromagnetic compatibility
EMI	Electromagnetic interference
FCC	Federal Communications Commission
FDA	Food and Drug Administration
GHz	Gigahertz
GST	Glucose sensor transmitter
H	Magnetic field strength
H-field	Magnetic field
Hz	Hertz
IAA	Interagency Agreement
ICD	Implantable cardioverter defibrillator
ICNIRP	International commission on non-ionizing radiation protection
IEEE	Institute of electrical and electronics engineers
IPG	Implantable pulse generator
IR detector	Infrared detector
J	Joule

J/m^2	Joule per meter squared
kHz	Kilohertz
LED	Light emitting diode
LNA	Low noise amplifier
m	Meter
Mast	A vertical rotating column in the AIT-2 that contains an array of 192 transmit and 192 receive antennas
MHz	Megahertz
mm	Millimeter
mmW	millimeter wave
mW/cm^2	Miliwatt per centimeter squared
MΩ	Megaohm
OEWG	Open ended wave guide
PMED	Personal medical electronic device
RF	Radio frequency
RMS	Root mean squared
S/m	Siemens per meter
T	Tesla
TENS	Transcutaneous electrical nerve stimulators
TSA	Transportation Security Administration
UPS	Uninterruptible power supply
V	Volt
V/m	Volt per meter
VCO	Voltage controlled oscillator
VDD	This is a cardiac device mode that stands for Ventricular pacing Dual sensing Dual response to sensing
VVI	This is a cardiac device mode that stands for Ventricular pacing Ventricular sensing and Inhibition by sensing
W	Watt
W/m^2	Watt per meter squared
WR28	Antenna or waveguide that is designed for frequencies between 26.5 GHz and 40.0 GHz
WR34	Antenna or waveguide that is designed for frequencies between 20.0 GHz to 33.0 GHz
µT	Microtesla
Ω	Ohm

Appendix B

Background information about the AIT-2 (Task 1 report)

Review of AIT-2 information provided by TSA and L3

Per task 1 of the TSA/FDA IAA, the FDA has thoroughly reviewed the AIT-2 information provided by TSA (CDs) and the open/closed calibration document provided by L3. The FDA used this information in performing tests and assessing risks for certain personal medical electronic devices (PMEDs) exposed to the AIT-2. The information is summarized below.

1. Summary review of the "ProVision2 Technical Data Package CDRL L016" pdf document, which is inside the "L3 PV2 TOP" CD.
   a. This document contains the following relevant information:
      - The transmitting and receiving antennas in the AIT-2 have a vertical polarization.
      - The antennas have a 50-65 degrees elevation beam-width, and a 75-90 degrees azimuth beam-width. The gain of the antennas is flat over the frequency range (24.25 GHz to 30 GHz) within +/- 2 dB.
      - The antennas have a 1.04 cm center to center spacing.
   b. However, the technical data package does not provide the following information that is needed for the investigation at the FDA.
      - There is no quantitative information about the movement of the antenna masts (e.g. movement speed, scan duration).
      - There is no quantitative description of the in-band (mmW) and out-of-band (spurious) emissions by the AIT-2. Spatial distribution of these electromagnetic fields is needed to assess the risks for persons with PMEDs.
        - There are no FCC reports about emissions from the AIT-2.
        - There is no assessment of the risks of human exposure to electromagnetic emissions by the AIT-2 in this document.
        - There is no information regarding the safety of PMEDs around the AIT-2 (e.g. quantitative exposure measurements, any information related to PMED).
2. Summary review of the "AIT-2 Emissions Test Report" zipped files, which are inside the "L-3 AIT2 DOCS" CD.
   a. The "AIT-1 and AIT-2 RF Exposure Compliance Test.pdf" document contains the CKC Laboratories Report No. 92757-31A entitled "Radio Frequency Addendum Exposure Report to 92757-31". Page 6 of this report [4] indicates, that the emissions from the AIT have a power density of 1.6×10^{-4} mW/cm^2 in the mmW operating frequency range of 24.25 GHz to 30 GHz at a distance of 3.5 cm. However, there is no mention of reference points for the 3.5 cm distance measurement. The report states that this power density level is below the US [5] and Canadian [6] limits for human exposure (referenced as 1 mW/cm^2). Regarding the measurement methods, the report states, "Measurements were

gathered with equipment stopped at a specific frequency. Calculations provided here are based on instantaneous peak measurements representing a worst case approach".

b. However, there is no detailed information about the following.
   - There is no information about the spatial distribution of the electric and magnetic fields in and around the AIT-2 beyond the 3.5 cm measurement point mentioned above. There is also no detailed description of the measurement techniques and instrumentation used for the measurement reportedly done at 3.5 cm.
   - There is no information that can be directly related to the safety of PMEDs in and around the AIT-2.

3. Summary review of "ProVision 2 Transmmitted Signal Testing With the Antenna Mast Stationary" hard copy document obtained directly from L3.
   a. This document includes the following:
      - Timing diagrams that show the duty cycle of the emitted pulse signal, and the pulse width, which help confirm that the AIT-2 emits the same waveform as the AIT-1.
      - Instructions to operate the AIT-2 in advanced mode enabling emission with stationary mast.
4. Summary review of the "AIT-2 Operator Manual.pdf", which is inside the "L-3 AIT2 DOCS" CD.
   a. This document contains basic information about the AIT-2, which is needed to carry out the testing at the FDA, such as:
      - standard operating procedures,
      - basic troubleshooting, and
      - cleaning and maintenance.

   This document has brief sections titled "1.2 System Safety" and "1.3 Important Precautions". We recommend expanding these sections to include summary of information about the safety of PMEDs in and around the AIT-2, and summary of information about the safety of human exposure to emissions from the AIT-2.

5. Summary review of the "Checkpoint Design Guide" pdf document, which is inside the "L-3 AIT2 DOCS" CD.
   a. The typical layout of a SSCP (Security Screening Check Point) area (which consists of AIT, Advanced Technology X-Ray device, Walk Through Metal Detectors, etc) is presented along with the SSCP Arrangement Recommended Spacing.
6. Summary review of the "FDAQuestionhighlightedforoperations – OIB.docx", which is inside the "L-3 AIT2 DOCS" CD.
   a. This document provides the typical location of security personnel operating the AIT-2 scanner and passengers who are scanned. This information is supported by the contents of "SOP for FDAwithFDAPW.docx" in the same CD.

Document Name	Summary of information in the document
"ProVision2 Technical Data Package CDRL L016"	• Antenna polarization. • Antenna beam width. • Antenna vertical spacing.
AIT-2 Emissions Test Report	• Measured power density at a distance of 3.5cm from the AIT antenna. • Compared measurements with US (1.1310) and Canadian (RSS-102) standard for human exposure.
ProVision 2 Transmitted Signal Testing With the Antenna Mast Stationary (obtained directly from L3)	• Timing diagrams of the pulses emitted by the AIT. • Instructions to operate the AIT in advanced mode.
AIT-2 Operator Manual.pdf	• Standard operating procedures. • Basic troubleshooting. • Cleaning and maintenance.
Checkpoint Design Guide	• Typical layout of airport security area.
FDAQuestionhighlightedforoperations – OIB.docx	• Typical locations of people around the AIT.

Table B.1: This is a summary of the information received from TSA and L3 regarding the AIT-2.

Appendix C

AIT-2 test locations and heights

C.1 Selecting AIT-2 electromagnetic emission measurement locations and heights

The electromagnetic emissions from the AIT-2 can be classified into two types: millimeter wave (mmW) emissions that are the intentional emissions or "in-band", and the spurious unintended "out-of-band" emissions. Both types of emissions have the potential to affect the PMEDs via electromagnetic disturbance (EMD) and cause electromagnetic interference (EMI) to the PMED. The in-band mmW and out-of-band emission measurements are further discussed in appendix E and appendix F respectively.

Understanding the spatial distributions of the in-band and the out-of-band emissions fields helps in the assessment of potential risks to the PMEDs and humans exposed to the fields. A high resolution and uniform spatial sampling of the electromagnetic fields around the AIT-2 was not possible given the limitations of the AIT-2 project and resources. Instead, attention was focused on 24 representative measurement points in and around the AIT-2 that are distributed three dimensionally. For these measurements, the coordinate system is oriented so the x-y plane is parallel to the ground supporting the AIT-2.

The 24 measurement points were chosen using four criteria:

1) the locations (x and y coordinates) of the measurement points should be representative of the places where people (security personnel or passengers) are likely to stand;

2) the heights (z coordinate) of the measurement points should be representative of the location of the PMEDs with respect to an average human, based on anthropomorphic data [7];

3) the measurement points should be spread out in space to assess the overall spatial distribution of emissions; and,

4) the measurement points should be chosen close to the most likely sources of in-band and out-of-band electromagnetic emissions in and around the AIT-2.

C.1.i Emission measurement locations around the AIT-2

The above mentioned criteria were applied to choose 6 locations in and around the AIT-2, and 4 different heights at each of these 6 locations. In total there were 24 measurement points (6 locations x 4 heights) in and around the AIT-2. Figure C.1 and figure C.2 illustrate the measurement locations and heights, respectively. Table C.1 and table C.2 summarize the rationale for picking the locations and heights, respectively.

The six locations were chosen with the following rationale. Passengers stand for five to ten seconds approximately 1.5 meters (5 feet) from the entrance gate of the AIT-2 (location 3) waiting to be scanned. Once a passenger enters the AIT-2, they are expected to stand at the center of the AIT-2 (location 1) for about 3 seconds. In addition, the passengers' body might be located closer to the AIT-2 interior wall because of their size or other reasons, which would place their body closer to the AIT-2 emitters array and thus increase their exposures to the in-band emission. For this reason, another measurement location was added inside the AIT-2 against the interior wall (location 2), where the maximum in-band emission is expected to be measured. The distance between location 2 and the radiating array of antennas of the AIT-2 is about 3 centimeters (cm).

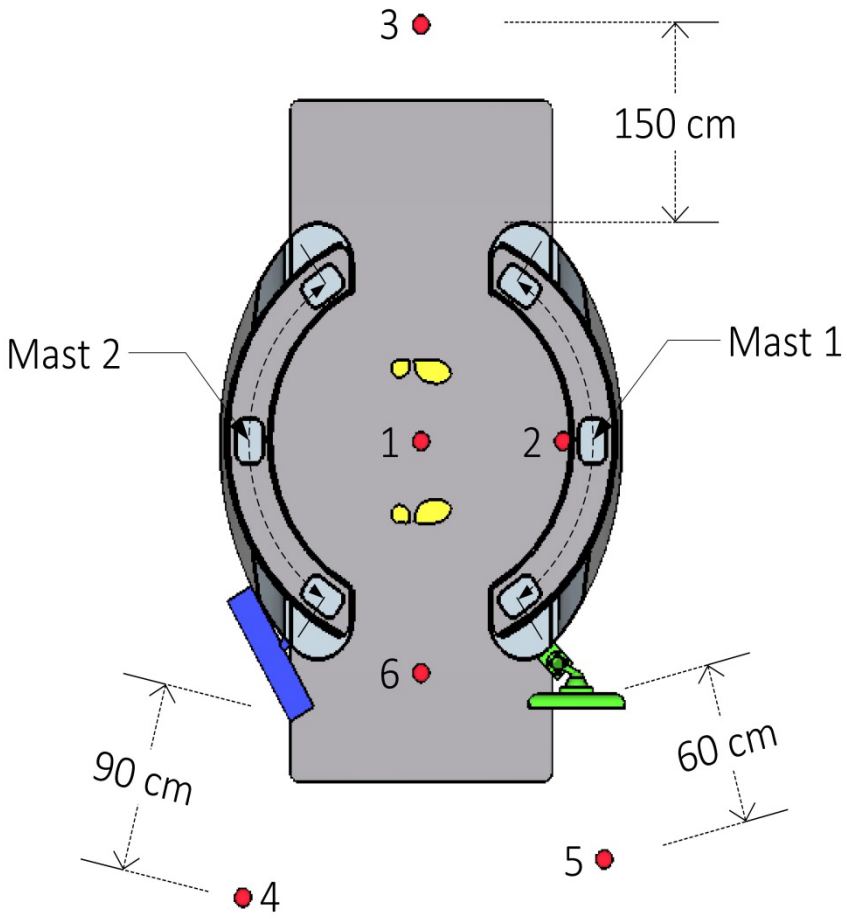

Figure C.1: The six locations in and around the AIT-2 chosen to perform the in-band and out-of- band emission measurements. The AIT-2 uninterruptable power supply (UPS) is shown to the left of location 6 in blue, and the AIT-2 computer monitor is shown to the right of location 6 in green.

The Standard Operating Procedure of the TSA, which is summarized in appendix B, specifies that officers may conduct secondary screening approximately 90 cm - 3 meters (3 feet to 10 feet) away from the AIT-2. Location 4 is 90 cm from the AIT-2 UPS that is hung just outside the AIT-2 exit. This location was chosen because it seems likely this spot would expose the security

personnel to both the mmW emissions and spurious emissions from the UPS during the secondary screening.

The security personnel typically would be expected to stand approximately 60 cm (2 feet) away from the computer monitor controlling the AIT-2, likely for about 30 minutes before personnel rotation. Location 5, which is 60 cm away from the computer monitor, was chosen since the location affords the security personnel a view of both the monitor and the passenger, and it also maximizes the likelihood of a direct line of sight exposure to the in-band emissions from the rotating mast.

There is spatial gap between locations that was filled with extra measurement location. Location 6 at the AIT-2 exit was chosen to fill the gap among locations 1, 4 and 5. This measurement location provides an opportunity to better understand the spatial distribution of the fields in and around the AIT-2.

Location #	Description	Rationale
1	Center of the AIT-2	Passengers stand here for about 3 seconds for security screening.
2	3 cm away from AIT-2 mast	Portions of the passenger's body might reach here during the 3 second scan. The in-band emissions have maximum field strength at this location.
3	1.5 meters away from the entrance of the AIT-2	Passengers typically might stand here for five to ten seconds waiting to be scanned.
4	90 cm away from the UPS	This represents the location with the worst case emission exposure (due to its relative proximity to the UPS and the masts) during secondary screening of the passengers, which takes place approximately 90 cm - 3 meters from the exit of the AIT-2.
5	60 cm away from the monitor	Security personnel location to observe passenger and watch the AIT-2 computer monitor.
6	Between the UPS and the monitor at the AIT-2 exit	Chosen to better understand the spatial variation of the fields between locations 1, 4, and 5.

Table C.1: Summary of the 6 locations where the in-band and out-of-band emission measurements were performed. The locations are based on information from TSA regarding the Standard Operating Procedure which is summarized in appendix B.

C.1.ii Emission measurement heights

The rationale for picking the 4 heights for each of the 6 locations was based on where the PMED might generally be expected to be located on or in the passenger's body. Patients place their PMEDs at heights ranging from a typical height of an ankle (e.g., insulin pump) to their head (e.g., deep brain stimulator), with many of the cardiac and neuro-stimulator implanted devices located at the chest/shoulder and sometimes waist level. Two aspects of the PMED placement were considered: typical placement positions, and an average placement height. The anthropomorphic data [7] for heights of human body parts have a large standard deviation to

cover a variety of body types, sexes, and ages which are difficult to filter down across the PMED types. For practical reasons, the decision was made to use a limited number of placements that results in the four heights specified in table C.2 and figure C.2.

A measurement point at 1.7 m height covers the expected maximum heights that an average patient might have a PMED placed at. This measurement point also would cover the exposure of typical PMEDs (typically placed slightly below the shoulder) for patients who might be much taller than average. The second measurement height is 1.3 m above the ground and is based on anthropomorphic data targeting PMEDs that are worn or implanted just below shoulder height. The third measurement height is 1 m above the ground targeting PMEDs that are worn at waist height. The fourth point at 25 cm height was chosen to target a potential location of an insulin pump worn just above the ankle or on lower leg areas. Overall, the spacing between the four measurement points was also considered so that it is as uniform as possible, which allows interpretation of any vertical variation of the data collected.

Height	Rationale
1.7 m	PMEDs in or on the head
1.3 m	PMEDs implanted or worn slightly below shoulder height
1 m	PMEDs implanted or worn at waist height
0.25 m	PMEDs, such as insulin pumps, placed just above ankles

Table C.2: Rationales for the 4 heights, where the in-band and out-of-band emission measurements were performed, based on anthropomorphic data for an average human [7].

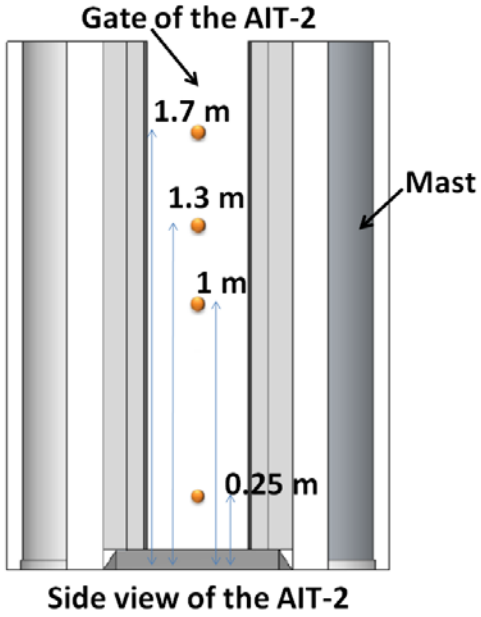

Figure C.2: These four heights were chosen to perform the emission measurements at the six locations shown in figure C.1. A side view of the AIT-2 shows the gate of the AIT-2, which is about 2 m tall.

C.2 Selecting locations and heights for PMED testing in and around the AIT-2

The in-band and out-of-band emissions of the AIT-2 were measured at the 24 points discussed above. The results of these emission measurements are discussed in appendix E and appendix F. The results were used to narrow down the locations and heights for PMED testing in and around the AIT-2. Below is a brief explanation for selecting the PMED testing points.

The data from the out-of-band emission of the AIT-2 showed that the spurious emission at all of the 24 measurement points were generally within the background noise level. Please see the discussions in appendix C which are summarized in table C.2 to table C.5. Based on this information, the PMED testing points were chosen using the observed spatial variation of the in-band emission levels at the 24 measurement points. In addition, the spurious measurement results showed that there is a spurious emission hot spot within 15 cm of the UPS front panel of the AIT-2, which was discovered by scanning the surroundings of the AIT-2 using the field measurement probes. Please see appendix F.2 for analysis of this spurious emission hot spot. From our understanding of the information from TSA this is not a location where people (passengers or security officers) would typically be standing and differs from locations 1 to 6 that are all more than 15 cm away from the UPS front panel. However, there is still some chance that people may walk very close to the UPS front panel. Therefore, a representative set of PMEDs were tested as close as possible to the UPS front panel of the AIT-2 at the height of 75 cm from the ground because this is the height where the hot spot of spurious emission was discovered. The representative set of PMEDs was chosen by selecting one PMED per device category and per manufacturer.

The in-band emissions of the AIT-2 peaked at location 2 at about 1.5 V/m. In fact, the magnitude of the highest electric field measured at location 2 is more than an order of magnitude higher than the highest electric field measured at any of the other 5 locations. The second highest electric field was measured at location 1. These values are discussed in detail in appendix E, and shown in figure E.10. Even though the peak electric field at location 1 (which is about 59 cm from the radiating antennas of the AIT-2) is about 20 times smaller than the peak electric field at location 2 (which is about 3 cm from the radiating antennas of the AIT-2) the exposure time at location 1 is significantly higher during the normal scanning operation of the AIT-2. A typical PMED at location 1 has an exposure time of about 0.23 seconds from each of the AIT-2 masts. On the other hand, a typical PMED at location 2 has an exposure time of only 10 milliseconds (ms) to the mast that is closest to the PMED. PMEDs may not respond to interference at such short time scales. In addition, location 1 is the primary spot where the passengers stand for scanning. Therefore, location 1 was chosen to be the primary PMED testing location. All of the PMEDs were tested at location 1 while the AIT-2 went through normal scanning operations. The set of PMEDs chosen for additional testing close to the UPS front panel were also tested at location 2 because this is the location that has the highest electric field strength despite the limited 10 ms exposure time. The exposure time at location 1 and location 2 is discussed thoroughly in appendix D, and summarized in table D.1.

The summary of in-band emissions measurements (figure E.11) shows that these are not significantly dependent on the height of the measurement point. The exposure time analysis (appendix D, figure D.5) shows that the exposure time of a 10 cm x 10 cm PMED does not depend on height especially for heights between 0.3 m and 1.7 m at location 1 and location 2. For these locations PMED testing can be performed at any of the 3 heights (1 m, 1.3 m, and 1.7 m). Thus, the PMED testing at location 1 and location 2 were done 1.3 m above the ground for cardiac devices, neuro-stimulators, and TENS. Insulin pumps can be worn at around a height of 0.25 m, which may have slightly different exposure time than other heights between 0.3 m and 1.7 m, especially at location 1. Therefore, one insulin pump type per manufacturer was tested at one more height (i.e. 0.25 m) both at location 1 and location 2.

The height for the PMED testing close to the UPS front panel was mainly based on the height of the UPS front panel from the ground, which is about 75 cm. Table C.3 summarizes the five points picked for PMED testing.

PMED testing point	PMEDs tested	Rationale
Location 1, height = 1.3 m	All PMEDs	There was a 0.23 seconds long exposure time to about 0.075 V/m peak electric field strength.
Location 1, height = 0.25 m	1 insulin pump type per manufacturer	There was about 0.23 seconds long exposure time to about 0.075 V/m electric field strength. Insulin pumps worn on ankles or lower leg areas may have slightly different (smaller) exposure times compared to those at heights between 0.3 m and 1.7 m.
Location 2, height = 1.3 m	1 PMED per device category per manufacturer	The maximum peak electric field strength (i.e. 1.5 V/m) was measured here despite the relatively short exposure time (i.e. 10 ms).
Location 2, height = 0.25 m	1 insulin pump type per manufacturer	The maximum peak electric field strength (i.e. 1.5 V/m) was measured here despite the relatively short exposure time (i.e. about 10 ms). Insulin pumps worn on ankles or lower leg areas may have slightly different (smaller) exposure times compared to

PMED testing point	PMEDs tested	Rationale
		those at heights between 0.3 m and 1.7 m.
UPS front panel, height = 75 cm	1 PMED per device category per manufacturer	There is a hot spot of spurious emission that can have electric fields as high as 100 V/m by the front panel of the UPS.

Table C.3: Rationales for the five PMED test points selected based on in-band and out-of-band emission data, and exposure time calculations.

Appendix D

Detailed pulse exposure time considerations

D.1 Introduction

The L3 ProVision mmW AIT-2 utilizes the frequency bandwidth of 5.75 GHz from 24.25 GHz to 30 GHz using a pulsed signal which also incorporates linear frequency sweeping (chirp) technique to acquire a cylindrical image of individuals who pass through security checkpoints. The total system scan time is usually roughly stated as 1.5 seconds; however, experiments set up in appendix E.2 show that it is close to 1.324 seconds.

During that time, two vertical antenna arrays (masts) rotate partially around the body being scanned. When an AIT-2 scan is activated, the masts accelerate to start moving along their curved path, and eventually decelerate until they stop after about a 120^0 travel. There are sensors throughout the masts' travel path with a spacing of roughly 0.5 cm. As the masts pass over each sensor, a vertical scan line is activated. A vertical scan line is a sequential top down activation of the 192 transmit and 192 receive antennas of a mast to capture a vertical image line. A single vertical scan line takes about 3.1 ms, which is 191 x 2 x 8.08 μs + 1 x 8.08 μs, because 191 of the antennas emit two consecutive 8.08 μs pulses, whereas the top most antenna emits only one 8.08 μs long pulse. There are 224 vertical scan lines, which last for about 3.1 ms each. However, due to the acceleration and deceleration of the masts along their curved path populated with sensors placed every 0.5 cm, the time gap between the vertical scan lines decreases and then increases during the 1.324 seconds long AIT-2 scan. Finally, each individual antenna in the mast transmits a 5.59 μs long chirp during an 8.08 μs pulse period. The timing diagram is shown in figure D.1. The operation of the AIT-2 is discussed further in appendix E.1.

A PMED inside the AIT-2 sees two different frequency repetitions as shown in figure D.2: i) an 8.08 μs pulse, which translates into 123.762 kHz, with a 70 % (i.e. 5.59 μs / 8.08 μs) duty cycle, and ii) a pulse that is at least 3.1 ms long, which translates into at most 322 Hz. The time gap between the first few scan lines is usually much larger than 3.1 ms as the masts accelerate past the first few sensors placed every 0.5 cm along their path. The 322 Hz frequency is close to the biological frequency of the heart as compared to the 123 kHz and 24.25 GHz to 30 GHz carrier frequencies. Depending upon the design of the low pass filter or digital filter at the front end of a PMED, 322 Hz could be detected by the PMED sensing circuitry. It is important to estimate the duration of the time that the PMED is exposed to the mmW radiation from the AIT-2.

D.2 Calculation of exposure times

The estimated exposure time of a 10 cm x 10 cm area, which for the present analysis is the assumed area of a PMED on a person, is estimated below to help quantify the EMI risks. The exposure time estimation is carried out for three of the six in-band and out-of-band emission measurement locations (i.e. location 1, location 2, and location 6). Figure D.3 points out these

three locations discussed in this appendix. The six in-band and out-of-band emission measurement locations are discussed in detail in appendix C.

These three locations (i.e. location 1, location 2, and location 6) were selected for the exposure time analysis because they received the strongest AIT-2 in-band emissions out of the six locations where in-band emission measurements took place. This is due to their relative proximity to the rotating masts, and it was confirmed by in-band measurements discussed in appendix E. The exposure time was estimated for just one of the 4 emission measurement heights (i.e. 1 meter). The four emission measurement heights are discussed in detail in appendix C. This height (i.e. 1 meter) was chosen because it is close to half of the height of the masts. It is expected that the pulse exposure time is maximum at a height which is in between the 192 vertical array of transmitting antennas. This approach enables the estimation of the maximum possible pulse exposure time of a PMED at each of the three locations with the strongest in-band emission levels (i.e. location 1, 2, and 6).

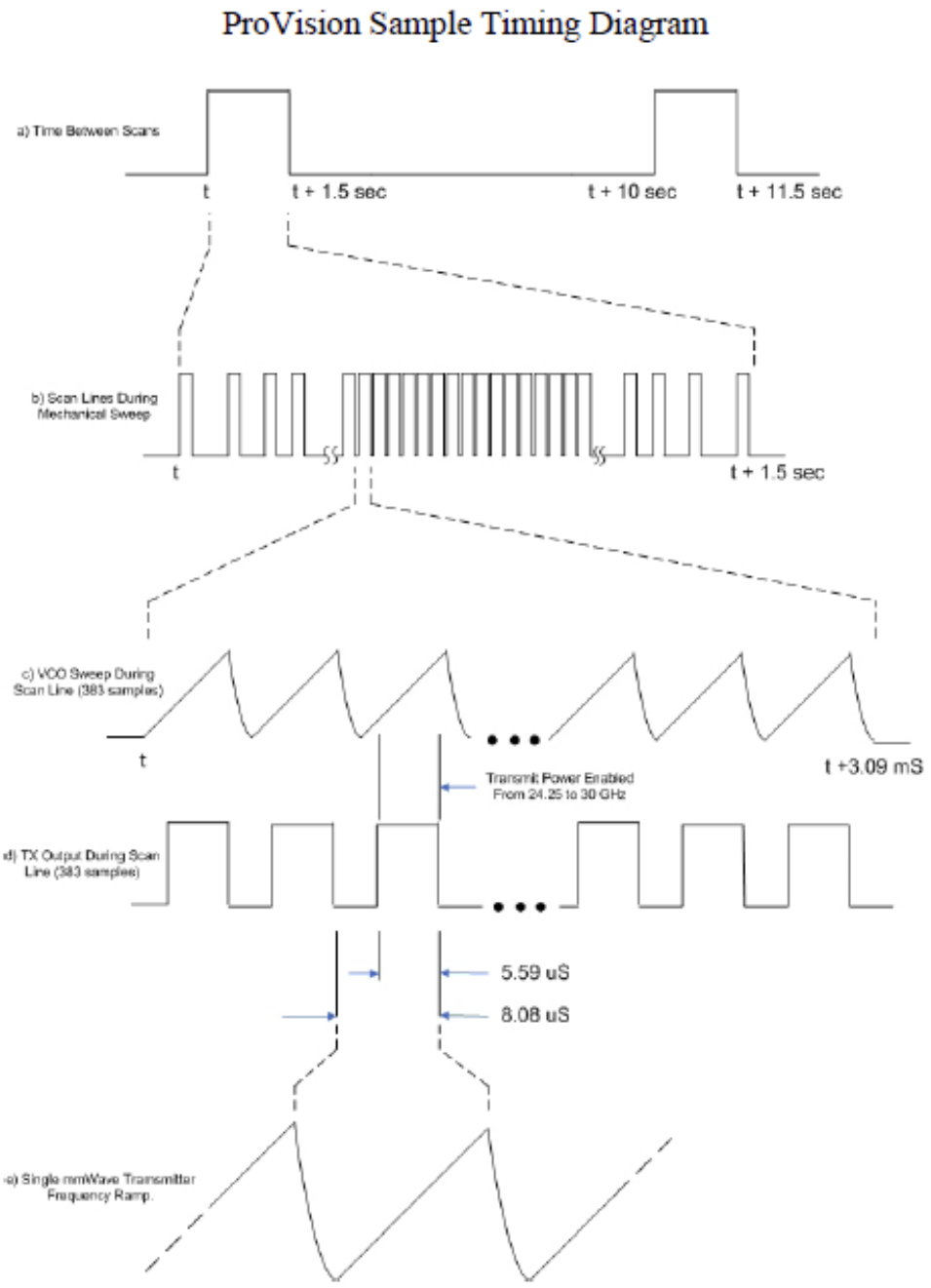

Figure D.1: AIT-2 mmW emission timing diagram.

The radiation pattern of the antennas of the AIT-2 was considered to estimate the exposure times. Each of the 192 transmitting antennas on the AIT-2 mast are specified to have an antenna beam width elevation of 50^0 (minimum) to 65^0 (maximum), and an antenna beam width azimuth of 75^0 (minimum) to 90^0 (maximum). The two masts rotate in a 120^0 arc while radiating. It was assumed that the transmitting antennas of the AIT-2 have an average beam width of 70^0, and that the PMED receives the emission isotopically. To simplify the calculations, the pulse exposure time of the PMED was calculated while considering the closest mast only. The other mast is

ignored in the following calculations. Symmetry arguments are later used to estimate the total pulse exposure time to emissions from both masts.

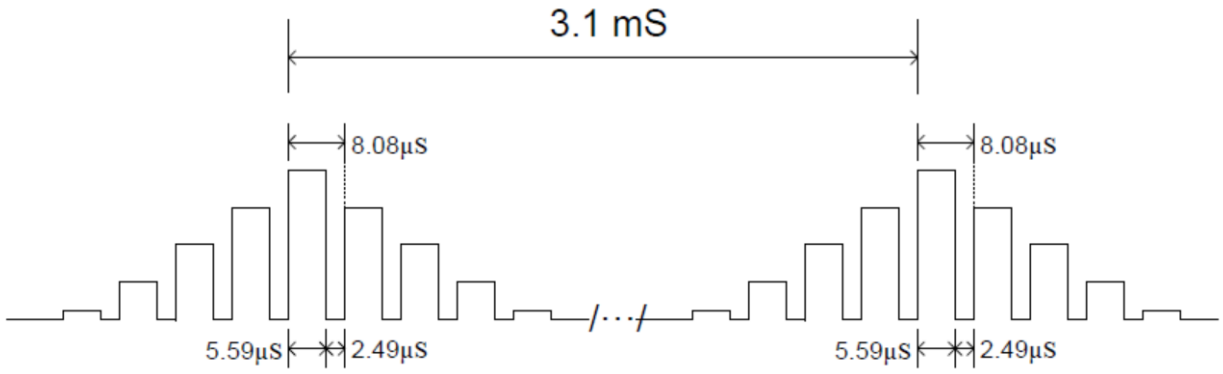

Figure D.2: Perceived exposure at a single point on a PMED (or a human body) when exposed to the AIT-2 screening system. The gap between the start of two vertical scan lines is at least 3.1 ms, and slightly varies as the masts accelerate and decelerate along their path.

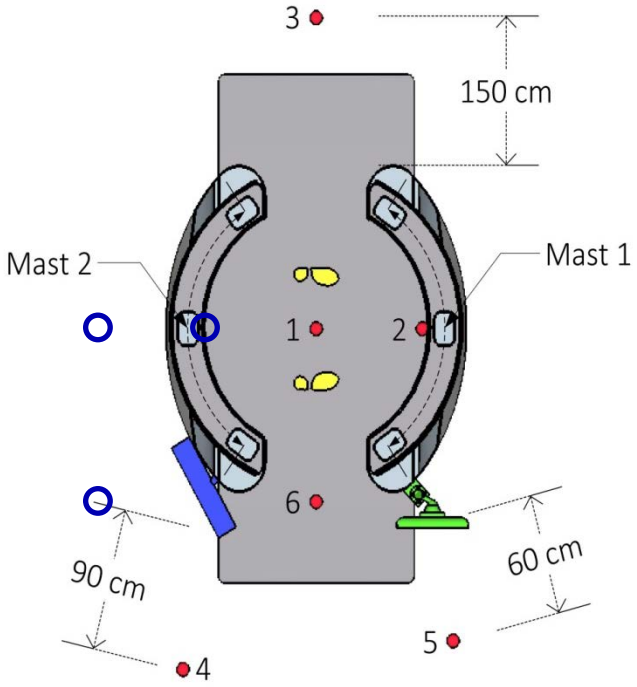

Figure D.3: This is a top down view of the AIT-2. The exposure times are calculated for location 1 (center of the AIT-2), location 2 (inner wall of the AIT-2) and location 6 (at the exit gate of the AIT-2) shown using red dots encircled with blue rings. These three locations were chosen because they received the highest in-band emission levels based on results from appendix E.

D.2.i Exposure time at location 2

The pulse exposure time at location 2 was estimated by: 1) calculating the arc length that the mast travels while directly irradiating the PMED within its beam width, and 2) calculating the

height of the portion of the mast which contains antennas that can directly irradiate the PMED. The arc length that is travelled by the mast while it irradiates the PMED was calculated using the geometric considerations illustrated in figure D.4, which shows a top down view of the AIT-2. The center of the AIT-2 is at point O. The center of the PMED, which is shown as a 10 cm long line E'E) is situated at point P. The mast sweeps along its 120^0 arc, through points T', C', M, C, and T. The mast clearly irradiates the PMED, while it sweeps between points C' and C, because the bore sights of its antennas pass through portions of the PMED. As the mast moves out of the arc between C and C', it continues to irradiate the PMED due to its wide beam width. However, there is a point T (or T') where the PMED stops being within the beam width of the antennas of the mast. The arc length between T and T' was numerically determined to be about 32 cm using the geometry of the problem defined in figure D.4. For location 2, the line PM is 3 cm long, which is the shortest distance between the PMED and the mast. The length of the PMED, which is line E'E, is 10 cm. The radius of the AIT-2, which is line OM, is approximately 59 cm.

The height of the portion of the mast that irradiates the PMED at location 2 was calculated using the geometric considerations shown in part a of figure D.5. The distance between the mast and the PMED (i.e. D) is 3 cm at location 2. Thus, the height (i.e. H) of the mast that can irradiate the PMED was determined to be 14 cm.

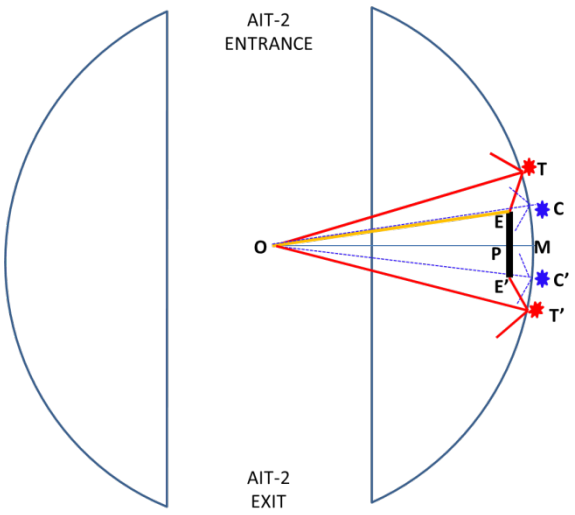

Figure D.4: This is top down view of the AIT-2. The geometrical considerations for calculating the pulse exposure time at location 2 are shown. Point O is the center of the AIT-2. Line E'E shows the PMED at location 2. The mast sweeps along an arc that passes through points T', C', M, C, and T; at each of these points, the beam width of the antennas are schematically illustrated using two lines that emanate from the points.

The mast travels along an approximately 1.23 meters long arc length. There are 224 vertical scan lines. As the mast sweeps through its arc, vertical scan lines are activated approximately every 0.5 cm (i.e. 1.23 meters / 224). Therefore, the PMED at location 2 sees 32 cm/0.5 cm = 64 vertical scan lines. Within each vertical scan line, the PMED at location 2 sees a portion of the mast that is just 14 cm long. This means the PMED at location 2 is irradiated by at most 14

antennas. Each of the antennas emits two consecutive 8.08 µs pulses with a 70 % duty cycle. The PMED at location 2 gets exposed to 14 x 64 x 2 = 1,792 pulses. This means the PMED at location 2 is exposed to about 10 ms of the mmW chirp radiation produced by the AIT-2 during one scan. This is considering only the exposure to radiation from the mast closest to the PMED at location 2.

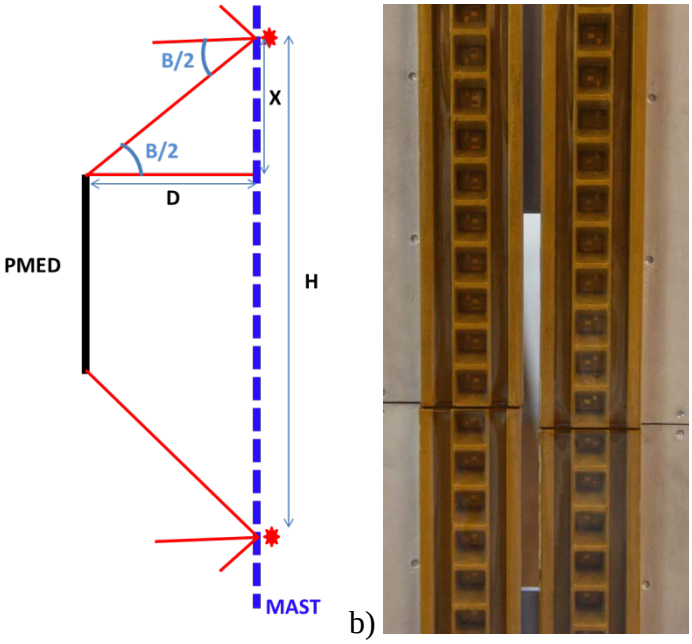

a) b)

Figure D.5: a) This is a schematic side view of the mast of the AIT-2, in which the antennas would be emitting waves to the left of the dotted blue line. The geometrical considerations to calculate the height (i.e. H) of the mast that can irradiate the PMED are shown. B is the beam width of the antennas. D is the distance between the PMED and the mast. b) This is a picture of the transmitting vertical array of antennas (left) and the receiving vertical array of antennas (right) on one of the masts of the AIT-2.

D.2.ii Exposure time at location 1

The pulse exposure time at location 1 was estimated by: 1) considering the number of vertical scan line emissions that directly irradiate the PMED, and 2) calculating the height of the portion of the mast containing antennas that can directly irradiate the PMED. The bore sight of the antennas of the AIT-2 always passes through location 1. Therefore, the PMED at location 1 is irradiated by all the 224 vertical scan lines as the mast travels along its approximately 1.23 meters arc length. The second calculation is carried out using the geometric consideration shown in part a of figure D.5. At location 1, the PMED is about 59 cm away from the mast. Therefore, the PMED at location 1 is irradiated by a portion of the mast that is about 92 cm long. In other words, the PMED at location 1 is irradiated by at most 92 antennas.

The PMED at location 1 sees 224 vertical scan lines from one of the masts. Therefore, the PMED sees 224 x 92 = 20,608 “antennas irradiating it”, as the mast swings by it once. This means that the PMED gets exposed to 20,608 x 2 = 41,216 pulses with a period of 8.08 µs and a

duty cycle of 70 %. The PMED at location 1 is exposed to 41,216 x 5.59 μs ~ 0.23 s of mmW chirp radiation produced by one of the AIT-2 masts during a single scan.

D.2.iii Exposure time at location 6

The calculation of the pulse exposure time of the PMED at location 6 is more complicated due to the geometry of the problem. Therefore, only a conservative upper limit is estimated. The PMED at location 6 can be irradiated by a portion of the mast that is as high as 1.7 meters long; this is assuming that the distance between the PMED and the mast can be as large as the diameter of the AIT-2. The PMED at location 6 is also assumed to be irradiated by all of the vertical scan lines that the mast generates over its 1.23 m long path (i.e. 224 vertical scan lines). Therefore, the PMED at location 6 can see as many as 224 x 170=38,080 "antennas irradiating it". This is equivalent to 38,080 x 2 = 76,160 pulses, or 76,160 x 5.59 μs ~ 0.43 s of mmW chirp exposure. Once again, this is a conservative estimate for the pulse exposure time of the PMED at location 6, to the radiation from just one of the masts.

D.3 Summary

Location 1 and location 6 are symmetrically situated between the two masts. Therefore, the above exposure time values, which are calculated for mast 1, directly apply to the other mast. On the other hand, the conservative estimates for location 6 can be used as a conservative estimate of the pulse exposure time at location 2 from the mast further away from it; because, location 2 is roughly a diameter away from the other mast, which is not close to it. Table D.1 summarizes the results of the pulse exposure time calculations for locations 1, 2, and 6, at a height of 1 m from the ground. The in-band emission peaks at location 2, and it progressively decreases at location 1 and location 6 which are generally further away from the mast. Therefore, the pulse exposure time for the strongest emission levels is 10 ms at location 2. Please see appendix E for more details about the relative magnitudes of the in-band emission levels at the different locations.

All of these exposure time calculations are done for a PMED with a size of 10 cm by 10cm. Appendix E provides a very conservative upper bound for the energy density at each of the six emission measurement locations. The upper bound calculation assumes that the exposure time (for a human or a PMED) is equal to the total number of pulses emitted from both masts (i.e. 171,584) times 5.59 μs, which is about 0.96 s. The calculation also assumes that all of those pulses produce the maximum electric field produced by the strongest among them. The exposure time results in this appendix are all smaller than 0.96 s. This shows that the energy density upper bound estimates in appendix E are indeed conservative.

Location	Number of antennas from mast 1 that irradiate the 10 cm by 10 cm PMED	Arc length travelled by mast 1 while it is irradiating the PMED	Number of pulses received from mast 1 during 1 scan	Duration of mmW chirp received from mast 1 during 1 scan	Duration of mmW chirp received from mast 2 during 1 scan
1	92	1.23 meters	41,216	0.23 s	0.23 s
2	14	32 cm	1,792	10 ms (mast closer to location 2)	< 0.86 s (mast further from location 2)
6	< 170	< 1.23 m	< 76,160	< 0.43 s	< 0.43 s

Table D.1: This summarizes the pulse exposure time calculations. These apply to a 10 cm by 10 cm PMED situated at 1 meter height above the ground, which is the height that would have the worst case exposure time. The results for location 6 are based on a conservative upper bound estimate. The PMED at location 2 is situated asymmetrically between the two masts; therefore, its exposure time depends on the mast that is considered. Location 1, 2, and 6 are shown in figure D.3.

Appendix E

AIT-2 in band emission measurements

E.1 Background of mmW AIT-2 system

The AIT-2 has two masts that contain antenna arrays. The masts are located inside acrylic shields on opposite sides of the stage where a person stands for imaging, as shown in figure E.1. During the normal scanning operation of the AIT-2, the masts are physically rotated in a 120^{o} arc in less than 1.5 s. Each mast consists of a vertical array of 192 transmitting antennas (12 boards containing 16 antennas each). Each mast also contains 192 receiving antennas to the right of the 192 vertically arranged transmitting antennas. As the masts physically rotate, 224 vertical scan lines are activated. A vertical scan line involves a top down activation of the 192 transmitting antennas of the masts. During a vertical scan line, the top most transmitting antenna is activated for 8.08 µs. The rest of the 191 antennas are activated for 16.16 µs each, as they emit two consecutive 8.08 µs pulses whose amplitude profile is identical. Therefore, a single vertical scan line takes 191 x 2 x 8.08 µs + 1 x 1 x 8.08 µs =3.095 ms. Each of the 224 vertical scan lines are triggered by sensors that sense the physical location of the masts as they rotate in the 120^{o} arc. These sensors are spaced with a gap of about 0.5 cm throughout the arc path of the masts. During the beginning of the 8.08 µs pulses, the transmitting antenna sweeps from 24.25 GHz to 30 GHz in 5.59 µs. Therefore, the duty cycle of each of the 8.08 µs pulses is about 70 %.

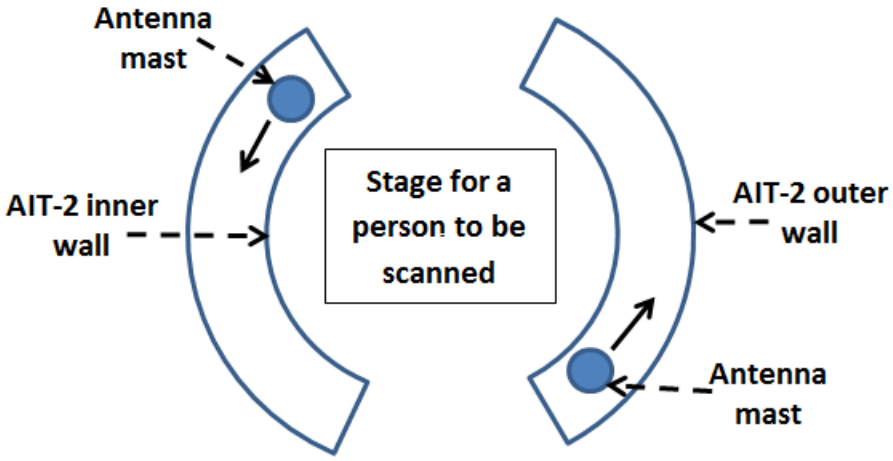

Figure E.1: Top view of the AIT-2 scan area showing direction of the antenna mast movement in one pass. The person who is scanned stands in between the two masts.

Figure E.2 shows pictures of the antennas on one of the masts of the AIT-2. These antennas are covered by a radome, and the distance between their rectangular aperture and the interior Plexiglas walls of the AIT-2 is about 2.8 cm. Each of the antennas is 8.5 mm by 9.5 mm. This means that the interior of the AIT-2 system, which is at least 2.8 cm away from the antennas, is within their far field; this is based on the Fraunhofer distance ($2D^2/\lambda$) of the antennas at the

relevant in-band frequencies (i.e. 24.25 GHz to 30 GHz). Part b of figure E.2 shows three of the vertically arranged transmitting antennas to the left of two of the vertically arranged receiving antennas. Note that the transmitting antennas are vertically shifted up by half of the vertical antenna dimension; this explains why the top most transmitting antenna is only activated for 8.08 µs during a vertical scan line, as opposed to the other 191 antennas that emit two consecutive 8.08 µs pulses.

a) 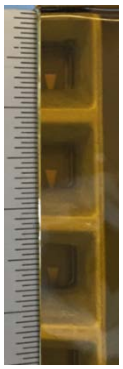 b) 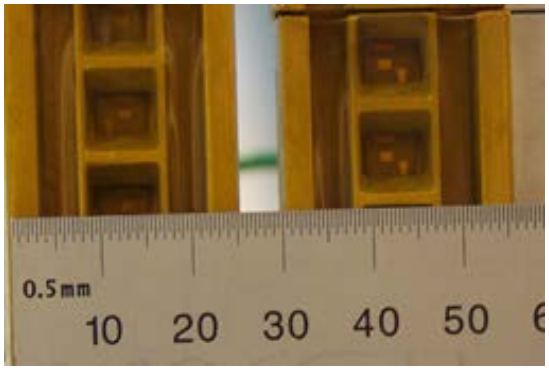

Figure E.2: The antennas in the AIT-2 system are 9.5 mm high vertically (see part a) and 8.5 mm (see part b) wide horizontally. Part b shows the transmitting (left) and receiving (right) antenna arrays next to each other.

E.2 Detection system to measure in band emissions from the AIT-2

A detection system was assembled at the FDA CDRH to measure the in-band emissions (i.e. 24.25 GHz to 30 GHz) from the AIT-2. The detection system consisted of equipment listed in table E.1. Figure E.3 illustrates how the detection system is assembled. The detection system captured the mmW signals emitted from the mast of the AIT-2 using either the horn antenna or the Open Ended Wave Guide (OEWG). The choice between the horn antenna and the OEWG was made based on the distance between the measurement point and the AIT-2 mast. Table E.2 shows the distances where the far fields of the three antennas start for the relevant frequency range. The horn antenna was used when the measurement point is farther than 44 cm from the AIT-2 mast, which guarantees that both the transmitting and receiving antennas are within each other's far field. On the other hand, the OEWG could be placed as close as 2 cm away from the AIT-2 mast, and both the transmitting and receiving antennas would be within each other's far field. The AIT-2 mast is enclosed inside the Plexiglas walls, hence, the closest measurement point to the AIT-2 mast is 2.8 cm away from the mast, which is a distance greater than the Fraunhofer distance of both the OEWG and the AIT-2 transmitting antennas. To summarize, the OEWG was used to make measurements at locations that are too close to the AIT-2 mast (i.e. less than 44 cm) where the far field gain of the horn antenna cannot be used. The smallest distance between a point in the interior of the AIT-2 and the mast is approximately 3 cm; at such a small separation distance, even the near field gain of the horn could not be used to make a measurement.

The OEWG is WR28 and not WR34, which would be ideal for the 24.25 GHz to 30 GHz frequencies generated by the AIT-2. However, WR34 OEWG could not be found for purchase as they are extremely rare. WR28 OEWG is specified to work between 26.5 GHz to 40 GHz; this fact was taken into consideration when interpreting the data collected using the WR28 OEWG.

Component	Brand / Model & Serial #	Purpose	Settings
Horn Antenna	Pasternack, PE9851-20, WR34, 20 dB Gain Horn Antenna.	Captured radiated signals at distances greater than ~ 44 cm from the AIT-2 masts.	Oriented for vertical polarization.
Open Ended Wave Guide (OEWG)	WR28, L shaped probe.	Captured radiated signals at distances less than ~ 44 cm from the AIT-2 masts.	Oriented for vertical polarization.
Low Noise Amplifier (LNA)	Miteq LNA, AMF-4F-20003000 29-10P-HS, 20-30 GHz, 27 dB gain, and 10 dBm output (min). SN: 1812845.	Amplified weak signals picked up by the antenna.	A heat sink was attached to the LNA.
Power supply for LNA	HP Power supply, 6216C, 0-25 V, 0-0.4 A. SN: 2805K-00885.	Powered the LNA.	15 V, and maximum current settings. + and – were connected to + and GND of the LNA respectively.
Diode detector	Krytar Diode Detector, 203BK, 0.01-40 GHz. SN: 00262.	Detected the envelope of the mmW signal picked up by the antenna, and amplified by the LNA.	The maximum power it can handle was 20 dBm.
Amplifier	Tektronix Differential Amplifier, AM 502. SN: B091755.	Amplified the voltage signal output by the diode.	The gain was 100. LF and HF are adjusted to create a

Component	Brand / Model & Serial #	Purpose	Settings
			pass band of .1 Hz – 1 MHz.
Oscilloscope	Agilent Four Channel Digital Storage Oscilloscope, 9104A, 1 GHz, 20 GSam. SN: MY51260124.	This read the output of the differential amplifier.	The voltage scale was dynamically adjusted based on signal strength.

Table E.1: List of components of the mmW detection system.

As shown in figure E.3, the horn antenna or the OEWG was connected to the LNA to amplify the received mmW signals. The output of the LNA was fed to the diode detector. The diode detector outputted a voltage signal that represented the envelope of the captured mmW signal. The voltage signal from the diode detector was amplified by the amplifier, and measured by the oscilloscope. There was a custom made 700 Ω resistor in parallel with the diode, followed by a BNC cable feeding into the 1 MΩ input impedance (+) port of the amplifier. There were two competing objectives which resulted in the use of the 700 Ω resistor as an optimum solution. The first objective was achieving high sensitivity to the voltage signals to be measured. High sensitivity could be accomplished by directly connecting the output of the diode to the port of the amplifier/oscilloscope with 1 MΩ input impedance. The second objective was achieving a very short response time (much smaller than 5.59 μs) to accurately measure the pulse with 8.08 μs period and 70 % duty cycle. If the response time is not short enough, the 5.59 μs long "on" time of the 8.08 μs pulse will have a distorted shape. The response time is determined by the effective RC constant of the diode and resistors connected to it before the measurement point. A very short response time could be achieved by connecting a 50 Ω resistor in parallel with the diode, followed by a BNC cable feeding into the 1 MΩ input impedance port of the amplifier/oscilloscope; however, this would significantly reduce the sensitivity. The compromise between these two competing objectives was to use the custom made 700 Ω resistor as described above. This achieved acceptable levels of sensitivity and response time.

Antenna	Dimensions	Fraunhofer distance ($2D^2/\lambda$) at λ=1 cm (f=30 GHz)
AIT-2 transmitting antenna	9.5 mm by 8.5 mm	~ 2 cm
WR34 horn antenna	35.56 mm by 47.24 mm	~ 44 cm
WR28 OEWG	7.112 mm by 3.556 mm	~ 1 cm

Table E.2: The Fraunhofer distance shows where the far field region of an antenna starts. This shows the maximum Fraunhofer distance of the three antennas for the relevant frequency range, which is 24.25 GHz to 30 GHz.

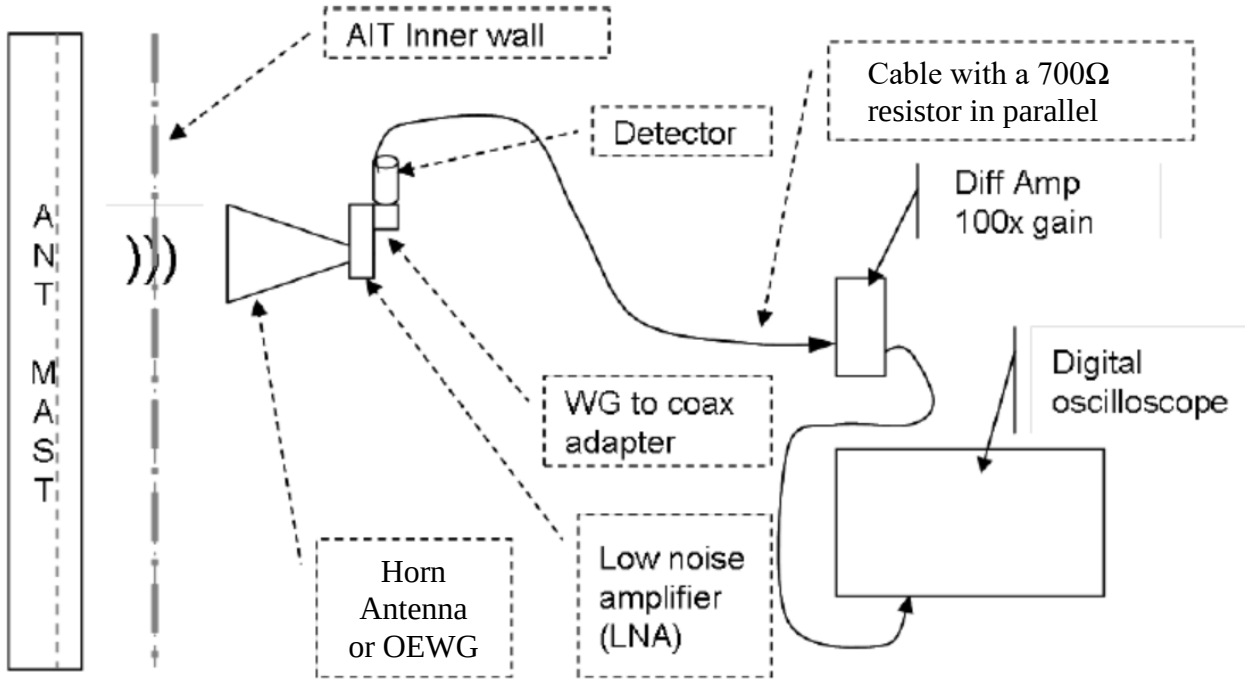

Figure E.3: The mmW detection system is illustrated. The detection system used a horn antenna or OEWG, depending on the measurement distance, to measure emissions from the AIT-2 mast. The antenna was connected to the LNA, the diode detector, the amplifier, and oscilloscope, in this order.

The oscilloscope of the detection system was connected to a computer recording the voltage signals. Figure E.4 shows an example of a recording using the detection system. The horn antenna was placed 170 cm above the ground at location 1. Location 1 is the center of the AIT-2 which is about 59 cm from the mast. Please see appendix C for more details about the locations and heights for the emission measurements.

Figure E.4 has five parts (a-e) that also illustrate the normal scanning operation of the AIT-2, which is described in appendix E.1 above. Part a shows 35 of the 224 vertical scan lines that are triggered as the masts rotate in their 120^{o} arc; a similar measurement with the OEWG, which has a broader beam width than the horn, proved that there are a total of 224 vertical scan lines and that the total duration of the AIT-2 scan is about 1.324 seconds. The amplitude of the signal from the vertical scan lines increases as the mast moves closer to the bore sight of the horn antenna of the detection system. The amplitudes decrease as the mast moves past the bore sight. The strongest pulses recorded are highlighted in red throughout the five parts of figure E.4 for easy comparison. Part b of figure E.4 shows a zoomed in picture of the three strongest vertical scan line signals. The separation between two vertical scan lines is roughly about 3.62 ms as the

masts move past the mid-point of their 120^{o} arc based on figure E.4 part b. As discussed in appendix E.1 above, a single vertical scan line is known to last for 3.095 ms, and the time gap between the start of consecutive vertical scan lines depends on the instantaneous speed of the mast along its 120^{o} arc.

Part c of figure E.4 shows pulses from a single vertical scan line. A vertical scan line consists of a top down firing of the vertical array of transmitting antennas on the AIT-2 mast. Part c shows that the amplitude of the signals generally depends on the vertical distance between the AIT-2 antennas and the bore sight of the receiving horn. The maximum signal amplitude is recorded during emission from the antenna closest to the bore sight of the receiving horn. Part d of figure E.4 illustrates that each of the transmitting AIT-2 antennas emit two consecutive pulses that look identical based on their amplitude profile; this fact is also discussed in appendix E.1 above. Part e zooms in on the strongest pair of 8.08 µs pulses recorded from one of the AIT-2 antennas, which must have been most aligned with the bore sight of the receiving horn. Part e further zooms in on the 8.08 µs pulses with roughly 70% duty cycle.

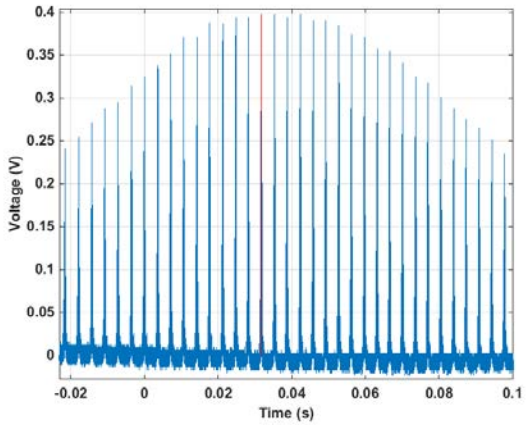

a) 35 vertical scan lines were captured as the masts rotate; the vertical scan line with the strongest signal is highlighted in red.

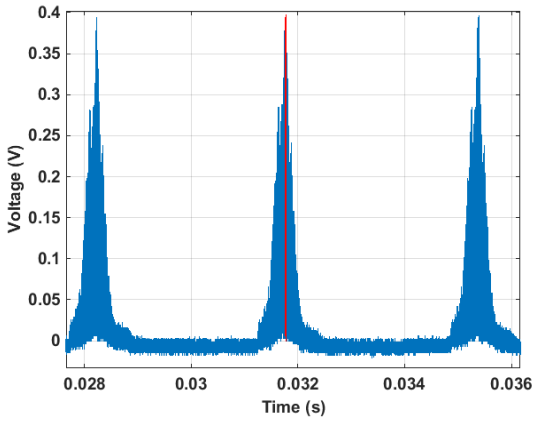

b) The signals from the three strongest vertical scan lines are shown closely after zooming in on the data.

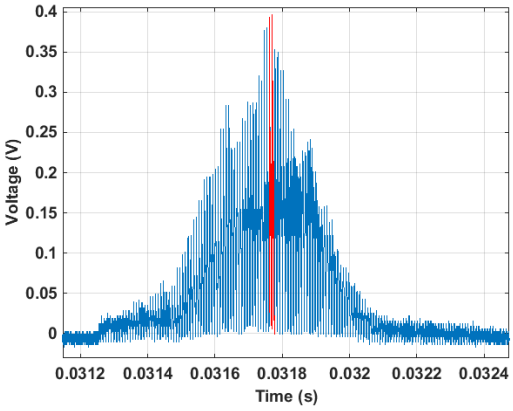

c) Further zooming shows the pairs of identical pulses emitted by each of the antennas activated top down during a vertical scan line.

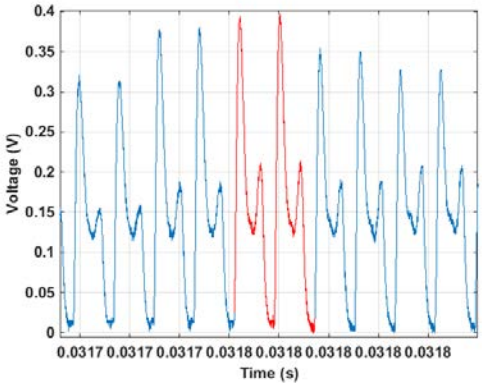

d) The pair of pulses emitted by the antenna whose bore sight was aligned with the receiving horn antenna is shown. These are the strongest measured pulses at this location and height, and they are almost identical based on their amplitude profile.

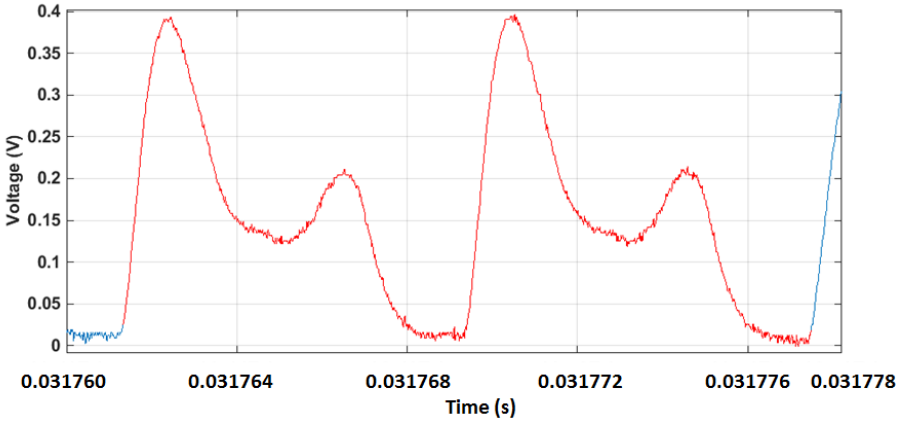

e) Finally, a close up view of the pair of pulses in part d is provided.

Figure E.4: These are signals recorded by the detection system (with horn antenna) at location 1, and 170 cm height from the ground, during the normal scanning operation of the AIT-2.

E.3 Calibration of the detection system to measure in band emissions from the AIT-2

The electric field strength is the crucial parameter to assess the safety of PMEDs and humans exposed to the AIT-2 in-band emissions. The detection system directly provided voltage signals such as the ones shown in figure E.4. A calibration experiment was designed to deduce the root mean square (RMS) power (in mW) received by the LNA of the detection system during the 5.59 µs long "on" time of the 8.08 µs pulse, given the voltage signals (in mV). This RMS power value can be used to calculate the RMS electric field strength at the aperture of the receiving antenna, given the appropriate gain of the antenna. The calibration experiment involved directly injecting signals (with known RMS power and frequency) to the LNA of the detection system, and recording the peak-to-peak amplitude of the voltage output of the detection system at the oscilloscope. Figure E.5 shows a schematic of the calibration experiment. The Agilent MXG Analog Signal Generator with model number N5183A and SN MY50140921 was used; the signal generator works over the range of frequencies between 100 kHz and 40 GHz. The antenna of the detection system (horn or OEWG) is not part of this calibration. All other components of the detection system, which are discussed in appendix E.2, were part of the calibration.

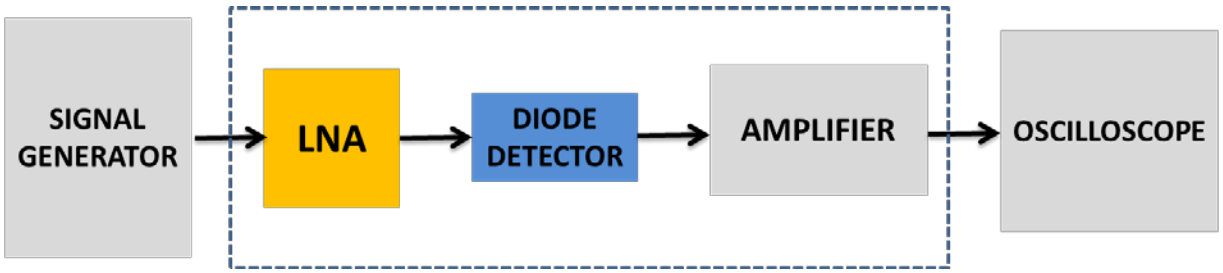

Figure E.5: Schematics of the experiment to calibrate the detection system. The dotted box shows the set of components that were calibrated.

The signal generator was programmed to output a rectangular pulse modulated signal that emulates the envelope of the in-band signal from the AIT-2. In particular, a pulse with 8.08 µs period and 70 % duty cycle was generated. The RMS power and center frequency of the pulse modulated signal were systematically varied using the signal generator. The center frequency was varied from 24.25 GHz to 30 GHz in increments of 0.25 GHz. For each of these frequencies, the RMS power of the pulse modulated signal was varied from -20 dBm to 10 dBm in increments of 2 dBm. These signals passed through a coax cable and a 40 dB attenuator, which have a combined loss of about 42 dB, before reaching the LNA. The insertion loss of the coax cable and the 40 dB attenuator was characterized in a separate experiment, and the results are shown in figure E.6. The signals, from the signal generator in figure E.5, got amplified by the LNA, and the diode detector extracted the rectangular envelope of the mmW signals it received. The output of the diode was amplified by the amplifier and recorded by the

oscilloscope. The settings shown in table E.1 were maintained for the components of the detection system, during the calibration. The peak-to-peak amplitude of the rectangular voltage pulses (with 8.08 µs period and 70 % duty cycle) was measured.

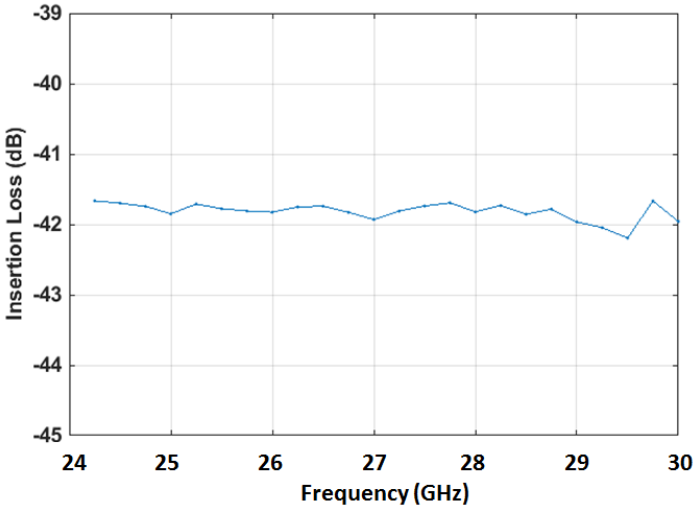

Figure E.6: The combined insertion loss of the coax cable and the 40 dB attenuators in between the signal generator and the LNA during the calibration of the detection system.

For each center frequency, the RMS power (in mW) fed to the LNA (during the "on" time of the 8.08 µs pulse) was plotted as a function of the peak-to-peak amplitude of the voltage (in mV) measured by the scope. Examples of these plots are shown for representative center frequencies (25 GHz, 27 GHz, 29 GHz and 30 GHz) in figure E.7. The RMS power fed to the LNA was determined by using the information from the power settings of the signal generator, and the measured insertion loss between the generator and the LNA (see figure E.6). Therefore, the RMS power fed to the LNA roughly varied between -62 dBm to -32 dBm in increments of 2 dBm (corresponding to the -20 dBm to 10 dBm power ramp executed in the signal generator, and approximately 42 dB insertion loss shown in figure E.6). Figure E.7 shows that a second degree polynomial fit describes the relationship between the RMS power during the "on" time of the 8.08 µs pulse (in mW) and the peak-to-peak voltage (in mV) measured in the oscilloscope, for each of the representative frequencies.

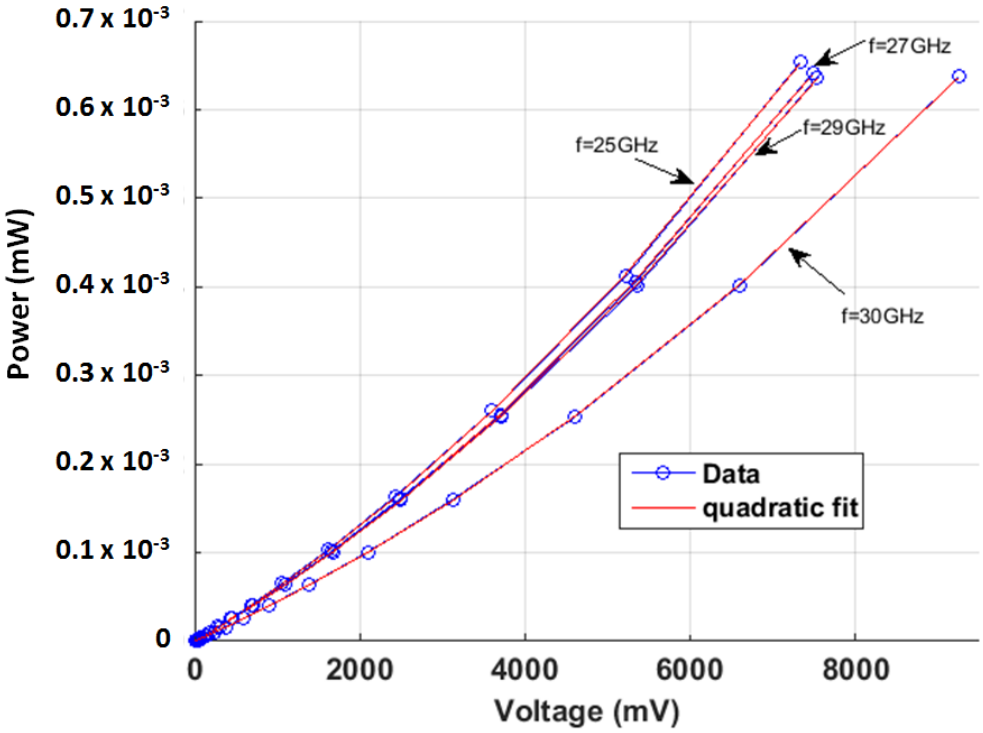

Figure E.7: This shows the RMS power (mW) fed to the LNA vs the peak to peak voltage (mV) determined from the scope. The calibration was done for center frequencies ranging from 24.25 GHz to 30 GHz in increments of 0.25 GHz; here, the data from only four representative frequencies are shown for simplicity. The data and its quadratic fit are shown.

The second degree polynomial fit was done for all the data collected at different frequencies (i.e. 24.25 GHz to 30 GHz in increments of 0.25 GHz). The three coefficients ('a', 'b', and 'c') of the fits are shown as a function of frequency in figure E.8. These coefficients enable the prediction of the RMS power (mW) fed to the LNA (during the "on" time of the 8.08 μs pulse) given the voltage (mV) read from the oscilloscope of the detection system, for a given frequency of mmW. This is the goal of the calibration experiment shown in figure E.5. The experiment produced a frequency dependent conversion mechanism from the instantaneous voltage (mV) measured by the oscilloscope of the detection system to the RMS power (mW) received by the LNA of the detection system.

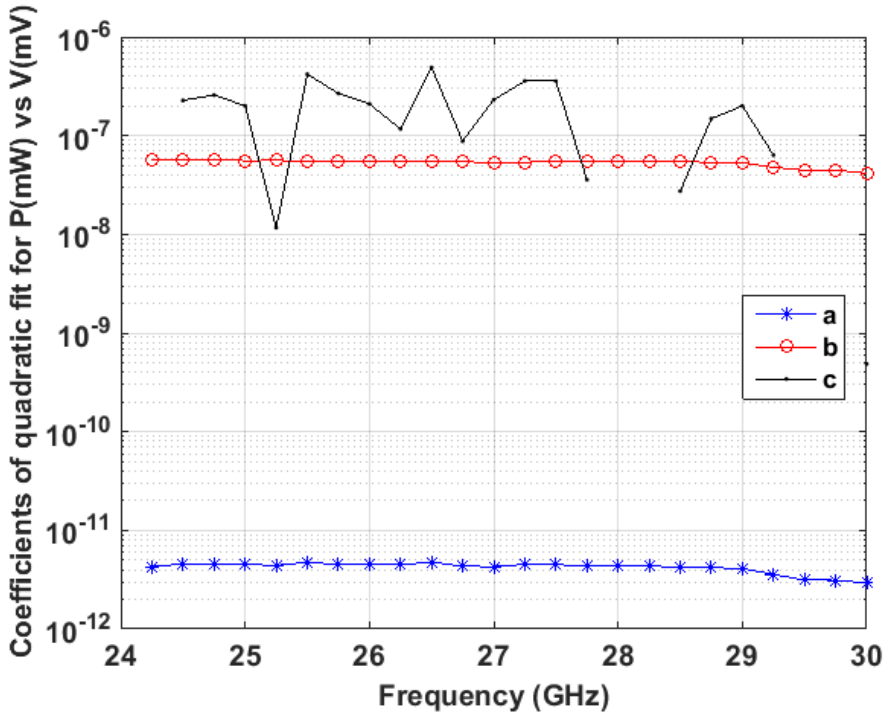

Figure E.8: These are the three coefficients of the second degree polynomial fit as a function of frequency. The fit was based on the power (mW) vs voltage (mV) plots shown in figure E.7. The 'a', 'b', and 'c' coefficients are associated with the quadratic, linear and constant terms of the second degree polynomial fit respectively.

E.4 Using the detection system to measure in band emissions from the AIT-2

The detection system that is illustrated in figure E.3 measured voltage vs time plots shown in figure E.4. Each of the instantaneous voltage (mV) values in figure E.4 corresponds to a unique mmW frequency generated by the AIT-2; because, the AIT-2 generates a chirp ramping from 24.25 GHz to 30 GHz within the first 5.59 µs of the 8.08 µs pulses. The appropriate calibration coefficients shown in figure E.8 can be used to determine the RMS power (mW) at the LNA (during the on time of the 8.08 µs pulse) given the voltage (mV) measured by the oscilloscope of the detection system. The antenna that is attached to the LNA of the detection system can be horn antenna or OEWG; as discussed in appendix E.2, the antenna that enabled a far field measurement of the radiation was selected. The relevant far field gain of the detection antenna can be used to calculate the power density at the antenna aperture using equation E.1. The equation shows that the power density (P_d) at the aperture of the antenna (i.e. either the horn or the OEWG) is the ratio of the RMS power received at the LNA during the "on" time of the pulse (P_{LNA}) to the effective aperture (A_e) of the antenna. The effective aperture of the antenna (i.e. either the horn or the OEWG) can be determined from relevant far field gain (G) and the relevant wavelength (λ). In equation E.1, the power density is in W/m^2, the P_{LNA} is in W, the gain is linear (as opposed to in dB), and the wavelength is in m. The far field gain of the WR34 horn antenna is 20 dBi (i.e. G=100), where the unit dBi emphasizes the comparison with an isotropic antenna. The far field gain of the OEWG is estimated to be approximately 5 dBi (i.e. G=3.16)

based on theoretical formulas and experimental results for the relevant frequency range of 24.25 GHz to 30 GHz. [14]

$$P_d = \frac{P_{LNA}}{A_e} = \frac{P_{LNA}}{G\lambda^2/4\pi}$$

Equation E.1

The power density (P_d) in W/m^2 at the aperture of the detection antenna (i.e. the horn or the OEWG) can be used to calculate the rms electric field strength (E) in V/m using equation E.2. The RMS electric field strength is the important parameter to characterize the in-band emission of the AIT-2. This parameter can be calculated as a function of frequency for the 5.59 µs chirp signal emitted by the AIT-2.

$$E = \sqrt{120\pi P_d}$$

Equation E.2

The representative voltage vs time data shown in figure E.4 is used to illustrate how the electric field strength was computed. Part a of figure E.9 shows one of the two pulses emitted by the antenna of the AIT-2 closest to the bore sight of the detection horn, which was located 170 cm from the ground at location 1 (center of the AIT-2). These instantaneous voltage (mV) values were used to calculate the RMS power (mW) values at the LNA of the detection system. This was done by using the second order polynomial fit coefficients shown in figure E.8. In particular, aV^2+bV+c is the RMS power (in mW) corresponding to an instantaneous voltage V (in mV) detected by oscilloscope of the detection system. The fit coefficients 'a', 'b', and 'c' are a function of frequency; therefore, the time from 0 µs to 5.59 µs should be mapped to frequencies ranging from 24.25 GHz to 30 GHz, based on the properties of the AIT-2 chirp emissions. The resulting power (mW) vs time signal is shown in part b of figure E.9.

a)

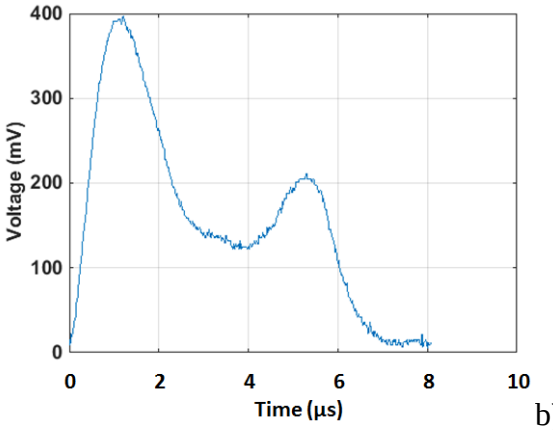

b)

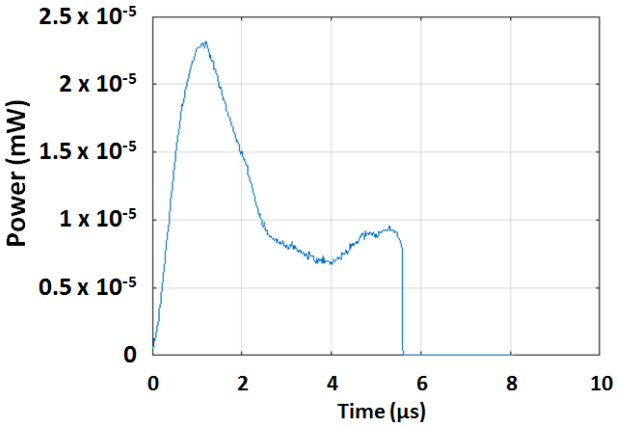

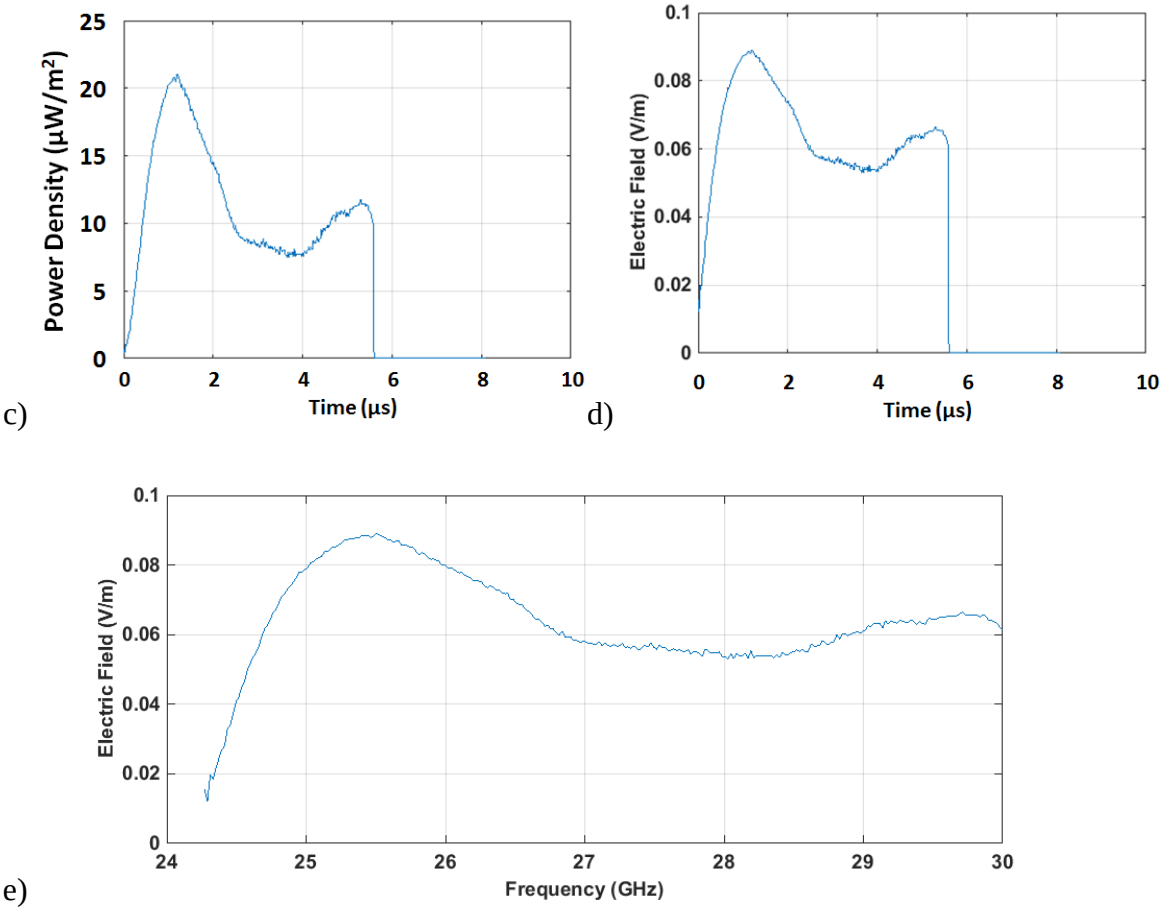

Figure E.9: These figures illustrate how the voltage vs time pulse captured from the oscilloscope of the detection system was analyzed to produce the relevant electric field strength parameter as a function of frequency. One of the pulses shown in part e of figure B.4 were used for this illustration (i.e. the pulse was measured 170 cm above the ground at location 1). a) voltage vs time captured by the oscilloscope. b) Power at the LNA of the detection system as a function of time. c) The power density at the aperture of the detection antenna (horn). d) The electric field strength at the aperture of the detection antenna as a function of time. e) The electric field strength at the aperture of the detection antenna as a function of frequency of the mmW emission.

The power received at the LNA of the detection system can be used to determine the power density at the aperture of the detection antenna. For the measurement at location 1, the horn antenna was used; because, location 1 was far enough (i.e. >44 cm) from the radiating antennas of the AIT-2 guaranteeing a far field measurement. Therefore, the linear far field gain of the WR34 horn antenna, which is 100, was used in equation E.1 to calculate the power density. The resulting power density vs time signal is shown in part c of figure E.9. The corresponding RMS electric field strength vs time signal is shown in part d using equation E.2. There is a 5.59 μs chirp, which ramps from 24.25 GHz to 30 GHz, at the beginning of the 8.08 μs pulse from the AIT-2 antenna. Therefore, the RMS electric field strength can also be mapped to a frequency axis, as in part e of figure E.9.

The data analysis illustrated in figure E.4 and figure E.9 was for the measurement at location 1 (center of AIT-2), 170 cm above the ground. The measurement was done using the horn antenna. There were 24 similar measurements done at 6 locations and 4 heights using either the horn antenna or the OEWG, depending on the distance from the AIT-2 antennas. The rationale for the choice of these locations and heights for the in-band emission measurement is discussed in appendix C in detail.

E.5 Summary of in-band emissions from the AIT-2

The electric field strength (in V/m) was measured at 24 emission measurement points (distributed over 6 locations and 4 heights) in and around the AIT-2, as a function of frequency ranging from 24.25 GHz to 30 GHz. The 6 locations and 4 heights are shown in figure E.10. Please see appendix C for discussion of the rationale for choosing these 24 (i.e. 6 locations x 4 heights) emission measurement points.

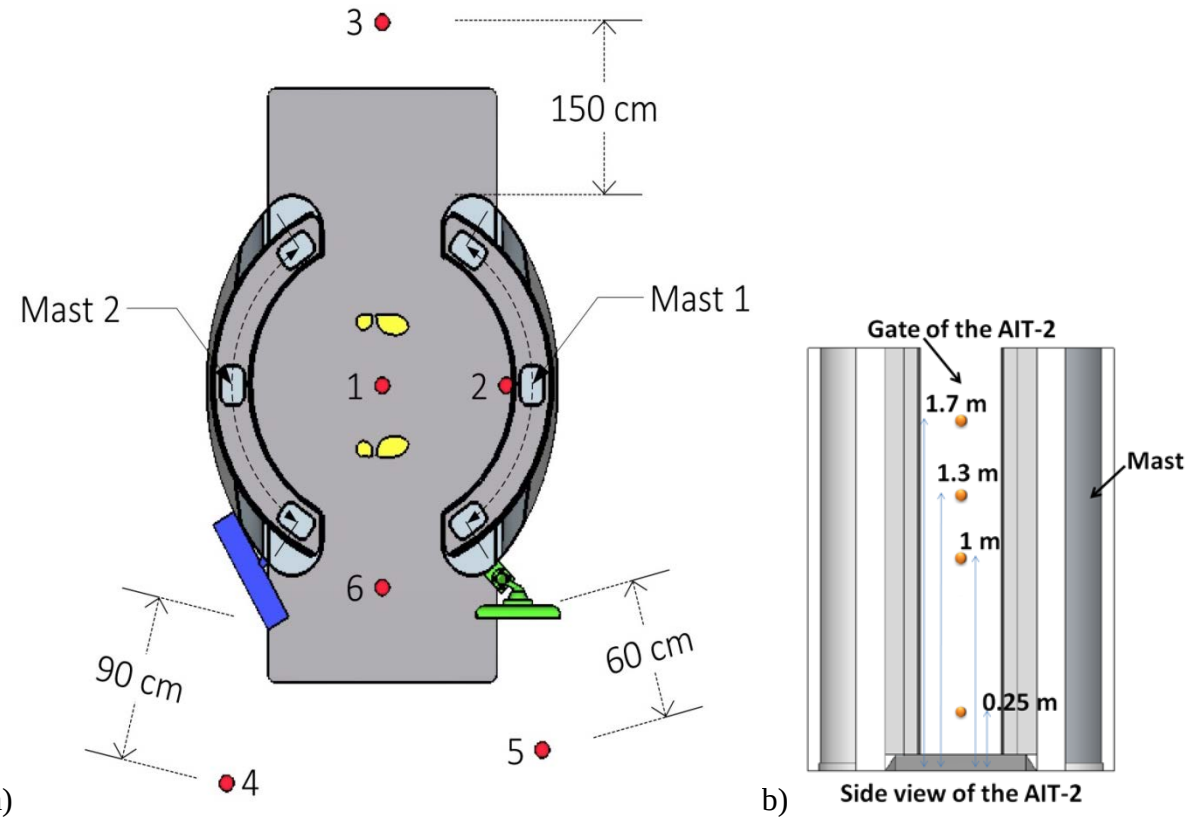

Figure E.10: These two schematics define the 24 emission measurement points distributed at 6 locations and 4 heights. a) This is the top view of the AIT-2, depicting the six locations in and around the AIT-2 chosen to perform the in-band emission measurements. The UPS is shown to the left of location 6 in blue, and the AIT-2 computer monitor is shown to the right of location 6 in green. b) This is the side view of the AIT-2 looking through the gate of the AIT-2. These four heights were chosen to perform the emission measurements at the six locations shown in part a.

The primary goal of the in-band emission measurement was to find out where the maximum electric field strength exists. Figure E.11 shows the variation of the electric field strength at the

6 different locations for each of the 4 heights. Location 2 has by far the strongest electric field strength as it is the closest location to the radiating antennas of the AIT-2 (about 3 cm away). Location 1 has the second largest electric field strength. In general, the electric field strength increases as the distance between the measurement location and the AIT-2 antennas decreases, as expected. Figure E.12 shows the electric fields as a function of the height of the measurement point for all the 6 measurement locations. The electric field does not show significant and / or systematic dependence on the height of the measurement point. Table E.3, table E.4 and table E.5 summarize the maximum, the mean and the minimum electric field values illustrated in figure E.12 and figure E.13.

The maximum, the mean and the minimum electric field values were calculated for each of the strongest measured pulses at each of the 24 measurement points. The strongest measured pulse at any measurement point was selected based on the zooming in process illustrated in figure E.4. Any one of the identical pair of pulses highlighted in red in figure E.4 can be considered as the strongest pulse for that measurement point. As shown in part e of figure E.9., the electric field is a function of frequency ranging from 24.25 GHz to 30 GHz for each of those pulses. Therefore, the maximum, the mean and the minimum electric field value was taken over electric field values corresponding to different frequency values for each of the strongest pulses measured at each of the 24 measurement points. These are the statistics of electric fields presented in tables E.3-5 and figures E.12-13.

Height	Maximum E-field (V/m) at location 1	Maximum E-field (V/m) at location 2	Maximum E-field (V/m) at location 3	Maximum E-field (V/m) at location 4	Maximum E-field (V/m) at location 5	Maximum E-field (V/m) at location 6
25 cm	0.1021	1.548	0.0397	0.0444	0.0385	0.0527
1 m	0.0783	1.433	0.029	0.0397	0.0295	0.0489
1.3 m	0.0892	1.5822	0.0276	0.0363	0.035	0.0487
1.7 m	0.0891	1.3048	0.0273	0.045	0.0406	0.0547

Table E.3: The maximum electric fields shown in figures E.12 and E.13 are summarized for the 24 measurement points distributed over 6 locations and 4 heights.

Height	Mean E-field (V/m) at location 1	Mean E-field (V/m) at location 2	Mean E-field (V/m) at location 3	Mean E-field (V/m) at location 4	Mean E-field (V/m) at location 5	Mean E-field (V/m) at location 6
25 cm	0.0728	1.3804	0.0262	0.029	0.0253	0.0358
1 m	0.0614	1.2666	0.0218	0.0243	0.0195	0.0361
1.3 m	0.0667	1.3164	0.0197	0.0254	0.0231	0.0338
1.7 m	0.0641	1.0821	0.0204	0.0314	0.0278	0.0375

Table E.4: The mean electric fields shown in figures E.12 and E.13 are summarized for the 24 measurement points distributed over 6 locations and 4 heights.

Height	Minimum E-field (V/m) at location 1	Minimum E-field (V/m) at location 2	Minimum E-field (V/m) at location 3	Minimum E-field (V/m) at location 4	Minimum E-field (V/m) at location 5	Minimum E-field (V/m) at location 6
25 cm	0.0077	0.2179	0.0006	0.0044	0.006	0.0004
1 m	0.0008	0.2383	0.0033	0	0	0
1.3 m	0.0057	0.2286	0.0043	0.0004	0.0005	0.0024
1.7 m	0.0121	0.1925	0.008	0.011	0.009	0.0081

Table E.5: The minimum electric fields shown in figures E.12 and E.13 are summarized for the 24 measurement points distributed over 6 locations and 4 heights.

The measurement at location 2 is the most important result as it provides the maximum in-band emission from the AIT-2. For this reason, this measurement was done under special operating mode of the AIT-2, where the radiating masts are fixed at the mid-point of their 120^{o} arc. This mode allows several automated measurements of the in-band emission without having to get the masts moving, which is time consuming. The stationary masts can be programmed to execute any number of 'open-closed calibrations'. Each 'open-closed calibration' takes about 2.6 s. There is about a 1 s software delay before an 'open-closed calibration' action can be repeated. An 'open-closed calibration' involves the software triggering of 224 vertical scan lines down the transmitting antennas of the masts. During the normal scanning operation of the AIT-2, vertical scan lines are triggered based on the location of the masts as they rotate along their semi-circular path. Each vertical scan line, within an 'open-closed calibration' always lasts about 3.1 ms. But, there is a 12 ms software delay in between consecutive scan lines executed during an 'open-closed calibration'. The vertical scan line emissions during the normal operation of the AIT-2 were proven to be the same as the vertical scan line emissions during the special 'open-closed calibration' mode of the AIT-2. The detection system was moved to several heights at location 2 to verify that the emission from the antennas does not depend on the height. It was also verified that the emission levels from both of the masts were the same.

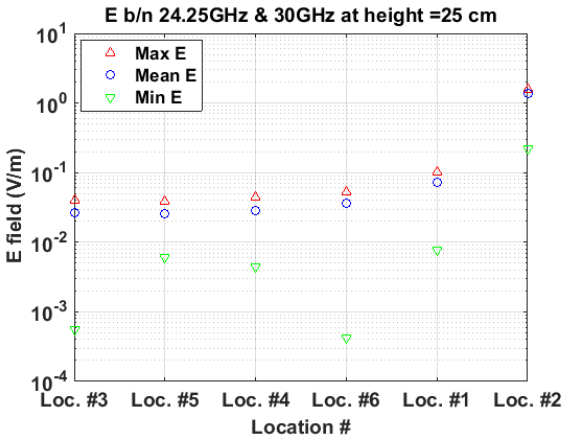

a)

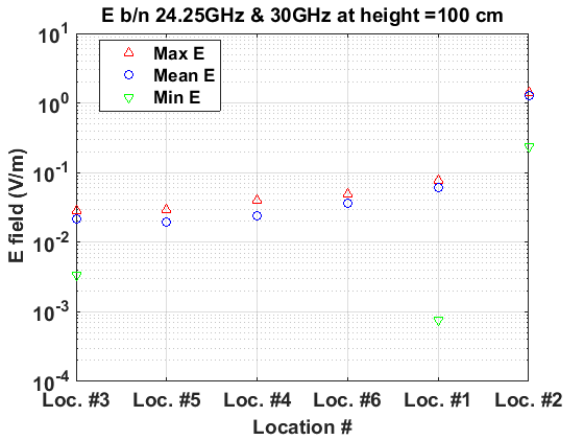

b)

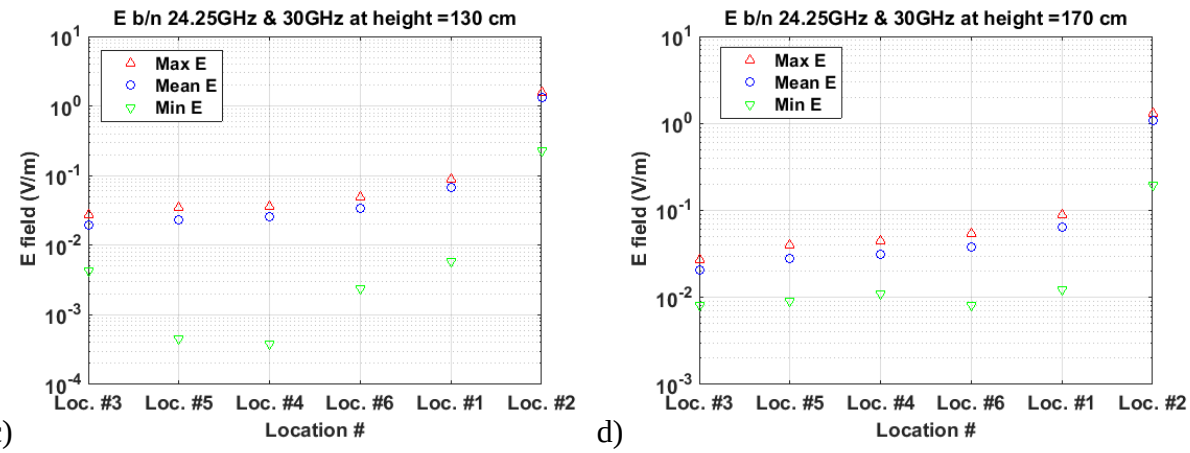

Figure E.11: The maximum, minimum and average electric field was taken over different frequencies for each of the strongest measured pulses (such as the one in part e of figure E.4) at each of the locations and heights. Then, the statistics of the field were plotted vs location for each of the measurement heights. Parts a, b, c, and d correspond to measurements at 25 cm, 100 cm, 130 cm and 170 cm from the ground, respectively.

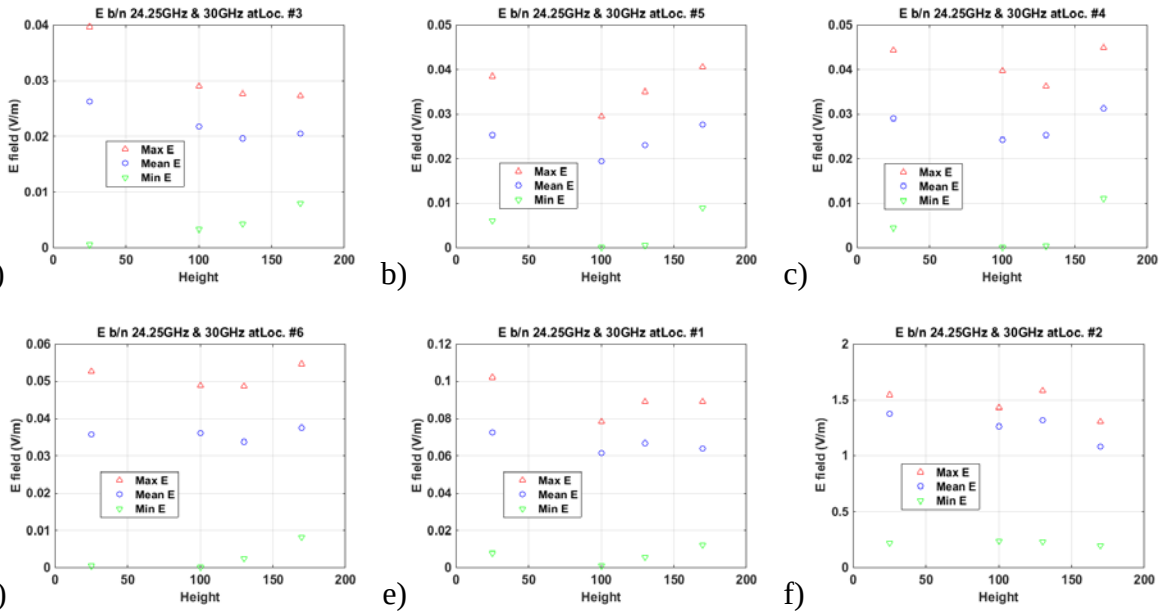

Figure E.12: The maximum, minimum and average electric field was taken over different frequencies for each of the strongest measured pulses (such as the one in part e of figure E.4) at each of the locations and heights. Then, the statistics of the field were plotted vs height for each of the measurement locations. Parts a, b, c, d, e, and f correspond to measurements at locations 3, 5, 6, 4, 1, and 2. The plots demonstrate that the electric field does not have any particular dependence on the height of the measurement point. The fluctuations are explained by the precisions of the measurement that is dependent on the alignment of the detection antenna.

The results obtained in this study generally agree with similar studies, within an order of magnitude. For instance, page 6 of [4] indicates, that the emissions from the AIT have a power density of 1.6×10^{-4} mW/cm^2 in the mmW operating frequency range of 24.25 GHz to 30 GHz at

a distance of 3.5 cm. However, there is no mention of reference points for the 3.5 cm distance measurement. The report states that this power density level is below the US [5] and Canadian [6] limits for human exposure (referenced as 1 mW/cm^2). Regarding the measurement methods, the reference [4] states, "Measurements were gathered with equipment stopped at a specific frequency. Calculations provided here are based on instantaneous peak measurements representing a worst case approach". Based on equation E.2, the reference [4] suggests that the measured electric field is about 0.8 V/m at 3.5 cm from a reference point that is not clearly specified. Part f of figure E.12 shows that the electric field is about 1.5 V/m at location 2, which is 2.8 cm from the aperture of the antennas of the AIT-2 mast. This shows that the results in this study do generally agree with similar studies in the past.

The energy density (J/m^2) is an important parameter when evaluating the safety of human and PMED exposure to electromagnetic radiation. The energy density is calculated by integrating the power density, which is calculated by equation E.1, over the relevant time. Figure E.13 shows the energy density (J/m^2) of the strongest pulse at each of the measurement points. This energy density was found by integrating the power density over the 5.59 µs during which the chirp (ramping from 24.25 GHz to 30 GHz) is emitted from the AIT-2. A very conservative upper bound on the energy density can be estimated by multiplying this by the total number of pulses that the AIT-2 emits during one full scan. This is very conservative because figure E.4 clearly shows that most of the 8.08 µs pulses (containing the 5.59 µs chirps) are much weaker than the strongest 8.08 µs pulse. In fact, most of the 8.08 µs are not even registered by the detection system during the measurement at location 2.

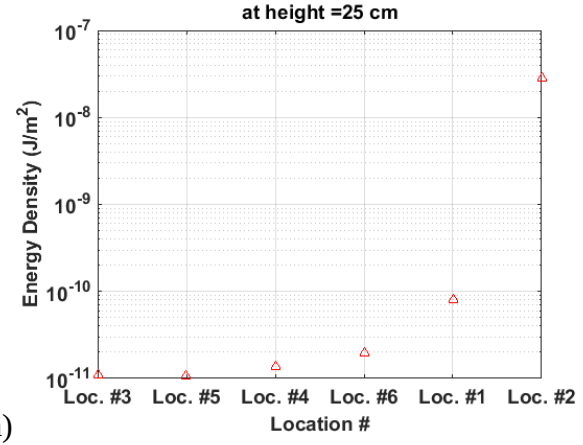

a)

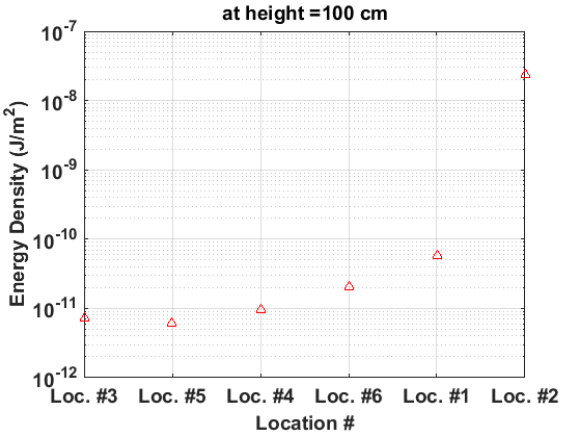

b)

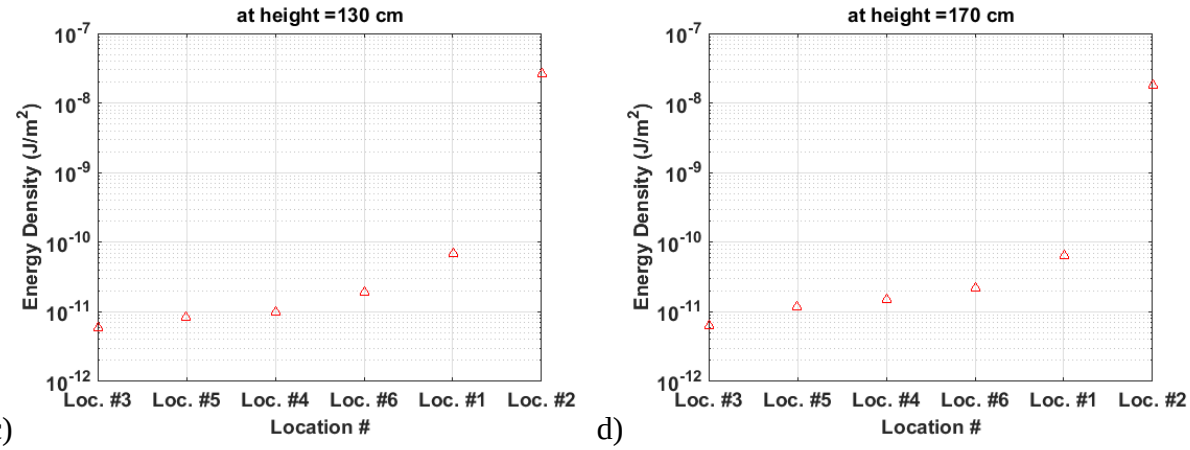

Figure E.13: This is the total energy density (J/m^2) during the 5.59 µs long duration of the chirp within the strongest 8.08 µs pulse. This is obtained by integrating the power density over time. Parts a, b, c, and d correspond to measurements at 25 cm, 100 cm, 130 cm and 170 cm from the ground, respectively.

The total number of 8.08 µs pulses emitted by the AIT-2 during one full scan is estimated as follows. During a single vertical scan line, there are 383 (i.e. 191 x 2 + 1) 8.08 µs long pulses. During a full AIT-2 scan, there are 224 vertical scan lines. Therefore, there are 224 x 383 = 85,792 of the 8.08 µs long pulses during a full AIT-2 scan from one mast. Thus, the energy density (J/m^2) shown in figure E.13 is multiplied by 2*85,792=171,584 to obtain a very conservative upper bound for the total energy density at the respective measurement points, during one full scan, from both masts. The result of this very conservative upper bound estimate is shown in figure E.14. It is important to note that the energy density is expected to be much smaller than this upper bound estimate, especially for the measurement at location 2. Because, the exposure time of an object at location 2 to the nearest mast is a small fraction of the time for a full scan. For instance, the typical PMED exposure time at location 2 is only about 10 ms from the mast closest to it. Please see table D.1 of appendix D for more details.

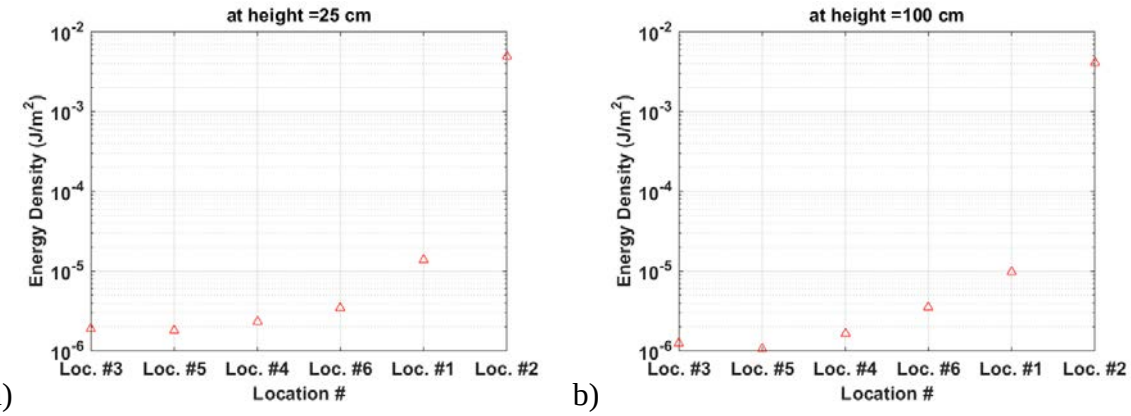

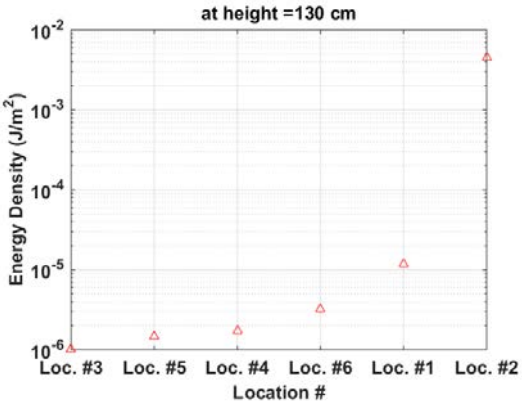

c)

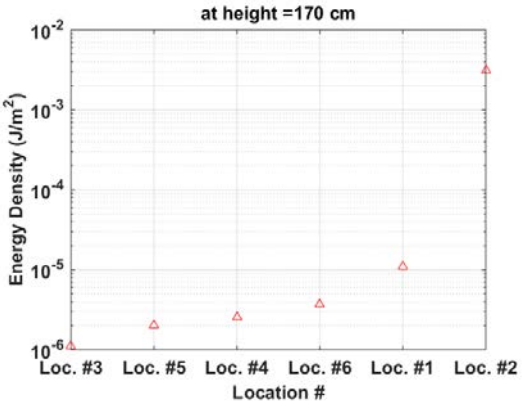

d)

Figure E.14: This is a very conservative upper bound for the total energy density (J/m^2) during one full scan of the AIT-2. This was obtained by multiplying the energy density of the strongest pulse by the total number of pulses. Parts a, b, c, and d correspond to measurements at 25 cm, 100 cm, 130 cm and 170 cm from the ground, respectively.

Appendix F

AIT-2 out of band emission measurements

F.1 Measurement of out-of-band emissions at fixed points in and around the AIT-2

The AIT-2 is designed to emit waves between 24.25 GHz and 30 GHz. These in-band emissions are characterized in appendix E. In this appendix, the radiated spurious or unintentional emissions (out-of-band emissions) from the AIT-2 are characterized. These unintentional emissions are generally emitted by the electrical and electronics components of a product and are expected to meet applicable regulatory requirements such as Federal Communication Commission's (FCC) title 47 CFR (Code of Federal Regulations) part 15 subpart B for emissions [8]. While the AIT-2 appears to have undergone thorough testing for these types of emissions and passed [8], the potential for some of the emitted fields to affect medical devices in and around the AIT-2 unit was examined via measurements and comparisons to applicable medical device EMC standards discussed below. It is important to note that the measurements in [8] were done at greater distances from the AIT-2 and direct comparisons with the results in this appendix are very difficult to make.

Table F.1 lists the measurement probes and base units used in making the out-of-band magnetic field emissions from the AIT-2 at frequencies ranging from 1 Hz to 1 GHz, and out-of-band electric field emission from the AIT-2 at frequencies ranging from 100 kHz to 60 GHz. Note that the EF-6091 E-field probe operates between 100 MHz - 60 GHz, and hence it measures both in-band and out-of-band emissions from the AIT-2. Each of these probes was used at all of the 24 emission measurement points. The 24 emission measurement points were distributed at 6 locations and 4 heights in and around the AIT-2, as shown in Figure F.1. Please see appendix C for detailed discussion of the rationale for choosing these locations and heights.

The measurements were carried out by putting the probes in place at each of the 24 emission measurement points while the AIT-2 went through normal scanning operations. The maximum field strength detected at each of the 24 measurement points was recorded. The maximum magnetic and electric fields that were recorded at the 24 measurement points are shown in table F.2 and table F.4 respectively; the peak values were measured over the frequency ranges specified which correspond to the frequency ranges of the probes in table F.1.

H-Field Measurement Equipment			
Base Unit	Probe	Frequency Range	Sensitivity
ELT-400 (2304/04)	B-Field Sensor (2300/90.10)	1 Hz - 400 kHz	60 nT
NBM-550 (2401/01B)	H-Field Probe (HF-3061)	300 kHz - 30 MHz	0.017 A/m
NBM-550 (2401/01B)	H-Field Probe (HF-0191)	27 MHz - 1 GHz	0.026 A/m

SRM-3000 (3001/01)	3-axis HF Antenna (3581/02)	100 kHz – 250 MHz	0.4 µA/m

E-Field Measurement Equipment			
Base Unit	Probe	Frequency	Sensitivity
NBM-550 (2401/01B)	E-Field Probe (EF-0391)	100 kHz – 3 GHz	0.2 V/m
NBM-550 (2401/01B)	E-Field Probe (EF-6091)	100 MHz – 60 GHz	0.7 V/m
SRM-3000 (3001/01)	3-axis EF Antenna (3501/02)	50 MHz – 3 GHz	125 µV/m

Table F.1: Test equipment (manufactured by Narda / L-3 Communications) for lower frequency radiated emission measurements.

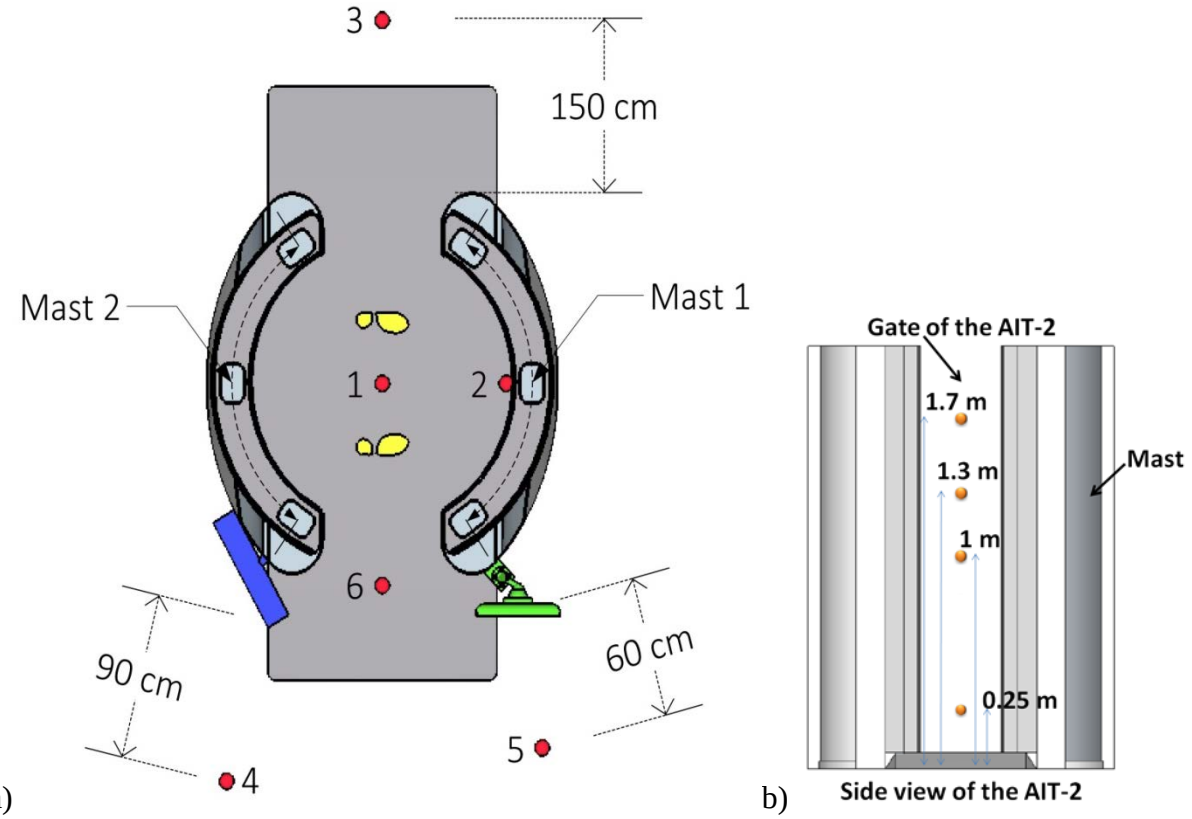

Figure F.1: These two schematics define the 24 emission measurement points distributed at 6 locations and 4 heights. a) This is the top view of the AIT-2, depicting the six locations in and around the AIT-2 chosen to perform the out-of-band emission measurements. The UPS is shown to the left of location 6 in blue, and the AIT-2 computer monitor is shown to the right of location 6 in green. b) This is the side view of the AIT-2 looking through the gate of the AIT-2. These four heights were chosen to perform the emission measurements at the six locations shown in part a.

Measurement Point		Peak Electric Field (V/m) at Different Frequency Ranges		
Location	Height (cm)	100 kHz – 3 GHz	100 MHz – 60 GHz	50 MHz – 3 GHz
1	25	0.39	0.29	0.194
	100	0.45	0.29	0.158
	130	0.44	0.35	0.196

Measurement Point		Peak Electric Field (V/m) at Different Frequency Ranges		
Location	Height (cm)	100 kHz – 3 GHz	100 MHz – 60 GHz	50 MHz – 3 GHz
	170	0.38	0.31	0.161
2	25	1.52	1.7	0.204
	100	0.99	1.18	0.234
	130	1.24	1.53	0.173
	170	1.03	0.94	0.171
3	25	0.38	0.53	0.165
	100	0.26	0.26	0.181
	130	0.29	0.28	0.212
	170	0.47	0.49	0.166
4	25	0.48	0.32	0.178
	100	0.33	0.28	0.178
	130	0.21	0.37	0.183
	170	0.39	0.35	0.19
5	25	0.62	0.39	0.163
	100	0.39	0.3	0.184
	130	0.32	0.3	0.169
	170	0.39	0.31	0.187
6	25	0.58	0.34	0.181
	100	0.46	0.47	0.18
	130	0.41	0.38	0.287
	170	0.53	0.44	0.191

Table F.2: Peak Electric Field measurements at the 24 points in and around the AIT-2 distributed over 6 locations and 4 heights. The measurements were carried out by putting the probes in place while the AIT-2 went through normal scanning operations.

Background Measurements		Peak Electric Field (V/m) at Different Frequency Ranges		
#	Condition	100 kHz – 3 GHz	100 MHz – 60 GHz	50 MHz – 3 GHz
1	1 week before installation of AIT-2	0.94	0.89	3.07
2	1 day before installation of AIT-2	1.03	0.94	0.186
3	During installation of AIT-2	1.23	1.26	0.873
4	With unplugged AIT-2	1.53	1.43	0.207
5	With plugged, but turned off AIT-2	2.37	1.81	0.195

Table F.3: Peak Electric Field measurements of the background noise in and around the AIT-2.

Prior to the 24 measurements in and around the AIT-2, the baseline environmental measurements were made five times. These background measurements were made: one week before the

installation of the AIT-2; one day before the installation of the AIT-2; during the AIT-2 installation; without the AIT-2 being plugged in; and with the UPS of the AIT-2 being plugged in, but with the AIT-2 being turned off. The background measurements were carried out by moving the probes throughout the vicinity of the AIT-2, and by recording the maximum electric or magnetic fields for the frequency ranges of the probes. The peak baseline electric and magnetic fields are shown in table F.3 and table F.5 respectively.

The emission levels from the baseline measurements were used to ensure that there were no other electromagnetic sources creating strong fields in the immediate environment of the AIT-2, and to assess the field strengths of the AIT-2 emission considering the background noise. The baseline measurements were necessary because the AIT-2 system was not located in an anechoic chamber. Emissions measurements were performed with the AIT-2 system with the mmW emitters active and moving through the same operation cycle used in the PMED testing.

Table F.2 and table F.4 report the highest emission field strength levels measured from the AIT-2 system at the frequency ranges, and the measurement points specified. These measurements may not reflect the highest level emitted by the AIT-2 because of temporal changes of the emissions. In general, most non-implantable active medical devices are tested for immunity to electric field strengths of 3 V/m or more depending upon the essential function of the device [9]. Non-implantable PMED immunity testing is typically done at power line frequencies with 3 A/m field strength in present standards. Implantable PMEDs can be tested to even higher levels. Present standards for implantable PMEDs check immunity to magnetic fields generally below 450 MHz at various field strengths up to 150 A/m. The spurious emission measurements presented here indicate the tested AIT-2 does not seem to emit very large spurious electric or magnetic fields. All of the peak field measurements at the 24 points in and around the AIT-2 are within the fluctuations in the baseline environmental noise shown in table F.3 and table F.5. It is important to note that a hot spot of emission was discovered at the front panel of the UPS (uninterruptible power supply) of the AIT-2. This is discussed in detail in appendix F.2.

It is worth noting that one of the probes used for the out-of-band emissions has a capability to measure the in-band emissions from the AIT-2 during the scanning operations, as well; this is the EF-6091 E-field probe that works with the NBM-550 (2401/01B) base unit over the frequency range of 100 MHz to 60 GHz shown in table F.1. The peak electric field measured at location 2, which is the closest location to the radiating mast of the AIT-2, is shown to be about 1.5 V/m in table F.2. This result approximately agrees with in-band emission measurement results shown in part f of figure E.11; the data in this figure was measured with a detection system that was specifically designed to be sensitive to the in-band emissions.

Measurement Point		Peak Magnetic Field (A/m) at Different Frequency Ranges					
Location	Height (cm)	10 Hz-400 kHz	1 Hz-400 kHz	300 kHz-30 MHz	27 MHz-1 GHz	100 kHz-10 Hz	10 MHz-250 MHz
1	25	0.182	0.456	0.027	0.0185	0.000141	0.000243
	100	0.15	0.413	0.0237	0.0186	0.000125	0.000258
	130	0.134	0.428	0.0204	0.0154	0.0000848	0.000252
	170	0.123	0.438	0.0107	0.0141	0.0000715	0.000258
2	25	0.201	0.448	0.0972	0.0771	0.000126	0.000245
	100	0.15	0.407	0.0521	0.0457	0.0000943	0.000259
	130	0.133	0.473	0.07	0.0503	0.00016	0.000247
	170	0.131	0.828	0.0463	0.0285	0.000132	0.00026
3	25	0.22	0.458	0.0149	0.0185	0.000391	0.000249
	100	0.199	0.449	0.0123	0.0131	0.000222	0.000261
	130	0.189	0.41	0.0156	0.0108	0.000101	0.000256
	170	0.192	0.395	0.0212	0.0189	0.000201	0.000257
4	25	0.154	0.432	0.0089	0.0111	0.000247	0.000257
	100	0.126	0.4	0.013	0.0108	0.000173	0.000258
	130	0.115	0.4	0.015	0.0152	0.0000857	0.000256
	170	0.117	0.414	0.0164	0.0141	0.000149	0.000253
5	25	0.12	0.416	0.0214	0.0114	0.000131	0.000249
	100	0.111	0.409	0.0176	0.0138	0.0000997	0.000256
	130	0.109	0.402	0.0203	0.0114	0.000105	0.000256
	170	0.112	0.392	0.0153	0.0101	0.000121	0.000265
6	25	0.166	0.415	0.0345	0.0267	0.0000955	0.000254
	100	0.144	0.417	0.0247	0.0234	0.000125	0.000253
	130	0.131	0.403	0.0257	0.0199	0.000125	0.000257
	170	0.139	0.384	0.0136	0.0171	0.000104	0.000255

Table F.4: Peak Magnetic Field measurements at the 24 points in and around the AIT-2 distributed over 6 locations and 4 heights. The measurements were carried out by putting the probes in place while the AIT-2 went through normal scanning operations.

Background Measurements		Peak Magnetic Field (A/m) at Different Frequency Ranges					
#	Condition	10 Hz-400 kHz	1 Hz-400 kHz	300 kHz-30 MHz	27 MHz-1 GHz	100 kHz-10 MHz	10 MHz-250 MHz
1	1 week before installation of AIT-2	0.211	21.5	0.0445	0.0259	0.000159	0.000233
2	1 day before installation of AIT-2	0.362	3.98	0.0537	0.0981	0.000287	0.000244

Background Measurements		Peak Magnetic Field (A/m) at Different Frequency Ranges					
#	Condition	10 Hz-400 kHz	1 Hz-400 kHz	300 kHz-30 MHz	27 MHz-1 GHz	100 kHz-10 MHz	10 MHz-250 MHz
3	During installation of AIT-2	0.341	6.05	0.0594	0.0607	0.000237	0.0198
4	With unplugged AIT-2	0.217	7.27	0.895	0.0567	0.000127	0.000234
5	With plugged, but turned off AIT-2	0.207	7.21	0.594	0.181	0.00231	0.000257

Table F.5: Peak Magnetic Field measurements of the background noise in and around the AIT-2.

F.2 Searching for and analyzing localized spurious emission hot spots on the surface of AIT-2

Appendix F.1 shows that the AIT-2 does not produce significant spurious, out-of-band emissions at the 24 measurement points. The 24 measurement points were chosen based on justifications stated in appendix C. In addition to measuring the peak electric and magnetic fields at the 24 points, all of the probes in table F.1 were diligently moved around throughout the immediate vicinity of the AIT-2. The goal was to find out any localized hot spots of spurious emission in and around the AIT-2. This approach resulted in the discovery of a localized spurious emission at the front panel of the UPS of the AIT-2.

The spurious emission hot spot was initially discovered around the UPS panel using the NBM-550 connected to the EF-0391 electric field probe. The probe is sensitive to electric fields with a frequency range of 100 kHz to 3 GHz. The electric field strength measured around the UPS was as strong as 100 V/m at times. The spatial variation of the electric field strength was mapped out by measuring the maximum electric field strength at various distances away from the UPS front panel. The probe was oriented in such a way that maximizes the measurement values. The probe was moved away from the front panel of the UPS systematically while recording the peak electric field at increasing distances. The closest distance between the axis supporting the probe and the front panel of the UPS with LEDs (light emitting diodes) is about 3 cm. Part a of figure F.2 illustrates how the probe was used to measure the electric field at increasing distances from the UPS front panel. The measurements are shown in figure F.3, which shows that the electric field decays to the background noise level at about 15 cm from the UPS front panel. This spurious hot spot was initially discovered and characterized using the EF-0391 electric field probe. The experiment was repeated using near field probes as shown in part b of figure F.2.

a)  b) 

Figure F.2: a) The electric field probe (model EF-0391) was initially used to discover that there is a hot spot of electric field in the vicinity of the UPS front panel of the AIT-2. b) The near field probe was then used to measure the fields in the vicinity of the UPS hot spot.

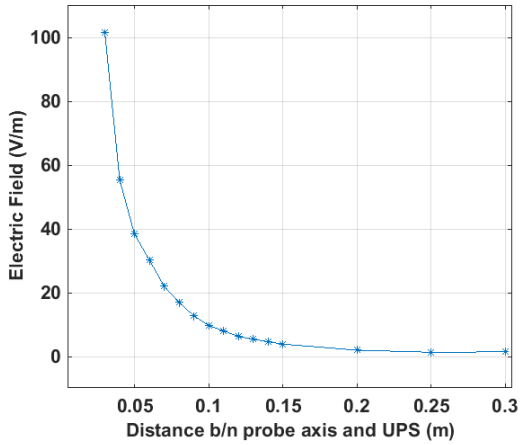

Figure F.3: The NBM-550 connected to the EF-0391 electric field probe was initially used to make these measurements in the vicinity of the UPS front panel of the AIT-2. The electric field decays to background noise levels after about 15 cm to 20 cm away from the UPS front panel of the AIT-2.

The localized spurious emission hot spot at the UPS front panel was further examined using the smaller near field magnetic and electric field probes. Part b of figure F.2 shows the Beehive 100C magnetic field probe being used to measure the near field around the UPS front panel. Table F.6 provides the information about the equipment used for the near field measurement. The near field probes were connected to a spectrum analyzer that was placed about 3m away from the UPS. The max (maximum) hold function of the spectrum analyzer was activated to measure the power spectrum between 3 MHz and 50 MHz. The probe was diligently moved around the front panel of the UPS measuring the spurious emission hot spot in all possible orientations while the max hold function of the spectrum continued to measure the maximum field. The spectrum that was measured is shown in figure F.4.

Equipment	Description

Beehive 100C	Magnetic field probe with: (0.85 in) Loop Diameter, and (1.0 in) Tip Diameter.
Beehive 100D	Electric field probe with: (0.08 in) Tip Diameter.
BNC Coaxial Cable	3.1 m RG58 cable
Spectrum Analyzer	N9030A PXA Signal Analyzer, 3 Hz to 50 GHz

Table F.6: Equipment used to do near field measurement of the electric and magnetic fields around the spurious emission hot spot at the UPS front panel of the AIT-2.

The Beehive 100C can be used to measure the magnetic flux density (B in Tesla) using equation F.1. P_{out} is the probe output power into 50 Ω termination in dBm. F is the frequency of the received signal in MHz. This equation is provided by the manufacturer of the probe; the equation guarantees a 3 dB accuracy (of power prediction given a known B) from DC to the 3 dB point of the probe, which is 50 MHz for the Beehive 100C.

$$B = 10^{(P_{out} - 85.1 - 20\log_{10} F)/20}$$

Equation F.1: This equation expresses the magnetic flux density (B) in terms of the power and frequency measured by the Beehive 100C near field magnetic probe. F is the frequency in MHz.

Figure F.4: This is the power spectrum of the spurious emission at the UPS between 3 MHz and 50 MHz. It was measured using the Beehive 100C magnetic probe. The vertical scale is 10 dB per division.

Equation F.1 was used to calculate the magnetic flux density (in T) as a function of frequency, and the equivalent magnetic field (in A/m). This is done using the data from the spectrum analyzer. The results are shown in figure F.5. These results were compared with the background magnetic field noise at these frequencies (i.e. 3 MHz to 50 MHz). The background measurements, shown in figure F.6, were obtained using the 3-axis HF antenna probe (3581/02) connected to the SRM-3000 (3001/01) base unit, which is specified in table F.1. Comparison of figure F.5 and figure F.6 shows that the magnetic field near the UPS (~ 0.04 A/m at around 25

MHz) is about 3 orders of magnitude higher than the magnetic field noise floor in and around the AIT-2 (~ 10^{-5} A/m at around 25 MHz).

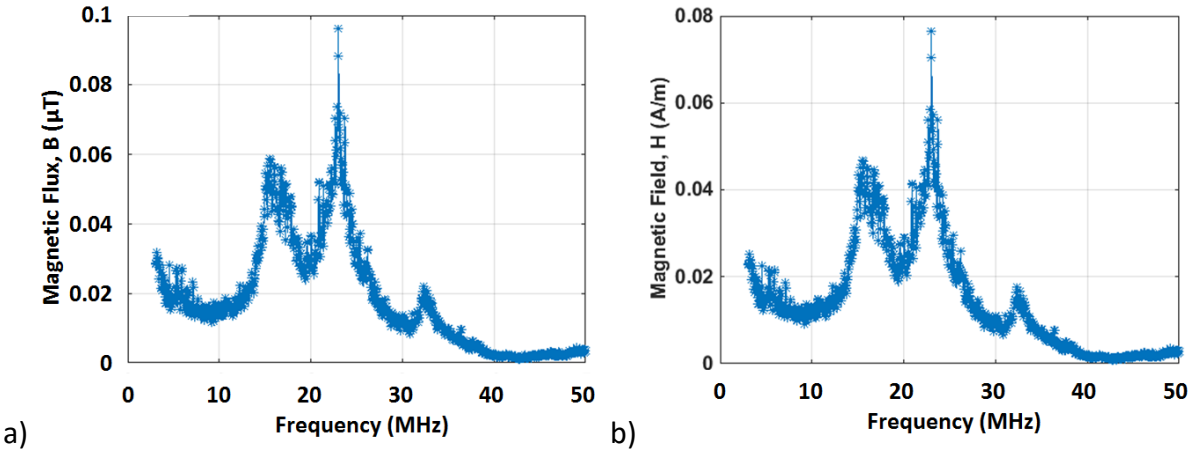

Figure F.5: The magnetic field flux density and the corresponding magnetic field are shown as a function of frequency. These were measured at the spurious emission hot spot of the UPS front panel using the Beehive 100C magnetic field probe.

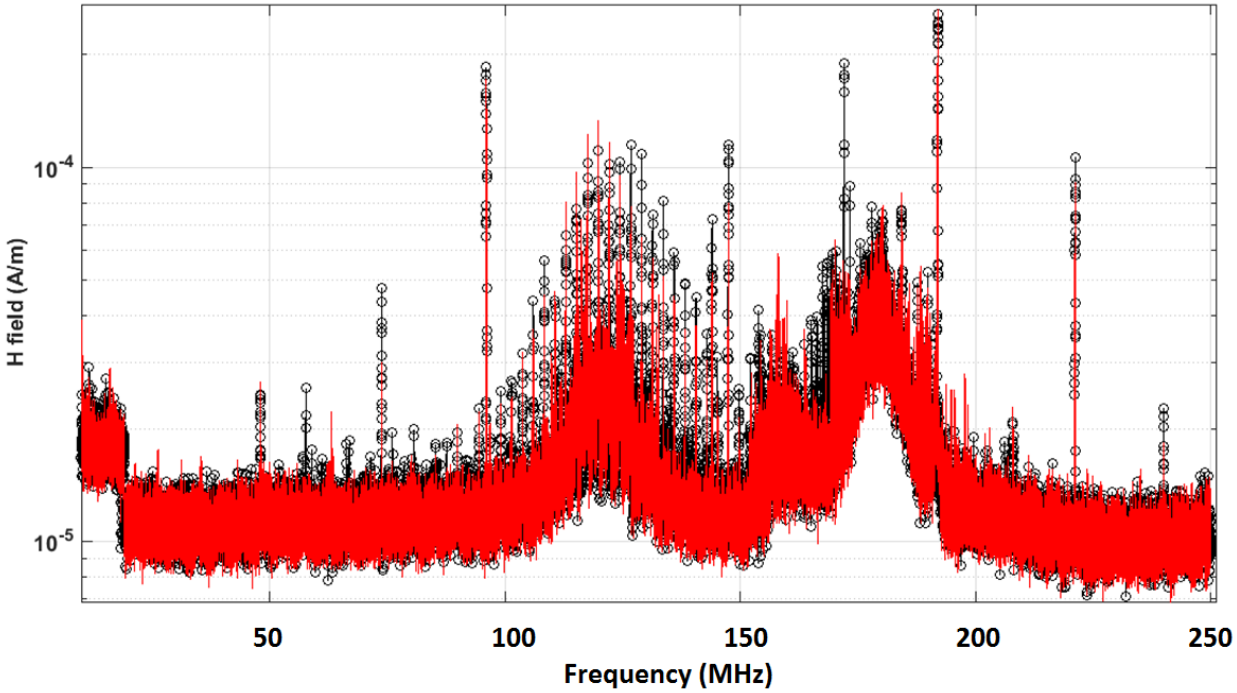

Figure F.6: This shows part of the raw spectrum data of the H field for the 24 fixed point measurements (in red) with the AIT-2 operating normal scans, and the 5 background condition measurements (in black) summarized in table F.4 and table F.5 respectively. These spectrums were measured using the 3-axis HF Antenna (3581/02) connected to the SRM-3000 (3001/01) base unit.

The Beehive 100D electric field probe, which is specified in table F.6, was also used to characterize the spurious emission around the UPS hot spot. The probe was connected to the

spectrum analyzer, and the spectrum shown in figure F.7 was measured. The probe was moved around within the UPS hot spot in all possible orientations while the spectrum analyzer measured the power spectrum with its max hold mode. The electric field was calculated using equation F.2, which is provided by the manufacturer of the probe. P_{out} is the probe output power into 50 Ω termination in dBm. F is the frequency of the received signal in MHz. The calculated electric field is shown in figure F.8. Measurements using the Beehive 100D tend to be less repeatable than shielded loop probes, due to the presence of common mode currents flowing on the outer surface of the probe or attached cable. Despite this uncertainty, figure F.8 shows that the electric field around the UPS spurious emission hot spot (50 V/m - 100 V/m) is much higher than background noise presented in table F.2 and table F.3 (<1 V/m).

$$E = 10^{(P_{out} - 113.2 - 20\log_{10} F)/20}$$

Equation F.2 This equation expresses the electric field (E) in terms of the power and frequency measured by the Beehive 100D near field electric probe.

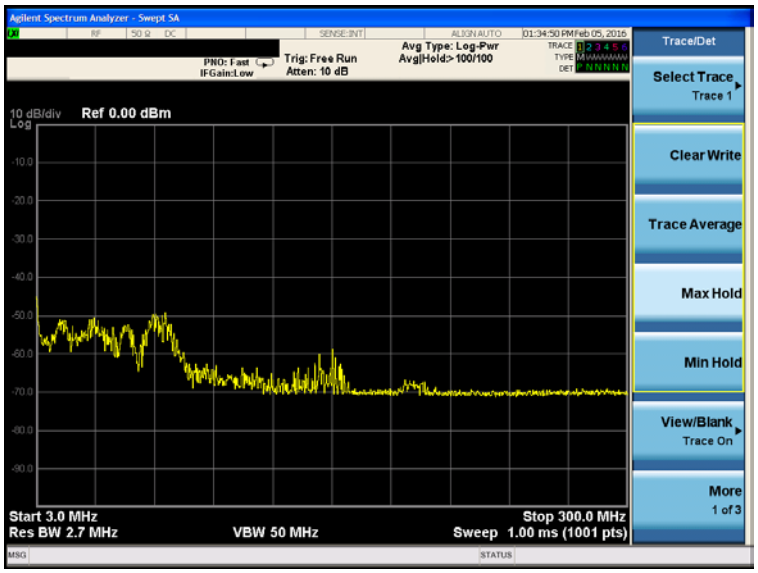

Figure F.7: This is the power spectrum of the spurious emission at the UPS between 3 MHz and 300 MHz. It was measured using the Beehive 100D electric probe. The vertical scale is 10 dB per division.

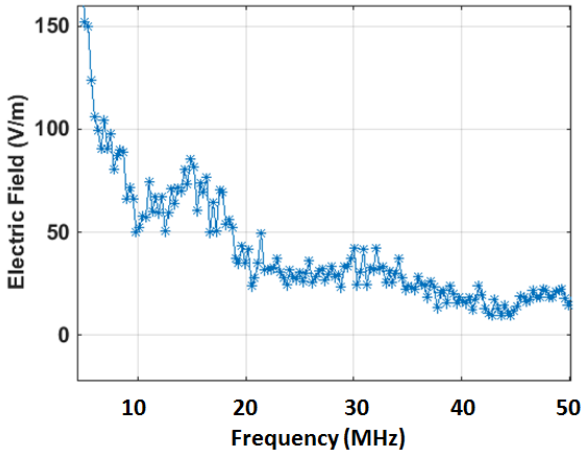

Figure F.8: The electric field is shown as a function of frequency. This was measured at the spurious emission hot spot of the UPS front panel using the Beehive 100D electric field probe. Please note that measurements using the Beehive 100D tend to be less repeatable than shielded loop probes.

To summarize, a hot spot of spurious emission was found at the front panel of the UPS of the AIT-2. The electric field around the hot spot can be as high as 100 V/m, and it decayed to the background noise level within about 15 cm of the front panel of the UPS. The magnetic field can be as high as 0.08 A/m. These spurious emissions were seen at frequencies roughly ranging from 10 MHz to 30 MHz based on the results shown in figure F.5. These field strengths are orders of magnitude higher than the background noise at these frequencies.

Appendix G

AIT-2 leakage current measurements

CDRH measured leakage currents of the AIT-2. The measurements were based on the leakage current safety standard discussion in IEC 60601-1, clause 8.7.3 [10]. The standard specifies limits for four types of leakage currents. These are: i) earth leakage current, ii) touch current, iii) patient leakage current, and iv) patient auxiliary current.

The first two types of leakage currents apply directly to the AIT-2. Earth leakage current is the current that leaks through the AIT-2 ground conductor in the AC power line. Touch current is the current that flows from any conductive component of the AIT-2's enclosure to protective earth through a person that touches the conductive component of the AIT-2.

The standard also specifies patient leakage current [10]. This is the current that flows from one part of equipment which is applied to a patient to ground through the patient. The patient leakage current is not directly applicable to the AIT-2 because the AIT-2 does not have parts that are designed to be applied directly to the person. However, CDRH measured all leakage currents that flow from any conductor on the AIT-2's surface, which may potentially contact the person, to ground through the person. In the results below, this is referred to as "surface to ground leakage current" of the AIT-2, and it is analogous to patient leakage current in the standard [10]. Please note that the measurement of surface to ground leakage current of the AIT-2 is identical to the measurement of the touch current. As shown in table G.1, the touch current and the patient leakage current of the AIT-2 are simply called the "surface to ground leakage current" of the AIT-2.

The fourth leakage current type specified in the standard is the patient auxiliary current [10]. This is the current that flows from one part of equipment which is applied to a patient to another part of the equipment which is applied to the patient through the patient. This is also not directly applicable to the AIT-2 because the AIT-2 does not have parts that are designed to be applied directly to the person. However, CDRH measured all leakage currents that may flow from any conductor on the AIT-2's surface to any other conductor on the AIT-2's surface through the person that may be standing inside the AIT-2. In the results below, this measurement is referred to as "surface to surface leakage current" of the AIT-2, and it is analogous to patient auxiliary current in the standard [10]. The relationship between the leakage currents defined in the standard [10] and the terminology used in this report is presented in table G.1.

Leakage current terminology defined in IEC 60601-1	Corresponding terminology for leakage current measurements of the AIT-2	Description
Earth leakage current	Earth leakage current	The current flowing in the protective earth circuit of the AIT-2
Touch current	Surface to ground leakage current	The current flowing between any conducting surface on the AIT-2 enclosure and protective earth through the subject
Patient leakage current	Surface to ground leakage current	The current flowing between any conducting surface on the AIT-2 enclosure and protective earth through the subject
Patient auxiliary current	Surface to surface leakage current	The current flowing between any two conducting surfaces on the AIT-2 enclosure through the subject

Table G.1: Terminology and description of leakage current measurements

The AIT-2 leakage current testing was performed using FLUKE Electrical Safety Analyzer ESA612 (see figure G.1), which is designed to satisfy the test standards including IEC 60601-1 [10]. In the sections below, the detailed test procedures and the results are presented.

Figure G.1: FLUKE Electrical Safety Analyzer ESA612 used for leakage current testing

G.1 Procedure for measuring leakage current testing

G.1.i Preparing the measurement equipment

1. Connect the Electrical Safety Analyzer ESA612 henceforth refered to as “Analyzer” to a properly grounded three-prong outlet.
2. Plug the AIT-2 power cable to the output outlet on the Analyzer.
3. Turn on the Analyzer.

G.1.ii Measuring earth leakage current

4. Select the µA key to measure the earth leakage current. Confirm normal polarity is displayed on the screen and record the displayed current.

5. Press the "Polarity" button to switch the polarity applied to Analyzer's test receptacles from normal to reverse. Record the displayed leakage current for reverse polarity

G.1.iii Measuring surface to ground leakage current

6. Connect the on end test lead to "V/Ω/A" jack and the other end to "Null" jack and press the soft key zero leads to cancel out the test lead resistance from the measurement.

7. Press the soft key labeled "Chassis" to measure surface to ground leakage current.

8. Apply the test lead to different points on the AIT-2, including screws and other conducting surfaces on the ceiling, the left wall, the right wall, and floor of the AIT-2. Record the displayed leakage current for each test.

9. Press the "Polarity" button to switch the polarity applied to Analyzer's test receptacles from normal to reverse. Repeat step 8.

The maximum surface to ground leakage current measured from various surfaces of the AIT-2 is presented in table G.2.

G.1.iv Measuring surface to surface leakage current

10. Press the soft key labeled "Lead to Lead" to measure the surface to surface leakage current for AIT-2.

11. Connect two banana plug test leads to the two banana plug receptacles on the header of the Analyzer.

12. Select the two conductors that are connected from the applied parts connection display.

13. Apply the test lead to all of the combinations of the different conducting points on the AIT-2 , including screws and other conducting surfaces on the ceiling, the left wall, the right wall, and floor of the AIT-2. Record the displayed leakage current for each test.

14. Press the “Polarity” button to switch the polarity applied to Analyzer’s test receptacles from normal to reverse. Repeat step 13.

The maximum surface to surface leakage current measured between various pairs of surfaces of the AIT-2 is presented in table G.2.

G.2 Results

The upper limits allowed by the standard [10], and the test results for the maximum leakage currents measured from the AIT-2 unit are summarized in table G.2. In all cases, the measured values were lower than the upper limits specified by the IEC 60601-1 standard [10].

Measurement Type	Surface 1 on AIT-2 surface	Surface 2 on AIT-2 surface	IEC 60601-1 limits	Maximum leakage current measurements	
				Normal polarity	Reversed polarity
Earth leakage current	N/A	N/A	5 mA	4.31 mA	4.51 mA
Surface to ground leakage current	Ceiling	N/A	100 µA	0.6 µA	0.6 µA
	Left wall	N/A	100 µA	0.5 µA	0.6 µA
	Right wall	N/A	100 µA	1 µA	1.1 µA
	Floor	N/A	100 µA	0.6 µA	0.6 µA
Surface to surface leakage current	Ceiling	Left wall	100 µA	0.4 µA	0.3 µA
	Ceiling	Right wall	100 µA	1.1 µA	1.2 µA
	Ceiling	Floor	100 µA	1.4 µA	1.5 µA
	Floor	Left wall	100 µA	0.6 µA	1.5 µA
	Floor	Right wall	100 µA	2.0 µA	2.2 µA
	Left Wall	Right wall	100 µA	0.4	1.5 µA

Table G.2: Maximum leakage current measurements for the AIT-2, and the corresponding upper limits set by the standard [10].

Appendix H

Procedures for testing personal medical electronic devices with the AIT-2

H.1 Procedure for testing implantable cardiac pacemakers for exposure in/near AIT-2

Setup monitoring system and torso simulator

1. Prepare the torso simulator for pacemaker testing as described in appendix I, and verify the appropriate conductivity of the saline (i.e. 0.27 S/m).
2. Mount the device under test (DUT) on the torso simulator. The DUT consists of the Implantable Pulse Generator (IPG) of the pacemaker and its monitoring or pacing leads shown in figure H.1. The leads should be secured on a predetermined curve drawn on the grid, which makes the required 225 cm^2 closed loop based on the testing standards [11]. There is a microwave absorber between the IPG (which is in air) and the saline. So, connect the IPG to the saline using a wire to complete the conduction loop.

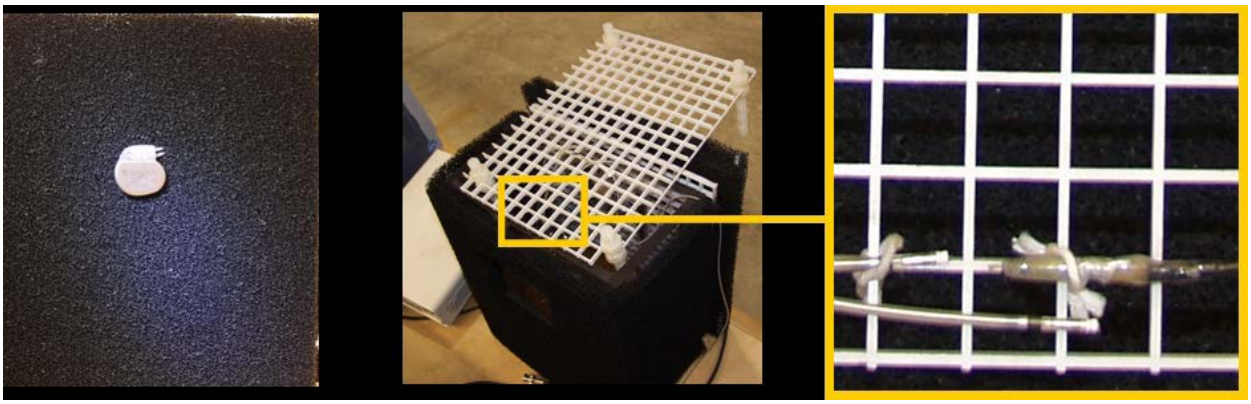

Figure H.1: This shows the installation of the DUT (pacemaker) on the torso simulator.

3. Connect DUT monitoring cable leading out of the torso simulator to a digital oscilloscope through a pre amplifier.
4. Connect DUT monitoring cable (with a BNC-T) to A/D converter which is linked with the controlling PC.
5. Connect the external simulated cardiac signal generator to the torso simulator. The simulated cardiac signal is generated according to the specifications in [11].
6. Place the infrared detection system to detect the AIT-2 mast passing through the center of the mast travel path. Connect the output of the infrared detection system to the A/D converter.
7. Set up the data acquisition software on the PC connected to the A/D converter.
8. Check torso simulator and cables on the oscilloscope to verify minimum noise from the exposure.
9. Program DUT according to the operating modes, and lead configurations in appendix J, and perform steps 10-11 for each of the lead configurations (i.e. unipolar and bipolar). If the DUT allows RF telemetry, set up the programmer to remotely monitor the activity of the DUT during the test; this provides an additional monitoring mechanism.
10. Start the external simulated cardiac signal generator. Determine the minimum voltage level needed to be applied to inhibit pacing. Double the minimum voltage level to find the voltage

level that needs to be applied for injected simulated heart signal test, at the current device settings. Once this is determined, turn the cardiac injected signal off.

11. To verify DUT operation, run a baseline test monitoring signals from the device while the DUT/torso simulator is still at a distance of at least 2 meters from the AIT-2 unit. Do the baseline test with and without the simulated cardiac signal.

Test the DUT in / near the AIT-2

12. Power the AIT-2, log on, and calibrate the system.
13. Set up the torso simulator at the center of the AIT-2 unit (location 1) and a height of 1.3 meter from the floor (see table C.3 of appendix C for the justification used to choose the test points). DUT monitoring and cardiac signal injection cables are fed in and out of the AIT-2 unit through hollow fiber glass tubing oriented parallel to the floor (perpendicular to the radiated electric field and wrapped with a millimeter wave absorber).
14. Record the DUT's orientation, operating mode, lead configurations, settings, and status (i.e. on or off) of the simulated cardiac signal on the data acquisition software.
15. Run the data acquisition software to start the experiment.
16. Command the AIT-2 system to activate a single scan.
17. During the scan (i.e. exposure), observe the DUT's output signal on the oscilloscope. Figure H.2 below is an example of DUT's output. At the same time, observe the screen of the programmer if the DUT is connected to the programmer using RF telemetry.

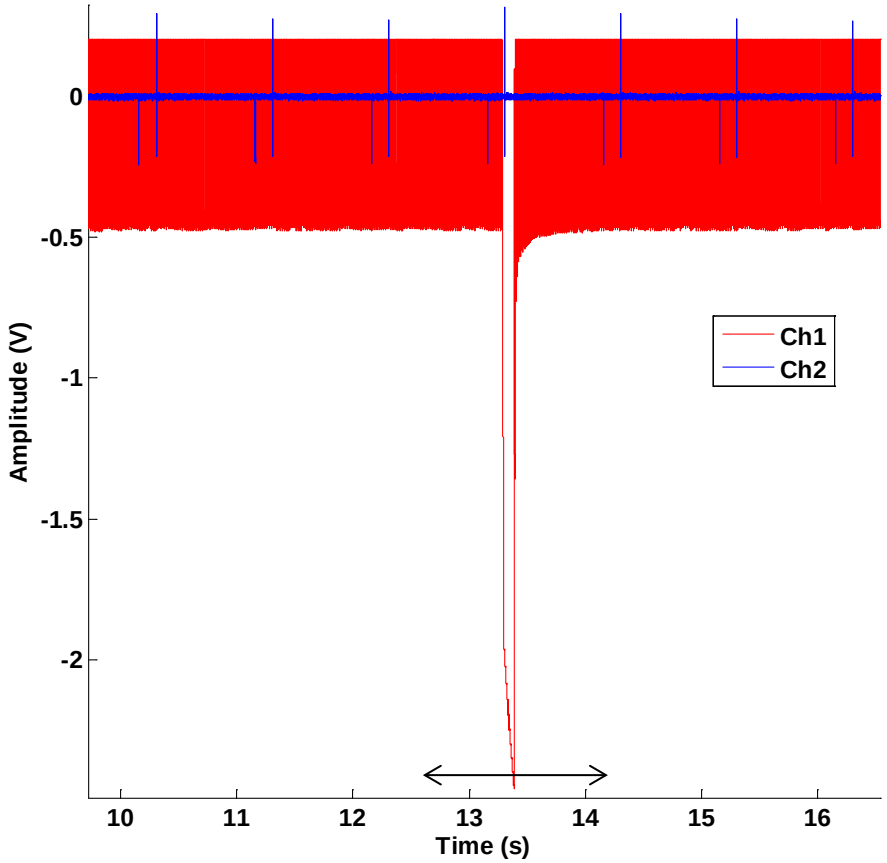

Figure H.2: Channel 2 shows the DUT Output. Channel 1 shows the Scanner Mast Motion Indicator. The black arrow shows the start and end of one scan which takes less than 1.5 s.

18. Repeat steps 16 and 17 five (5) times, recording any effects or spurious data over 30 seconds period.
19. Repeat steps 14 to 18 with the simulated cardiac signal on.
20. Rotate the IPG of the DUT by 90 degrees to a new orientation as shown in figure H.3 and repeat steps 14 - 19.
21. Repeat steps 14 to 20 after changing the lead configuration of the DUT (from unipolar to bipolar).

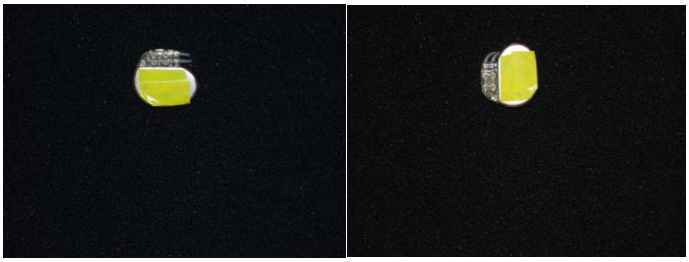

Figure H.3: The first figure shows the DUT in horizontal orientation, the second shows the DUT in vertical orientation.

22. If the device is designated for extensive testing, change the measurement point to each of the three measurement points selected in appendix C (i.e. location 1, location 2, and near the UPS), and repeat steps 14 to 21. One device type per manufacturer is chosen for extensive testing.
23. Retrieve any relevant files saved by the device programmer, and save them along with the data that is automatically saved by the data acquisition software.
24. Finally, program the device to a mode that saves its battery life.

H.2 Procedure for testing ICDs for exposure in/near AIT-2

Setup monitoring system and torso simulator

1. Prepare the torso simulator for ICD testing as described in appendix I, and verify the appropriate conductivity of the saline (i.e. 0.27 S/m).
2. For safety reasons, check that the ICD therapy functionality is turned OFF using the programmer, before touching it. The ICD therapy functionality needs to be turned on with minimum energy levels only during the actual test.
3. Mount the device under test (DUT) on the torso simulator. The DUT consists of the ICD's Implantable Pulse Generator (IPG) and its monitoring or pacing leads shown in figure H.4. The leads should be secured on a predetermined curve drawn on the grid, which makes the required 225 cm^2 closed loop based on the testing standards [11]. There is a microwave absorber between the IPG (which is in air) and the saline. So, connect the IPG to the saline using a wire to complete the conduction loop.

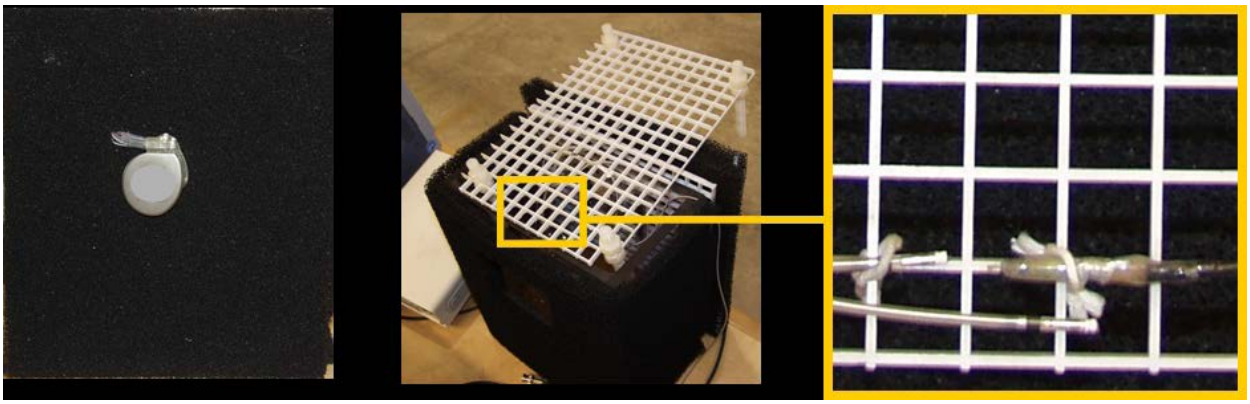

Figure H.4: This shows the installation of the DUT (ICD) on the torso simulator.

4. Connect DUT monitoring cable leading out of the torso simulator to a digital oscilloscope through a pre amplifier.
5. Connect DUT monitoring cable (with a BNC-T) to A/D converter which is linked with the controlling PC.
6. Connect the external simulated cardiac signal generator to the torso simulator. The simulated cardiac signal is generated according to the specifications in [11].
7. Place the infrared detection system to detect the AIT-2 mast passing through the center of the mast travel path. Connect the output of the infrared detection system to the A/D converter.
8. Set up the data acquisition software on the PC connected to the A/D converter.
9. As a safety measure, make sure that voltage protection circuits are present on all cables coming out of the torso simulator.
10. Check torso simulator and cables on the oscilloscope to verify minimum noise from the exposure.
11. As a safety measure, program the ICD to set the shock therapy levels to minimum energy levels, without touching the ICD. Once this is done, recognize the risk of shocking during steps 12-14, and avoid touching the ICD without protective gloves. If signs of ICD shock therapy sequence are seen during steps 12-14, be prepared to safely unplug the measurement equipment, and program the ICD shock therapy off.
12. Program DUT according to device operating modes, and settings in appendix J, and perform steps 13-14. If the DUT allows RF telemetry, set up the programmer to remotely monitor the activity of the DUT during the test. This provides an additional monitoring mechanism.
13. Start the external simulated cardiac signal generator. Determine the minimum voltage level needed to be applied to inhibit pacing. Double the minimum voltage level to find the voltage level that needs to be applied for injected simulated heart signal test. Once this is determined, turn the cardiac injected signal off.
14. To verify DUT operation, run a baseline test monitoring signals from the device while the DUT/torso simulator is still at a distance of at least 2 meters from the AIT-2 unit. Do the baseline test with and without the simulated cardiac signal.
15. As a safety measure, program the ICD to make sure that its shock therapy functionality is OFF while it is still situated on the torso, without touching it.

<u>Test the DUT in / near the AIT-2</u>

16. Power the AIT-2, and log on, and calibrate the system.

17. Set up the torso simulator at the center of the AIT-2 unit (location 1) and a height of 1.3 meter from the floor (see table C.3 of appendix C for the justification used to choose the test points). DUT monitoring and cardiac signal injection cables are fed in and out of the AIT-2 unit through hollow fiber glass tubing oriented parallel to the floor (perpendicular to the radiated electric field and wrapped with a millimeter wave absorber).
18. As a safety measure, program the ICD to set the shock therapy to minimum energy levels, without touching the ICD. Once this is done, recognize the risk of shocking during steps 19 to 27, and avoid touching the ICD without protective gloves. If signs of ICD shock therapy sequence are seen during steps 19 to 27, be prepared to safely unplug the measurement equipment, stop the AIT-2 scanning, and program the ICD shock therapy off.
19. Record the DUT's orientation, operating mode, settings, and status (on or off) of the simulated cardiac signal on the data acquisition software.
20. Run the data acquisition software to start the experiment.
21. Command the AIT-2 system to activate a single scan.
22. During the scan (i.e. exposure), observe the DUT's output signal on the oscilloscope. Figure H.5 below is an example of DUT's output. At the same time, observe the screen of the programmer if the DUT is connected to the programmer using RF telemetry.

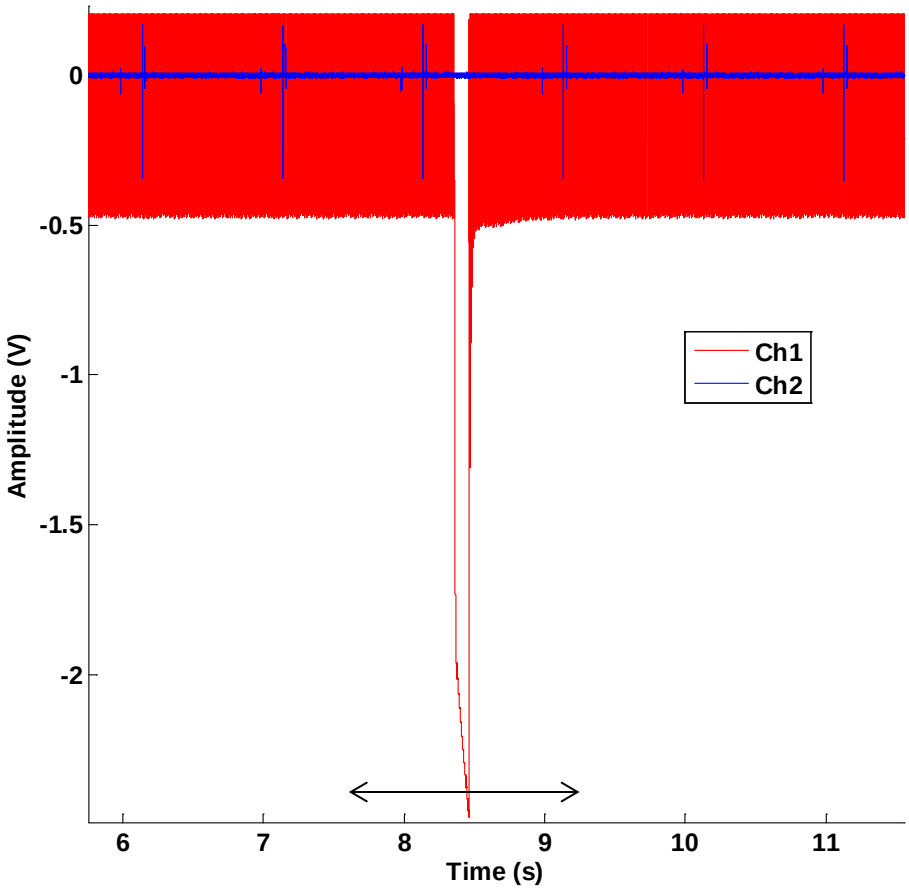

Figure H.5: Channel 2 shows the DUT Output. Channel 1 shows the Scanner Mast Motion Indicator. The black arrow shows the start and end of one scan which takes less than 1.5 s.

23. Repeat steps 21 and 22 five (5) times, recording any effects or spurious data over 30 seconds period.
24. Repeat steps 19 to 23 with the simulated cardiac signal on.
25. Rotate the IPG of the DUT by 90 degrees to a new orientation as shown figure H.6 and repeat steps 19 to 24.

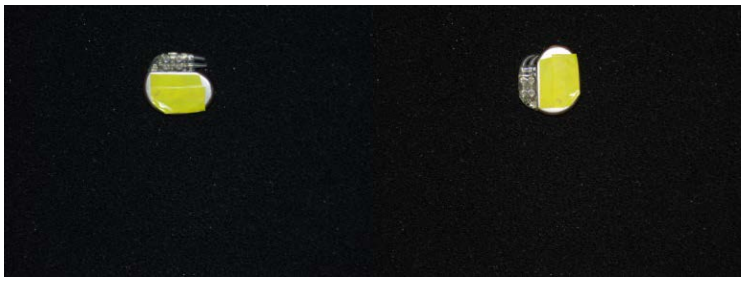

Figure H.6: The first figure shows the DUT in horizontal orientation, the second shows the DUT in vertical orientation.

26. If the device is designated for extensive testing, change the measurement point to each of the three measurement points selected in appendix C (i.e. location 1, location 2, and near the UPS), and repeat steps 19 to 25. One device type per manufacturer is chosen for extensive testing.
27. Retrieve any relevant files saved by the device programmer, and save them along with the data that is automatically saved by the data acquisition software.
28. Finally, program the ICD to make sure that its shock therapy functionality is OFF while it is still situated on the torso, without touching it. Besides, program the device to save its battery life.

H.3 Procedure for testing neuro-stimulators for exposure in/near AIT-2

Setup monitoring system and torso simulator

1. Prepare the torso simulator for neuro-stimulator testing as described in appendix I, and verify the appropriate conductivity of the saline (i.e. 0.27 S/m).
2. Mount the device under test (DUT) on the torso simulator. The DUT consists of the neuro-stimulator's Implantable Pulse Generator (IPG) and its leads shown in figure H.7. There is a millimeter-wave absorber between the IPG (which is in air) and the saline. So, connect the IPG to the saline using a wire to complete the conduction loop.

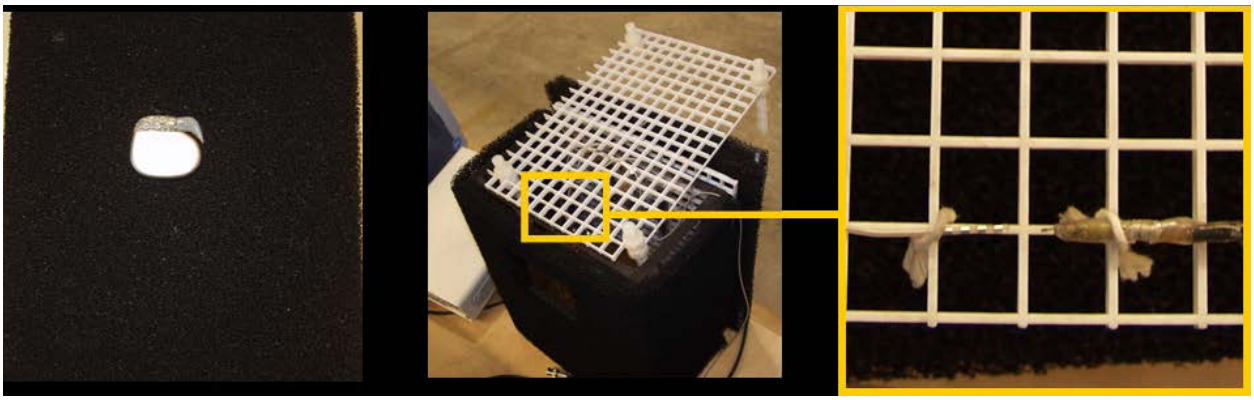

Figure H.7: This shows the installation of the DUT (neuro-stimulator) on the torso simulator.

3. Connect DUT monitoring cable leading out of the torso simulator to a digital oscilloscope through a pre amplifier.
4. Connect DUT monitoring cable (with a BNC-T) to A/D converter which is linked with the controlling PC.
5. Place the infrared detection system to detect the AIT-2 mast passing through the center of the mast travel path. Connect the output of the infrared detection system to the A/D converter.
6. Set up the data acquisition software on the PC connected to the A/D converter.
7. Check torso simulator and cables on the oscilloscope to verify minimum noise from the exposure.
8. Program DUT according to the device operating modes, and settings in appendix J and perform step 9 for each of the settings. If the DUT allows RF telemetry, set up the programmer to remotely monitor the activity of the DUT during the test. This provides an additional monitoring mechanism.
9. To verify DUT operation, run a baseline test monitoring signals from the device while the DUT/torso simulator is at a distance of at least 2 meters from the AIT-2 unit.

<u>Test the DUT in / near the AIT-2</u>

10. Power the AIT-2, log on, and calibrate the system.
11. Set up the torso simulator at the center of the AIT-2 unit (location 1) and a height of 1.3 meter from the floor (see table C.3 of appendix C for the justification used to choose the test points). DUT monitoring cables are fed out of the AIT-2 unit through a hollow fiber glass tubing oriented parallel to the floor (perpendicular to the radiated electric field and wrapped with a millimeter wave absorber).
12. Record the DUT's orientation, operating mode and settings on the data acquisition software.
13. Run the data acquisition software to start the experiment.
14. Command the AIT-2 system to activate a single scan.
15. During the scan (i.e. exposure), observe the DUT's output signal on the oscilloscope. Figure H.8 below is an example of DUT's output. At the same time, observe the screen of the programmer if the DUT is connected to the programmer using RF telemetry.

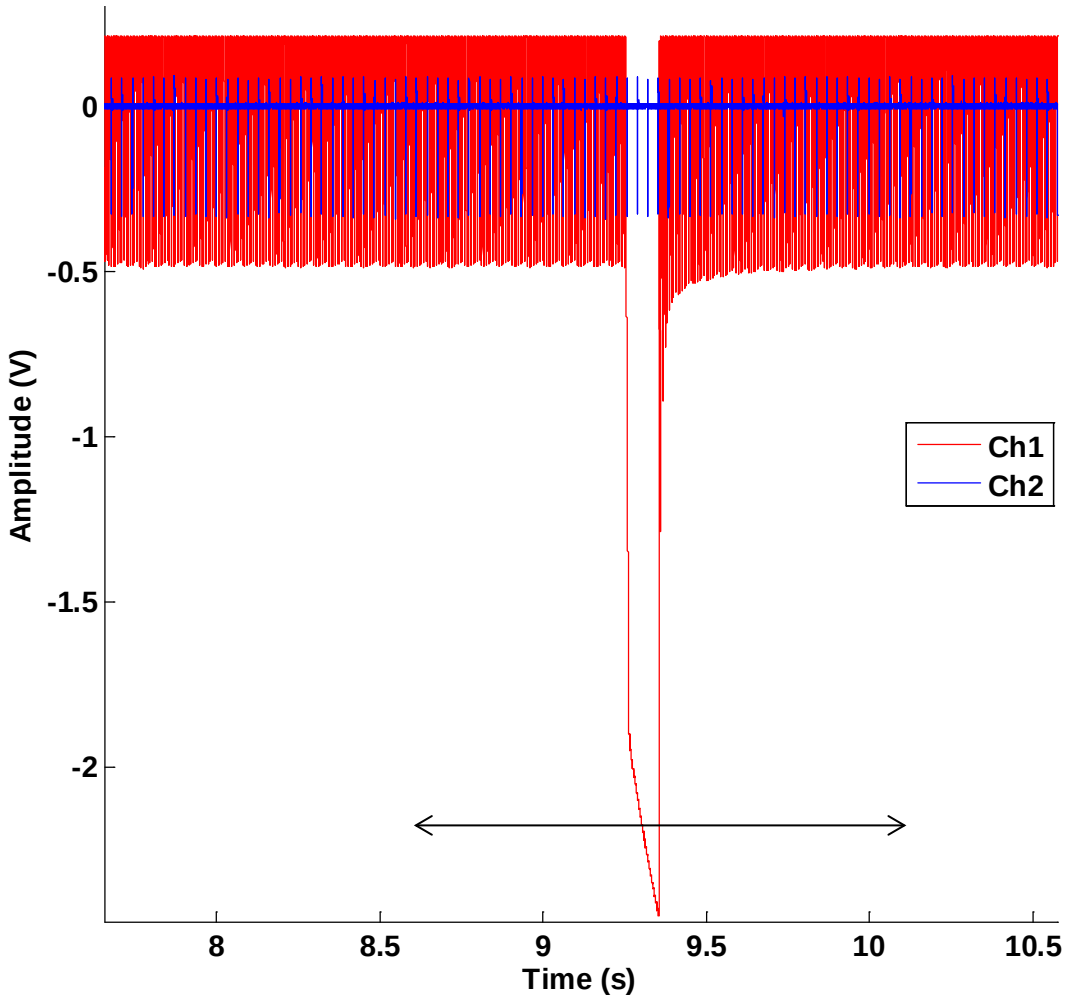

Figure H.8: Channel 2 shows the DUT Output. Channel 1 shows the Scanner Mast Motion Indicator. The black arrow shows the start and end of one scan which takes less than 1.5 s.

16. Repeat steps 14 and 15 five (5) times, recording any effects or spurious data over 30 seconds period.
17. Rotate the IPG of the DUT by 90 degrees to a new orientation as shown in Figure H.9 and repeat steps 12 to 16.
18. If the device has a magnet mode, switch from continuous (cycling) mode to the magnet mode and repeat steps 12 to 17. This is done by moving the magnet across the device.

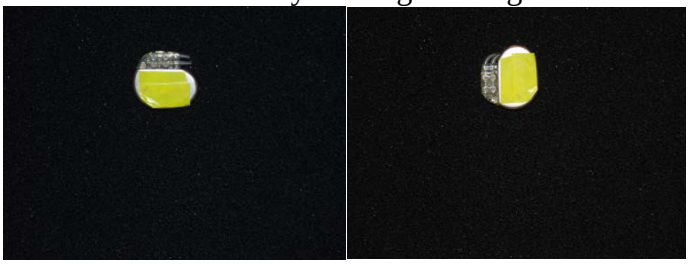

Figure H.9: The first figure shows the DUT in horizontal orientation, the second shows the DUT in vertical orientation.

19. If the device is designated for extensive testing, change the measurement point to each of the three measurement points selected in appendix C (i.e. location 1, location 2, and near the UPS), and repeat steps 12-18. One device type per manufacturer is chosen for extensive testing.
20. Retrieve any relevant files saved by the device programmer, and save them along with the data that is automatically saved by the data acquisition software.
21. Finally, program the device to a mode that saves its battery life.

H.4 Procedure for testing insulin pumps for exposure in/near AIT-2

Setup monitoring system and torso simulator

1. Prepare the torso simulator for insulin pump testing as described in appendix I.
2. Mount the devices under test (DUT) on the torso simulator. The DUT consists of an insulin pump, a glucose sensor transmitter (GST), a smart phone (iPhone), and a translator which enables communication of the insulin pump with the smart phone. The GST is attached to a load that simulates a human body with constant glucose levels. The DUT should be mounted on the outside of the torso simulator as shown in figure H.10 a. Figure H.10 b shows a 10 turn, 5 cm diameter, loop antenna that is mounted behind the millimeter-wave absorber of the torso simulator. The loop antenna is intended to monitor activations of the insulin pump motor which displaces the cylinder delivering insulin. The loop antenna may also record other communication signals from the insulin pump, and hence the loop antenna signal needs to be interpreted carefully. Since the signal from the loop antenna can be noisy, a complementary method was developed to measure the displacement of the insulin pump cylinder. This is done by using a high precision digital displacement meter. This digital displacement meter is used to measure the location of the insulin pump cylinder before and after exposure to the potential source of electromagnetic interference. The difference between the two displacement readings is compared with the expected result considering the experimental uncertainties of the measurement.

a)  b)  c) 

Figure H.10: a) This shows the installation of three components of the DUT on the exterior surface of the torso simulator. These are: the translator, the insulin pump, and the Glucose Sensor Transmitter (GST). b) The 10 turn, 5 cm diameter loop antenna was mounted inside the torso simulator behind the insulin pump. c) The smart phone that communicates with the insulin pump through the translator was also installed on the other side of the torso simulator.

3. Connect DUT monitoring cable leading out of the torso simulator to a digital oscilloscope through a pre amplifier. The DUT monitoring cable transmits signals from the loop antenna

which is designed to monitor activations of the insulin pump motor as it pushes the cylinder delivering insulin.

4. In addition, connect the above DUT monitoring cable (with a BNC-T) to A/D converter which is linked with the controlling PC.
5. Set up a data acquisition software (MATLAB based) on the PC connected to the A/D converter.
6. Place the infrared detection system to detect the AIT mast passing through the center of the mast travel path. Connect the output of the infrared detection system to the A/D converter.
7. Check the torso simulator and cables on the oscilloscope to verify minimum noise from the exposure.
8. Set up the DUT according to each of the three device test modes specified in Appendix J (i.e. idle mode, alarm mode, and bolus delivery mode) and perform step 9 for each of the modes. These test modes are chosen in accordance with [15].
9. To verify DUT operation, run a baseline test monitoring signals from the device while the DUT/torso simulator is at a distance of at least 2 meters from the AIT-2 unit.

Test the DUT in / near the AIT-2

10. Power the AIT-2, log on, and calibrate the system as necessary.
11. Set up the torso simulator at the center of the AIT-2 unit (location 1) and a height of 1.3 meter between the DUT and the floor (see table C.3 of appendix C for the justification used to choose the test points). DUT monitoring cables are fed out of the AIT-2 unit through a hollow fiber glass tubing oriented parallel to the floor (perpendicular to the radiated electric field and wrapped with a millimeter-wave absorber).
12. Record the DUT's orientation, operating mode and settings in the data acquisition software. Use the high precision displacement meter to measure the position of the insulin pump cylinder before exposure.
13. Run the data acquisition software to start the experiment.
14. Command the AIT-2 system to activate a single scan.
15. During the scan (i.e. exposure), use the oscilloscope to observe the signal from the loop antenna, which monitors the activations of the insulin pump motor. Figure H.11 below shows an example of signal from the loop antenna monitoring the insulin pump and the signal showing the movements of the AIT-2 mast.

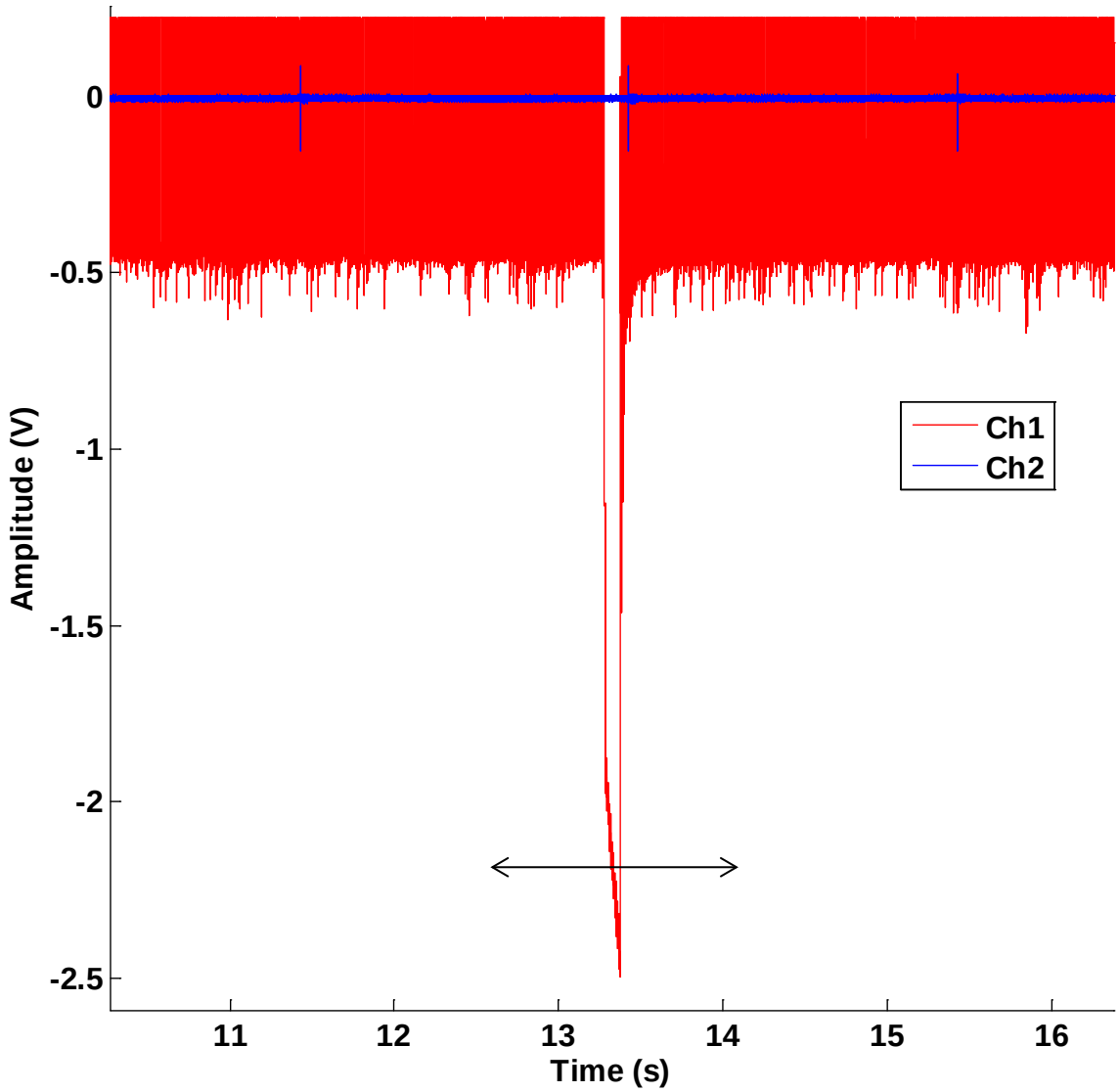

Figure H.11: Channel 1 shows the loop antenna output monitoring the insulin pump motor activations. Channel 2 shows the Scanner Mast Motion Indicator, which is generated by the infrared detection system set up in step 6. The black arrow shows the start and end of one scan which takes less than 1.5 s.

16. Repeat steps 14 and 15 five (5) times, recording any effects or spurious data over a 30 second period. In addition, physically measure any net displacement of the cylinder of the insulin pump after the 5 AIT-2 scans using the high precision displacement meter. Finally, use the smart phone, which communicates with the insulin pump using a translator device, to look for any abnormalities that may happen after the 5 AIT-2 scans. If the insulin pump is designed to test the communication to the glucose sensor transmitter (GST), check if any of the test packets that are sent every 0.5 s are lost or corrupted due to potential electromagnetic interference; typical insulin pumps communicate with the glucose sensor transmitter (GST) once every 5 minutes.
17. Rotate the insulin pump by 90 degrees to a new orientation as shown in figure H.12 and repeat steps 12 to 16.

18. Change the mode of the DUT to the rest of the three device test modes specified in appendix J (i.e. idle mode, alarm mode, and bolus delivery mode) and repeat steps 12 to 17.

Figure H.12: The first figure shows the insulin pump in horizontal orientation, the second shows the insulin pump in vertical orientation.

19. If the insulin pump is designated for extensive testing, change the measurement point to each of the three measurement points selected in appendix C (i.e. location 1, location 2, and near the UPS), and repeat steps 12-18. The extensive testing of insulin pumps at location 1 and location 2 shall also be done at two heights, which are 0.25 m and 1.3 m. One device type per manufacturer is selected for extensive testing.
20. Retrieve any relevant files saved by the device, and save them along with the data that is automatically saved by the data acquisition software.
21. Finally, turn off the devices and remove their batteries, as appropriate, before storing them.

H.5 Procedure for testing TENS for exposure in/near AIT-2

Setup monitoring system and torso simulator

1. Prepare the torso simulator for TENS testing as described in appendix I.
2. Mount the device under test (DUT) on the torso simulator. The DUT consists of a TENS device that is connected to a loop of the TENS leads as shown in figure H.13. The DUT is placed on the millimeter-wave absorber material of the torso simulator. The leads of the TENS are terminated by a 500 Ω resistor, which is connected to a coaxial cable, based on the testing standard in [16].

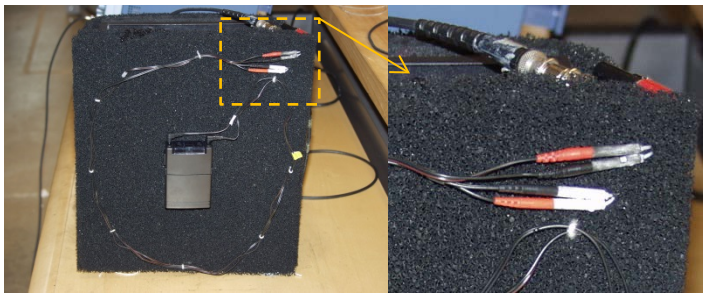

Figure H.13: This shows the installation of the DUT (TENS device) on the torso simulator.

3. Connect DUT monitoring coaxial cable leading out of the torso simulator to a digital oscilloscope through a pre amplifier.
4. Connect DUT monitoring cable (with a BNC-T) to A/D converter which is linked with the controlling PC.
5. Set up a data acquisition software (MATLAB based) on the PC connected to the A/D converter.

6. Place the infrared detection system to detect the AIT mast passing through the center of the mast travel path. Connect the output of the infrared detection system to the A/D converter.
7. Check the torso simulator and cables on the oscilloscope to verify minimum noise from the exposure.
8. Program DUT according to each of the device settings, and operating modes specified in appendix J (i.e. normal mode, modulated mode, and burst mode) and perform step 9 for each of the settings.
9. To verify DUT operation, run a baseline test monitoring signals from the device while the DUT/torso simulator is at a distance of at least 2 meters from the AIT-2 unit.

Test the DUT in / near the AIT-2

10. Power the AIT-2, log on, and calibrate the system.
11. Set up the torso simulator at the center of the AIT-2 unit (location 1) and a height of 1.3 meter from the floor (see table C.3 of appendix C for the justification used to choose the test points). DUT monitoring cables are fed out of the AIT-2 unit through a hollow fiber glass tubing oriented parallel to the floor (perpendicular to the radiated electric field and wrapped with a millimeter wave absorber).
12. Record the DUT's orientation, operating mode and settings on the data acquisition software.
13. Run the data acquisition software to start the experiment.
14. Command the AIT-2 system to activate a single scan.
15. During the scan (i.e. exposure), observe the DUT's output signal on the oscilloscope. Figure H.14 below is an example of DUT's output.

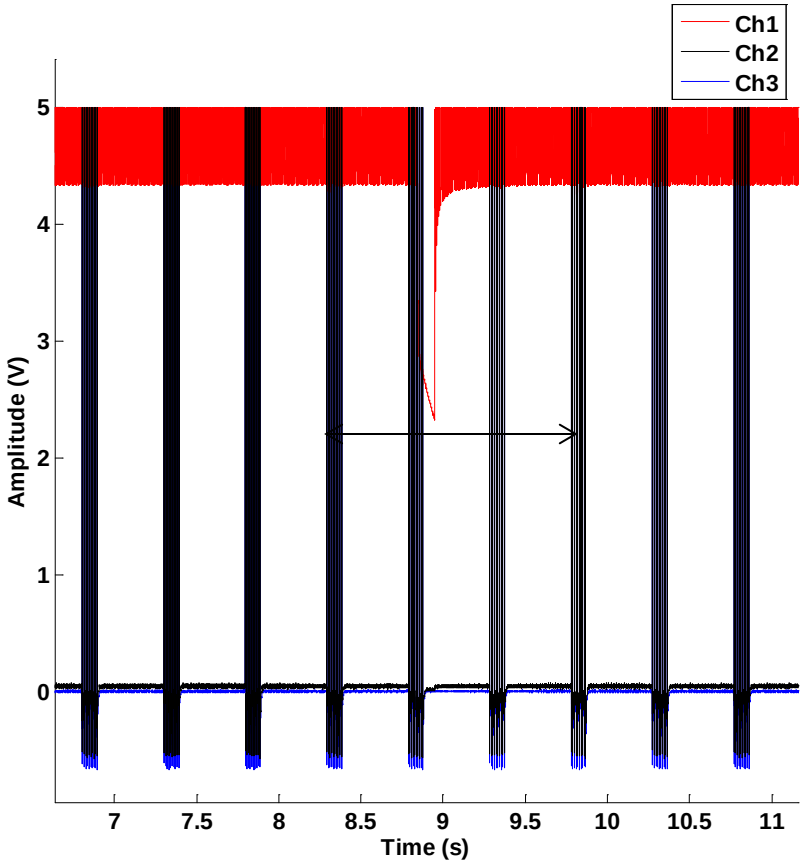

Figure H.14: Channel 2 and 3 show the DUT Output. Channel 1 shows the Scanner Mast Motion Indicator. The black arrow shows the start and end of one scan which takes less than 1.5 s.

16. Repeat steps 14 and 15 five (5) times, recording any effects or spurious data over 30 seconds period.
17. Rotate the TENS device by 90 degrees to a new orientation as shown in figure H.15 and repeat steps 12 to 16.

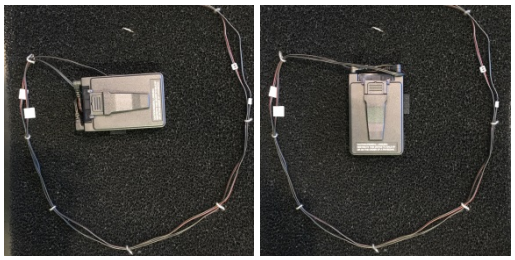
Figure H.15: The first figure shows the TENS in horizontal orientation, the second shows the TENS in vertical orientation.

18. If the device is designated for extensive testing, change the measurement point to each of the three measurement points selected in appendix C (i.e. location 1, location 2, and near the UPS), and repeat steps 12-17. One TENS device has been chosen for extensive testing.
19. Finally, turn off the devices and remove their batteries, as appropriate, before storing them.

Appendix I

Torso simulator

Engineers in the CDRH designed torso simulators (phantoms) for EMC testing of active, implantable PMEDs (such as pacemakers, ICDs and neuro stimulators), and external PMEDs (such as insulin pumps, and TENS) in conjunction with the mmW AIT units operating between 24.25 GHz to 30 GHz [17]. The design of the torso simulators for the PMEDs is discussed here.

I.1 Torso simulator for active implantable PMEDs

The torso simulator for active implantable PMEDs (pacemakers, ICDs, and neuro-stimulators) uses saline with a resistivity of 375 Ω cm (saline conductivity of 0.27 S/m), which is developed for work at much lower frequencies as specified in [11, 12]. Based on previous studies [17], the susceptibility of the PMED to mmW emissions is maximized if the Implantable Pulse Generator (IPG) is placed outside the saline in air. Thus, the torso simulator featured exposure of the device's IPG in air and placement of the device's stimulation and / or sensing leads in the saline (see Figure I.1 and Figure I.2). The signal path was completed by connecting the device IPG, which is in air, to the saline using a conducting wire. The completion of this signal path is particularly important for unipolar lead configuration. Commercially available mmW absorbing material was placed between the device IPG and the saline to minimize reflection from the surface of the saline.

I.1.i Torso simulator for cardiac PMEDs

Annex A.2.5 of the cardiac device testing standard [11] states that the layout of the cardiac PMED lead configuration is not critical at frequencies between 450 MHz and 3 GHz; section 4.9.2.3 of the standard [11] proposes a generic spiral lead configuration that can be easily repeated at these frequencies. On the other hand, Annex A.1 and Annex L.5 of the testing standard [11] recommend a closed loop lead configuration of about 225 cm^2 area for frequencies less than 450 MHz. This area is based on the estimated effective induction area of an open loop of a cardiac PMED lead inside a human body. The cardiac PMEDs tested in and around the AIT-2 may face spurious emissions that can be lower than 450 MHz; for example, the hot spot of spurious emission near the AIT-2 UPS front panel emitted at frequencies between 10 MHz to 30 MHz (please see appendix F.2 for more details). Therefore, it was decided to use a closed loop lead configuration of about 225 cm^2 for cardiac PMED testing, based on the recommendations of [11] for low frequency testing. As shown in figure I.1 and figure I.2, the cardiac PMED sits in air outside the saline, and the IPG is attached to the saline using a conducting wire. This configuration was taken into account while measuring the area of the closed loop formed by the cardiac PMED, the leads, and the saline.

As shown in figure I.1 and figure I.2, the electrical signals in the saline of the torso simulator of implantable PMEDs were sensed by an electrode that was connected to an oscilloscope through an amplifier. For cardiac PMEDs, an arbitrary waveform generator (AWG) was used to generate simulated cardiac signal according to the specifications in annex J of the standard [11]. The simulated cardiac signal was injected into the saline using an electrode.

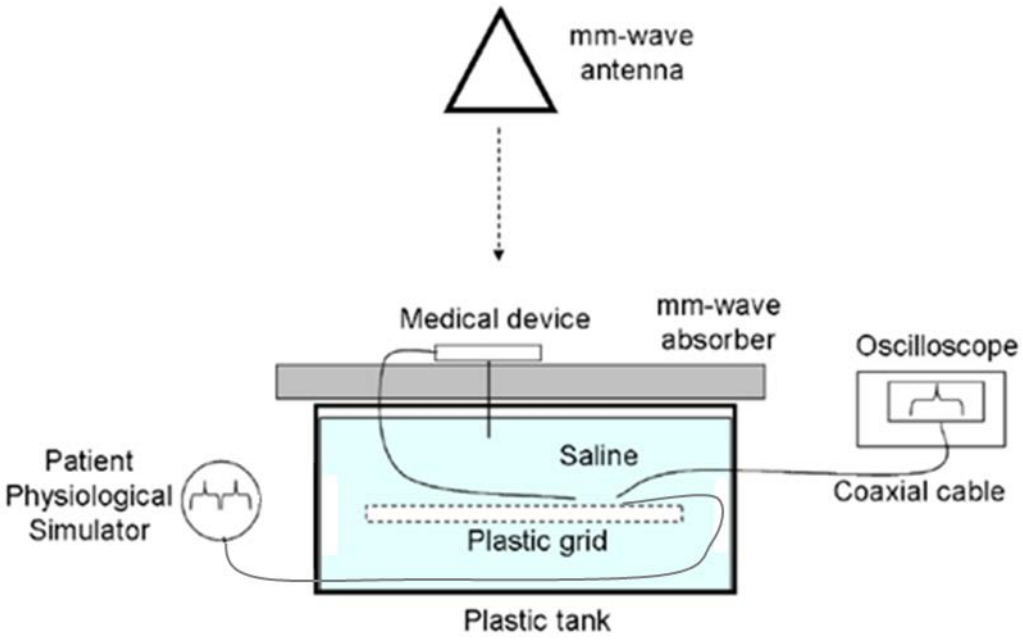

Figure I.1: Schematics of the horizontal torso simulator for cardiac PMEDs irradiated with the mmW AIT-2 simulator system.

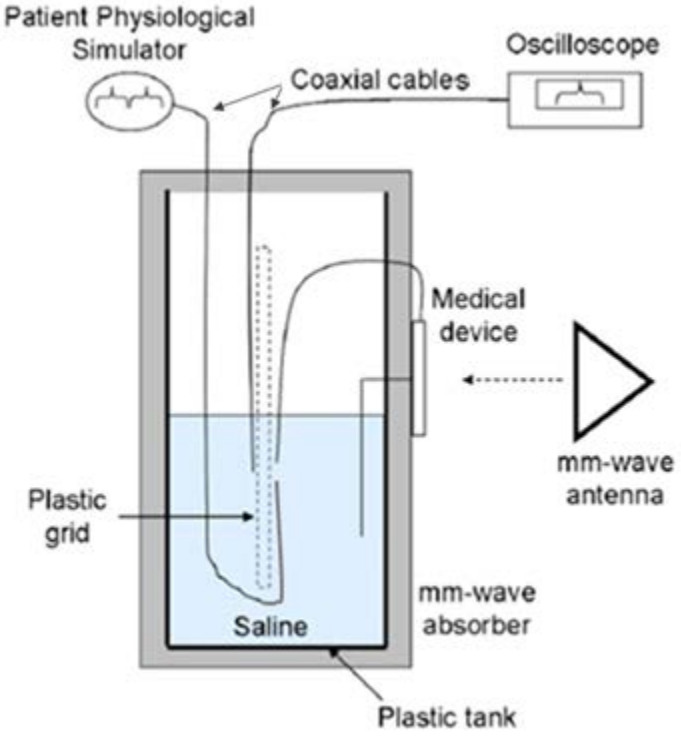

Figure I.2: Schematics of the vertical torso simulator for cardiac PMEDs irradiated with the mmW AIT-2 system.

I.1.ii Torso simulator for neuro-stimulator PMEDs

The torso simulator for testing neuro-stimulators was similar to the one designed to test cardiac PMEDs. The only difference was the absence of the AWG generating simulated cardiac signals, which involved injecting a simulated cardiac signal into the saline. In addition, the leads of the neuro-stimulator were arranged in a different manner from the cardiac leads.

The neuro-stimulator testing standard recommends three different lead configurations that correspond to three different frequency ranges. Clause 27.104 of the neuro-stimulator standard [12] recommends the use of a well-defined spiral lead configuration, which has prescribed relations between the median radius of the spiral and the length of the lead, for protection from magnetic fields with frequencies ranging from 10 Hz to 30 MHz. Clause 27.105 of [12] recommends the use of L shaped lead configuration for protection from electric fields from 30 MHz to 450 MHz. Clause 27.106 of [12] recommends the use of a simpler spiral for protection from electromagnetic fields from 450 MHz to 3 GHz.

Based on the results of appendix E and appendix F, the strongest emission occurred roughly between 10 MHz and 30 MHz at the front panel of the UPS. Therefore, it was important to configure the leads based on the prescription for protection from magnetic fields from 10 Hz to 30 MHz, as there is a higher probability of exposure to these fields. The part of the neuro-stimulator that is most susceptible to the electric fields is the connector header of the IPG, which was directly exposed to the fields in air. Therefore, the spiral shaped lead configuration was used instead of the L shape to prioritize testing of magnetic fields from 10 Hz to 30 MHz and electromagnetic fields from 450 MHz to 3 GHz. Depending on the length of the leads, the spirals specified by clause 27.104 and 27.106 of [12] may be slightly different. Whenever such discrepancies arose the lead that maximized the area of the loop was chosen.

I.2 Torso simulator for active external PMEDs

The main difference between the torso simulator for implantable and external PMEDs is that the torso for the external PMEDs does not have a saline. The torso for external PMEDs simply consists of a box that is surrounded by a mmW absorber. The external PMEDs (insulin pump and TENS) are installed outside the mmW absorber facing the incoming waves directly. The insulin pump may have other accompanying accessories such as a Glucose Sensor Transmitter (GST), a translator, and a smart phone. All of these accessories are also installed outside the mmW absorber facing the incoming waves. A 5cm diameter 10 turn loop antenna is placed underneath the insulin pump behind the mmW absorber; this is used to monitor the activations of the motor of the insulin pump. In the case of TENS, their leads were simply arranged outside the mmW absorber to form a loop that is as large as possible to test for susceptibilities to magnetic fields. The TENS device itself was also placed on top of the mmW absorber to maximize the exposure. The leads of the TENS were terminated by a 500 Ω resistor, which is connected to a coaxial cable, based on the relevant testing standard [16].

Appendix J

PMED device under test settings

PMED sample devices included implantable cardiac pacemakers, implantable cardioverter defibrillators, neuro-stimulators, insulin pumps, and TENS. Each PMED has a number of settings and functions that can be used to treat patients. With some PMEDs there are many settings and thousands of possible combinations. For this project, key functions and settings were used for the devices based upon experience with the devices, history of EMI issues, and suggestions by the device manufacturers. The following information provides more details about these sample PMEDs (i.e. device under test (DUT)) and the settings on these devices used during EMC testing.

H.1 Pacemaker and ICD test settings

The DUT for cardiac PMEDs involves an implantable pulse generator (IPG) and a sensing or pacing lead. The DUT was physically set up inside the torso simulator by putting the leads inside the saline and the IPG in air. The IPG was connected to the saline using a conducting wire that completed the circuit. Please see appendix I for details about the setup of the torso simulator for cardiac PMEDs.

The implantable cardiac devices (pacemaker and ICD) were tested both with and without injected simulated cardiac signal. Table J.1 describes the major device modes and functions typical for these device types. DDD settings were used in lieu of VVI and AAI modes; because, the DDD mode enables testing both of the channels (i.e. ventricular and atrial) using all the functions (i.e. atrial and ventricular sensing, atrial and ventricular pacing, atrial and ventricular inhibition, triggered ventricular pacing). If a cardiac device is a single chamber device, the VVI mode is tested.

The sensing and pacing polarities of pacemakers could either be unipolar or bipolar. Therefore, the pacemakers are tested both with unipolar and bipolar settings even though the unipolar settings are the ones that are more susceptible to electromagnetic interference. If the unipolar setting is not available, the pacemaker is tested only with the bipolar setting. The sample ICD devices also operate only in bipolar setting, and they were tested as such.

The cardiac rate response functionality allows the device to sense the heart rate and make adjustments to the device output rate. The device tries to replicate the normal heart behavior and changes the pacing rate in response to patient needs for their physical activity. This setting was disabled because it introduces significant waiting time period after cardiac device setup until the device settles back to normal condition.

The maximum sensitivity settings were used to increase the likelihood of observing a device failure due to EMI during the test. The settings involved with each device category are shown in table J.2.The refractory setting for implantable pacemakers and ICDs is the time period when the device becomes unresponsive to the cardiac signals and does not sense.

Some ICDs have a “monitor only” mode that can be used to perform the test safely without delivering an electric shock. For ICDs that do not have this safe mode, the actual device output for cardiac shock was set at minimum energy to prevent equipment damages or personal injuries.

DDD	Dual (i.e. atrial and ventricular) pacing, Dual (i.e. atrial and ventricular) sensing and inhibition of each chamber when sensed from the same chamber
VVI	Ventricular pacing, Ventricular sensing and Inhibition upon ventricular sensing.

Table J.1: Test mode used for implantable cardiac devices. Note that VVI are used only for the appropriate single chamber devices that do not support DDD.

Device Category	Maximum Sensitivity Setting
Implantable Pacemaker	Atrial Amplitude: 3.5 V Atrial Pulse Width: 340 µs - 400 µs Minimum Atrial Sensitivity Values: 0.1 mV – 0.5 mV Minimum Atrial Refractory: 125 - 325 ms Ventricular Amplitude: 3.4 V - 3.5 V Ventricular Pulse Width: 340 µs - 400 µs Minimum Ventricular Sensitivity values: 0.25 mV - 1 mV Minimum Ventricular Refractory: 125 ms - 200 ms
Implantable Cardioverter Defibrillator (ICD)	Atrial Amplitude: 3.5 V Atrial Pulse Width: 400 µs Atrial Sensitivity: 0.15 mV - 0.2 mV Atrial Refractory: 93 ms - 375 ms Right Ventricular Amplitude: 3.5 V Right Ventricular Pulse Width: 400 µs Left Ventricular Amplitude: 3.5 V Left Ventricular Pulse Width: 400 µs Ventricular Sensitivity: 0.15 mV - 0.5 mV Ventricular Refractory: 125 ms - 150 ms Shock: Monitor only or Minimum Energy

Table J.2: These are the range of values used to test the cardiac PMEDs under conditions of maximum sensitivity.

J.2 Neuro-stimulator test settings

The device under test (DUT) for neuro-stimulator PMEDs involves an implantable pulse generator (IPG) and a lead. The DUT was physically set up inside the torso simulator by putting the leads inside the saline and the IPG in air. The IPG was connected to the saline using a conducting wire that completed the circuit. Please see appendix I for details about the setup of the torso simulator for neuro-stimulators.

There are three fundamental parameters that can be used to define the output of a signal from a neuro-stimulator. These are: the amplitude of the output current/voltage, the pulse width, and the pulse rate. The values of these three parameters that were used are shown in table J.4, along with other parameters. Some neuro-stimulators stimulate continuously under their normal mode whereas others stimulate cyclically. The cyclical operation is defined with the duration of the on time and the off time for the output signal.

Some neuro-stimulators operate both in normal mode and magnet mode. The magnet mode is turned on by swiping a magnet above the IPG of the neuro-stimulator. The magnet mode can be used to modify (e.g. enhance the amplitude, change the pulse width …) the stimulation or to turn the stimulation off. If the magnet mode involves enhanced stimulation, it lasts for a preprogrammed period of time before the device goes back to its normal mode. If the magnet is used to turn off the device, the device can be turned back on using the same magnet.

Neuro-stimulator parameters	Recommended Sensitivity Settings
Amplitude of output current/voltage (normal mode)	1.5 mA, 5mA, 5V
Pulse Width (normal mode)	210 μs, 250 μs
Pulse Rate (normal mode)	20 Hz, 25 Hz, 30 Hz, 31Hz, 45Hz,
On Time (normal mode)	10s, 30 s
Off Time (normal mode)	0.1s, 150 s
Magnet mode current	1.75 mA
Magnet mode on time	30 s
Magnet mode pulse width	500 μs

Table J.3: These are the values used to test the neuro-stimulators based on recommendations from the manufacturers.

J.3 Insulin pump test settings

The device under test (DUT) for insulin pump PMEDs may consist of an insulin pump, a translator, a glucose sensor transmitter (GST), and a smart phone. The components of the DUT were physically set up on the exterior surface of the torso simulator. Please see appendix I for details about the setup of the torso simulator for external PMEDs such as insulin pumps.

There were three kinds of insulin pumps tested. The first kind was regular insulin pumps that communicate with the GST once every five minutes. The second kind was a special insulin pump that is designed to solely test the communication with a 2 Hz GST at a relatively high 2 Hz rate. The third kind was insulin pumps that do not have the capability to communicate with a GST. The first kind of insulin pumps mentioned above also communicates with a smart phone through a frequency translator. Insulin pumps are typically tested under three modes (i.e. idle mode, alarm mode, and bolus mode) according to the relevant standard [15].

The special insulin pump, which is designed to test the communication with GST at a relatively high rate of 2 Hz, does not have a cylinder and cannot be tested with alarm mode and bolus mode. It was only tested with the idle mode while it communicated at a 2 Hz rate; we call this "PING at 2 Hz" mode. The screen on this insulin pump indicates if there are any bad or lost packets during the communication with the GST. All other insulin pumps (other than the ones of the second kind mentioned above) were tested using the idle mode, alarm mode, and bolus mode.

The insulin pumps were set up to deliver the smallest measurable amount of bolus during the bolus delivery mode test. Most of the insulin pumps were set up to deliver just 1 unit of bolus. However, one insulin pump had to be set up to deliver 16 units of bolus because that was the smallest that could be reliably measured.

J.4 TENS test settings

The device under test (DUT) for TENS PMEDs consists of the TENS device and the accompanying leads. The components of the DUT were physically set up on the exterior surface of the torso simulator. Please see appendix I for details about the setup of the torso simulator for external PMEDs such as TENS.

The three parameters that define the output of most TENS devices are frequency, pulse width, and amplitude of the output current. Some of the TENS devices can also be configured in different modes such as: normal mode, modulated mode, and burst mode. If a TENS device does not have a modulated mode and burst mode, it is only tested with the normal mode which is the default mode. The parameters and modes shown in table J.4 were used to test the TENS devices.

Parameters	Values
Current in arbitrary units	3 out of 8
Frequency	8 Hz, 10 Hz, 100 Hz
Pulse Width	150 µs, 180 µs
Mode	Normal, Modulated, Burst

Table J.4: These are the parameter values, and modes used to test the TENS.

Appendix K

Findings for PMED Testing in the AIT-2

The results of PMED test in the AIT-2 are presented in this appendix. The general PMED settings and explanation about the test modes are in appendix J.

Device	Location	Height	Test Mode	Lead Configuration	Cardiac Signal	Orientation	Observed Reaction
A1	1	1.3 m	DDD	Unipolar	On	Horizontal	None
						Vertical	None
					Off	Horizontal	None
						Vertical	None
				Bipolar	On	Horizontal	None
						Vertical	None
					Off	Horizontal	None
						Vertical	None
	2	1.3 m	DDD	Unipolar	On	Horizontal	None
						Vertical	None
					Off	Horizontal	None
						Vertical	None
				Bipolar	On	Horizontal	None
						Vertical	None
					Off	Horizontal	None
						Vertical	None
	UPS	0.75 m	DDD	Unipolar	On	Horizontal	None
						Vertical	None
					Off	Horizontal	None
						Vertical	None
				Bipolar	On	Horizontal	None
						Vertical	None
					Off	Horizontal	None
						Vertical	None
A2	1	1.3 m	DDD	Unipolar	On	Horizontal	None
						Vertical	None
					Off	Horizontal	None
						Vertical	None
				Bipolar	On	Horizontal	None
						Vertical	None
					Off	Horizontal	None
						Vertical	None
	2	1.3 m	DDD	Unipolar	On	Horizontal	None
						Vertical	None
					Off	Horizontal	None
						Vertical	None

Device	Location	Height	Test Mode	Lead Configuration	Cardiac Signal	Orientation	Observed Reaction
				Bipolar	On	Horizontal	None
						Vertical	None
					Off	Horizontal	None
						Vertical	None
	UPS	0.75 m	DDD	Unipolar	On	Horizontal	None
						Vertical	None
					Off	Horizontal	None
						Vertical	None
				Bipolar	On	Horizontal	None
						Vertical	None
					Off	Horizontal	None
						Vertical	None
A3	1	1.3 m	DDD	Unipolar	On	Horizontal	None
						Vertical	None
					Off	Horizontal	None
						Vertical	None
				Bipolar	On	Horizontal	None
						Vertical	None
					Off	Horizontal	None
						Vertical	None
	2	1.3 m	DDD	Unipolar	On	Horizontal	None
						Vertical	None
					Off	Horizontal	None
						Vertical	None
				Bipolar	On	Horizontal	None
						Vertical	None
					Off	Horizontal	None
						Vertical	None
	UPS	0.75 m	DDD	Unipolar	On	Horizontal	None
						Vertical	None
					Off	Horizontal	None
						Vertical	None
				Bipolar	On	Horizontal	None
						Vertical	None
					Off	Horizontal	None
						Vertical	None
A4	1	1.3 m	DDD	Unipolar	On	Horizontal	None
						Vertical	None
					Off	Horizontal	None
						Vertical	None
				Bipolar	On	Horizontal	None
						Vertical	None
					Off	Horizontal	None

Device	Location	Height	Test Mode	Lead Configuration	Cardiac Signal	Orientation	Observed Reaction
						Vertical	None
	2	1.3 m	DDD	Unipolar	On	Horizontal	None
						Vertical	None
					Off	Horizontal	None
						Vertical	None
				Bipolar	On	Horizontal	None
						Vertical	None
					Off	Horizontal	None
						Vertical	None
	UPS	0.75 m	DDD	Unipolar	On	Horizontal	None
						Vertical	None
					Off	Horizontal	None
						Vertical	None
				Bipolar	On	Horizontal	None
						Vertical	None
					Off	Horizontal	None
						Vertical	None
A5	1	1.3 m	DDD	Unipolar	On	Horizontal	None
						Vertical	None
					Off	Horizontal	None
						Vertical	None
				Bipolar	On	Horizontal	None
						Vertical	None
					Off	Horizontal	None
						Vertical	None
	2	1.3 m	DDD	Unipolar	On	Horizontal	None
						Vertical	None
					Off	Horizontal	None
						Vertical	None
				Bipolar	On	Horizontal	None
						Vertical	None
					Off	Horizontal	None
						Vertical	None
	UPS	0.75 m	DDD	Unipolar	On	Horizontal	None
						Vertical	None
					Off	Horizontal	None
						Vertical	None
				Bipolar	On	Horizontal	None
						Vertical	None
					Off	Horizontal	None
						Vertical	None
A6	1	1.3 m	DDD	Unipolar	On	Horizontal	None
						Vertical	None

Device	Location	Height	Test Mode	Lead Configuration	Cardiac Signal	Orientation	Observed Reaction
					Off	Horizontal	None
						Vertical	None
				Bipolar	On	Horizontal	None
						Vertical	None
					Off	Horizontal	None
						Vertical	None
A7	1	1.3 m	DDD	Unipolar	On	Horizontal	None
						Vertical	None
					Off	Horizontal	None
						Vertical	None
				Bipolar	On	Horizontal	None
						Vertical	None
					Off	Horizontal	None
						Vertical	None
A8	1	1.3 m	DDD	Unipolar	On	Horizontal	None
						Vertical	None
					Off	Horizontal	None
						Vertical	None
				Bipolar	On	Horizontal	None
						Vertical	None
					Off	Horizontal	None
						Vertical	None
A9	1	1.3 m	VVI	Unipolar	On	Horizontal	None
						Vertical	None
					Off	Horizontal	None
						Vertical	None
				Bipolar	On	Horizontal	None
						Vertical	None
					Off	Horizontal	None
						Vertical	None
A10	1	1.3 m	VVI	Unipolar	On	Horizontal	None
						Vertical	None
					Off	Horizontal	None
						Vertical	None
				Bipolar	On	Horizontal	None
						Vertical	None
					Off	Horizontal	None
						Vertical	None
A11	1	1.3 m	DDD	Unipolar	On	Horizontal	None
						Vertical	None
					Off	Horizontal	None
						Vertical	None
				Bipolar	On	Horizontal	None

Device	Location	Height	Test Mode	Lead Configuration	Cardiac Signal	Orientation	Observed Reaction
						Vertical	None
					Off	Horizontal	None
						Vertical	None
A12	1	1.3 m	DDD	Unipolar	On	Horizontal	None
						Vertical	None
					Off	Horizontal	None
						Vertical	None
				Bipolar	On	Horizontal	None
						Vertical	None
					Off	Horizontal	None
						Vertical	None
A13	1	1.3 m	DDD	Bipolar (Note: A13 works only with bipolar pacing.)	On	Horizontal	None
						Vertical	None
					Off	Horizontal	None
						Vertical	None
A14	1	1.3 m	DDD	Unipolar	On	Horizontal	None
						Vertical	None
					Off	Horizontal	None
						Vertical	None
				Bipolar	On	Horizontal	None
						Vertical	None
					Off	Horizontal	None
						Vertical	None

Table K.1 Test data of sample Implantable Pacemakers. Pacemakers A1, A2, A3, A4, and A5 were selected for additional testing.

Device	Location	Height	Test Mode	Lead Configuration	Cardiac Signal	Orientation	Observed Reaction
B1	1	1.3 m	DDD	Bipolar	On	Horizontal	None
						Vertical	None
					Off	Horizontal	None
						Vertical	None
	2	1.3 m	DDD	Bipolar	On	Horizontal	None
						Vertical	None
					Off	Horizontal	None
						Vertical	None
	UPS	0.75 m	DDD	Bipolar	On	Horizontal	None
						Vertical	None
					Off	Horizontal	None
						Vertical	None
B2	1	1.3 m	DDD	Bipolar	On	Horizontal	None
						Vertical	None
					Off	Horizontal	None

						Vertical	None
	2	1.3 m	DDD	Bipolar	On	Horizontal	None
						Vertical	None
					Off	Horizontal	None
						Vertical	None
	UPS	0.75 m	DDD	Bipolar	On	Horizontal	None
						Vertical	None
					Off	Horizontal	None
						Vertical	None
B3	1	1.3 m	DDD	Bipolar	On	Horizontal	None
						Vertical	None
					Off	Horizontal	None
						Vertical	None
	2	1.3 m	DDD	Bipolar	On	Horizontal	None
						Vertical	None
					Off	Horizontal	None
						Vertical	None
	UPS	0.75 m	DDD	Bipolar	On	Horizontal	None
						Vertical	None
					Off	Horizontal	None
						Vertical	None
B4	1	1.3 m	VVI	Bipolar	On	Horizontal	None
						Vertical	None
					Off	Horizontal	None
						Vertical	None
	2	1.3 m	VVI	Bipolar	On	Horizontal	None
						Vertical	None
					Off	Horizontal	None
						Vertical	None
	UPS	0.75 m	VVI	Bipolar	On	Horizontal	None
						Vertical	None
					Off	Horizontal	None
						Vertical	None
B5	1	1.3 m	DDD	Bipolar	On	Horizontal	None
						Vertical	None
					Off	Horizontal	None
						Vertical	None
B6	1	1.3 m	DDD	Bipolar	On	Horizontal	None
						Vertical	None
					Off	Horizontal	None
						Vertical	None
B7	1	1.3 m	DDD	Bipolar	On	Horizontal	None
						Vertical	None
					Off	Horizontal	None
						Vertical	None

B8	1	1.3 m	VDD	Bipolar	On	Horizontal	None
						Vertical	None
					Off	Horizontal	None
						Vertical	None
B9	1	1.3 m	VVI	Bipolar	On	Horizontal	None
						Vertical	None
					Off	Horizontal	None
						Vertical	None
B10	1	1.3 m	DDD	Bipolar	On	Horizontal	None
						Vertical	None
					Off	Horizontal	None
						Vertical	None
B11	1	1.3 m	DDD	Bipolar	On	Horizontal	None
						Vertical	None
					Off	Horizontal	None
						Vertical	None
B12	1	1.3 m	DDD	Bipolar	On	Horizontal	None
						Vertical	None
					Off	Horizontal	None
						Vertical	None
B13	1	1.3 m	DDD	Bipolar	On	Horizontal	None
						Vertical	None
					Off	Horizontal	None
						Vertical	None
B14	1	1.3 m	VVI	Bipolar	On	Horizontal	None
						Vertical	None
					Off	Horizontal	None
						Vertical	None
B15	1	1.3 m	VVI	Bipolar	On	Horizontal	None
						Vertical	None
					Off	Horizontal	None
						Vertical	None

Table K.2 Test data of sample Implantable Cardioverter Defibrillators. ICDs B1, B2, B3, and B4 were selected for additional testing.

Device	Location	Height	Test Mode	Orientation	Observed Reaction
C1	1	1.3 m	Normal	Horizontal	None
				Vertical	None
			Magnet	Horizontal	None
				Vertical	None
	2	1.3 m	Normal	Horizontal	None
				Vertical	None
			Magnet	Horizontal	None
				Vertical	None
	UPS	0.75 m	Normal	Horizontal	None
				Vertical	None
			Magnet	Horizontal	None
				Vertical	None
C2	1	1.3 m	Normal	Horizontal	None
				Vertical	None
			Magnet	Horizontal	None
				Vertical	None
	2	1.3 m	Normal	Horizontal	None
				Vertical	None
			Magnet	Horizontal	None
				Vertical	None
	UPS	0.75 m	Normal	Horizontal	None
				Vertical	None
			Magnet	Horizontal	None
				Vertical	None
C3	1	1.3 m	Normal	Horizontal	None
				Vertical	None
			Off	Horizontal	None
				Vertical	None
C4	1	1.3 m	Normal	Horizontal	None
				Vertical	None
			Off	Horizontal	None
				Vertical	None
C5	1	1.3 m	Normal	Horizontal	None
				Vertical	None

Device	Location	Height	Test Mode	Orientation	Observed Reaction
			Off	Horizontal	None
				Vertical	None
C6	1	1.3 m	Normal	Horizontal	None
				Vertical	None
			Off	Horizontal	None
				Vertical	None
C7	1	1.3 m	Normal	Horizontal	None
				Vertical	None
			Off	Horizontal	None
				Vertical	None
C8	1	1.3 m	Normal	Horizontal	None
				Vertical	None
			Off	Horizontal	None
				Vertical	None
C9	1	1.3 m	Normal	Horizontal	None
				Vertical	None
			Off	Horizontal	None
				Vertical	None
C10	1	1.3 m	Normal	Horizontal	None
				Vertical	None
			Off	Horizontal	None
				Vertical	None
C11	1	1.3 m	Normal	Horizontal	None
				Vertical	None
			Off	Horizontal	None
				Vertical	None

Table K.3 Test data of sample Implantable Neuro-stimulators. Neuro-stimulators C1, and C2 were selected for additional testing. Neuro-stimulators C1, and C2 also had the magnet mode which enables the device to be turned off and / or mode switched. The rest of the neuro-stimulators (i.e. C3 to C11) do not have magnet mode, which enables turning off the device; therefore, they were also tested after turning them off using the clinician programmer.

Device	Location	Height	Test Mode	Orientation	Observed Reaction
D1	1	0.25 m	1 Unit Bolus	Horizontal	None
				Vertical	None
			Alarm	Horizontal	None
				Vertical	None
			Idle	Horizontal	None
				Vertical	None
		1.3 m	1 Unit Bolus	Horizontal	None
				Vertical	None
			Alarm	Horizontal	None
				Vertical	None

Device	Location	Height	Test Mode	Orientation	Observed Reaction
			Idle	Horizontal	None
				Vertical	None
	2	0.25 m	1 Unit Bolus	Horizontal	None
				Vertical	None
			Alarm	Horizontal	None
				Vertical	None
			Idle	Horizontal	None
				Vertical	None
		1.3 m	1 Unit Bolus	Horizontal	None
				Vertical	None
			Alarm	Horizontal	None
				Vertical	None
			Idle	Horizontal	None
				Vertical	None
	UPS	0.75 m	1 Unit Bolus	Horizontal	None
				Vertical	None
			Alarm	Horizontal	None
				Vertical	None
			Idle	Horizontal	None
				Vertical	None
D2	1	0.25 m	PING at 2Hz	Horizontal	None
				Vertical	None
		1.3 m	PING at 2Hz	Horizontal	None
				Vertical	None
	2	0.25 m	PING at 2Hz	Horizontal	None
				Vertical	None
		1.3 m	PING at 2Hz	Horizontal	None
				Vertical	None
	UPS	0.75 m	PING at 2Hz	Horizontal	None
				Vertical	None
D3	1	0.25 m	16 Unit Bolus	Horizontal	None
				Vertical	None
			Alarm	Horizontal	None
				Vertical	None
			Idle	Horizontal	None
				Vertical	None
		1.3 m	16 Unit Bolus	Horizontal	None
				Vertical	None
			Alarm	Horizontal	None
				Vertical	None
			Idle	Horizontal	None
				Vertical	None
	2	0.25 m		Horizontal	None

Device	Location	Height	Test Mode	Orientation	Observed Reaction
			16 Unit Bolus	Vertical	None
			Alarm	Horizontal	None
				Vertical	None
			Idle	Horizontal	None
				Vertical	None
		1.3 m	16 Unit Bolus	Horizontal	None
				Vertical	None
			Alarm	Horizontal	None
				Vertical	None
			Idle	Horizontal	None
				Vertical	None
	UPS	0.75 m	16 Unit Bolus	Horizontal	None
				Vertical	None
			Alarm	Horizontal	None
				Vertical	None
			Idle	Horizontal	None
				Vertical	None
D4	1	1.3 m	1 Unit Bolus	Horizontal	None
				Vertical	None
			Alarm	Horizontal	None
				Vertical	None
			Idle	Horizontal	None
				Vertical	None
D5	1	1.3 m	1 Unit Bolus	Horizontal	None
				Vertical	None
			Alarm	Horizontal	None
				Vertical	None
			Idle	Horizontal	None
				Vertical	None
D6	1	1.3 m	1 Unit Bolus	Horizontal	None
				Vertical	None
			Alarm	Horizontal	None
				Vertical	None
			Idle	Horizontal	None
				Vertical	None
D7	1	1.3 m	1 Unit Bolus	Horizontal	None
				Vertical	None
			Alarm	Horizontal	None
				Vertical	None
			Idle	Horizontal	None
				Vertical	None
D8	1	1.3 m	1 Unit Bolus	Horizontal	None

Device	Location	Height	Test Mode	Orientation	Observed Reaction
				Vertical	None
			Alarm	Horizontal	None
				Vertical	None
			Idle	Horizontal	None
				Vertical	None
D9	1	1.3 m	1 Unit Bolus	Horizontal	None
				Vertical	None
			Alarm	Horizontal	None
				Vertical	None
			Idle	Horizontal	None
				Vertical	None

Table K.4 Test data of sample Insulin Pumps. D1, D2 and D3 were selected for additional testing.

Insulin pump D2 is a special insulin pump designed solely to test the communication between the insulin pump and the GST; it communicates with the special test GST at a 2 Hz rate. Insulin pump D1, D5, D6, D7, and D8 are regular insulin pumps that communicate with a Glucose Sensor Transmitter (GST) once every five minutes, making it harder to detect the effect of electromagnetic interference on the communication scheme. Insulin pump D3, D4, and D9 are regular insulin pumps that do not have the capability to communicate with a GST.

D2 does not have a reservoir for insulin delivery, and it is only tested with the "PING at 2 Hz" mode, which is an idle mode. Most of the insulin pumps are tested while delivering just 1 unit of bolus. However, D3 was tested while delivering 16 units of bolus because its cylinder does not move in small enough increments to make accurate measurements of the cylinder's displacement. D1, D2, and D3 were selected for additional testing.

Device	Location	Height	Test Mode	Orientation	Observed Reaction
E1	1	1.3 m	Normal	Horizontal	None
				Vertical	None
	2	1.3 m	Normal	Horizontal	None
				Vertical	None
	UPS	0.75 m	Normal	Horizontal	Sporadic subtle EMI that was mainly seen under limited circumstances (please see appendix L for details)

Device	Location	Height	Test Mode	Orientation	Observed Reaction
				Vertical	Sporadic subtle EMI that was mainly seen under limited circumstances (please see appendix L for details)
E2	1	1.3 m	Normal	Horizontal	None
				Vertical	None
			Modulated	Horizontal	None
				Vertical	None
			Burst	Horizontal	None
				Vertical	None
E3	1	1.3 m	Normal	Horizontal	None
				Vertical	None
			Modulated	Horizontal	None
				Vertical	None
			Burst	Horizontal	None
				Vertical	None
E4	1	1.3 m	Normal	Horizontal	None
				Vertical	None
			Modulated	Horizontal	None
				Vertical	None
			Burst	Horizontal	None
				Vertical	None

Table K.5 Test data of sample Transcutaneous Electrical Nerve Stimulators (TENS). E1 was selected for additional testing. The TENS device E1 showed sporadic subtle EMI effects that are discussed at length in appendix L.

Appendix L

Testing of TENS near the UPS of the AIT-2

L.1 Motivation

The out of band emission measurements in appendix F showed that there is a hot spot of spurious emission at the UPS (uninterruptible power supply) of the AIT-2. The field strengths were shown to decay to the background level within about 15 cm of the front panel of the UPS. Since it is plausible to have a PMED within 15 cm of the front panel of the UPS, CDRH decided to test some of the PMEDs there. Please see appendix C for detailed discussion of the choice of locations to perform the PMED testing.

None of the pacemakers, ICDs, neuro-stimulators, and insulin pumps tested immediately next to the front panel of the UPS was affected by an electromagnetic interference (EMI). However, there was one TENS device that was affected by EMI when it was tested using a low battery voltage condition, which is not advised by the TENS manufacturer's labeling, within less than 2 cm of the front panel of the UPS. This is the E1 TENS mentioned in table K.5 of appendix K. A newer TENS unit with the same model name as E1 but different serial number was also tested to check for reproducibility of the results; this newer TENS is called E1.2 from now on. The additional TENS testing results near the UPS of the AIT-2 are discussed next.

L.2 Experimental results and analysis

L.2.i Testing TENS with a low battery voltage condition

Figure L.1 illustrates the EMI that was observed when the E1 TENS, which was being operated under low battery voltage (i.e. < 6 V) condition, was placed within less than 2 cm of the front panel of the UPS of the AIT-2. The E1 TENS is mentioned in table K.5 of appendix K. The E1 TENS was affected by EMI under all of its three available frequency settings (i.e. 0.3 Hz, 8 Hz, and 80 Hz). However, the study was focused on just one of these frequency settings (i.e. 8 Hz) to simplify the presentation. The EMI resulted in an increase in the number of 'individual pulses' from 3 to 5 when parts b and c of figure L.1 are visually compared with part a. This was roughly driven by a ~ 7 % increase in the pulse width of the underlying signal that is modulating the continuous wave (CW) output of the TENS at 8 Hz, and a ~ 7 % decrease in the width of the 'individual pulses' whose number has increased consequently; for the baseline case, part c of figure L.1 shows that the pulse width of the modulating signal is about 0.56 s, and the 'individual pulses' have a width that is at most ~ 65 ms. The BNC cable picking up the signal from the E1 TENS also picked up some noise from the UPS spurious emission resulting in the background fluctuations in part b of figure L.1 as compared with part c, which is the baseline.

The user manual of the E1 TENS recommended the use of full battery voltage (i.e. 9 V). The low battery voltage (i.e. < 6 V) facilitated the EMI shown in figure L.1. The low battery voltage

condition experiment was shown to be reproducible using the E1.2 TENS. The results of the experiments with E1 and E1.2 TENS are summarized in table L.1.

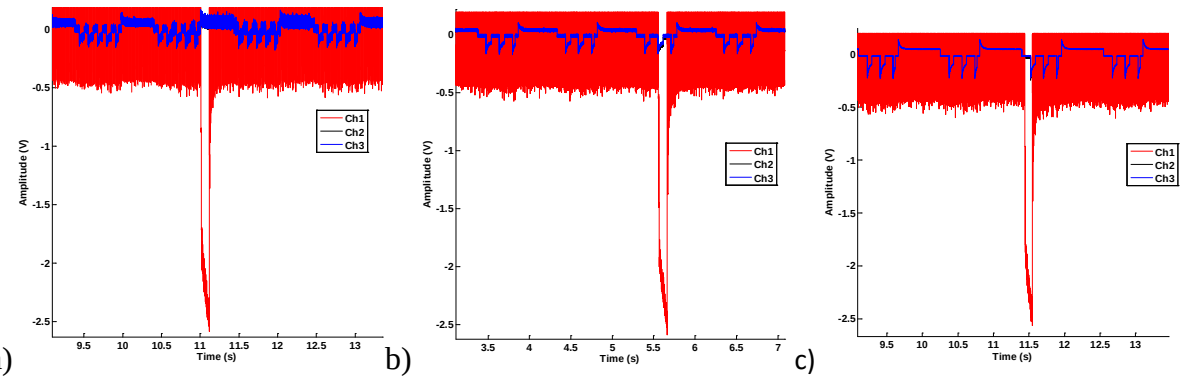

Figure L.1: 'Ch 2' and 'Ch 3' are almost identical signals from the two channels of the E1 TENS using low battery voltage (i.e. < 6 V). 'Ch 1' is the signal from the IR detector showing the movement of the masts. Note that the EMI changed the number of pulses from 3 (in parts b and c) to 5 in part a. a) The E1 TENS was placed 0 cm away (i.e. touching) from the front panel of the UPS. b) The E1 TENS was placed 2 cm away from the front panel of the UPS. c) The E1 TENS was placed 2 meters away from the front panel of the UPS (baseline).

L.2.ii Testing TENS with the proper full battery voltage condition

Figure L.2 shows an example of the output of the E1 TENS with the proper full battery voltage (i.e. 9 V) which contrasts with the E1 TENS output with a low battery voltage shown in figure L.1. The E1 TENS was not functioning properly when it was used with the low battery voltage. This was also indicated by its dim output lights which are designed to alert the user of the low battery voltage condition. The same observation was made about the E1.2 TENS.

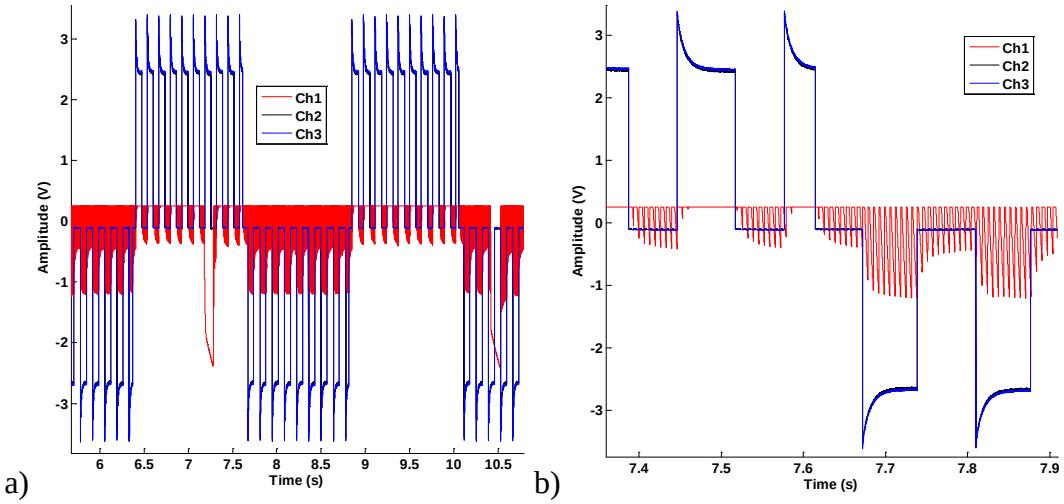

Figure L.2: a) An example of the output of the E1 TENS when the proper full battery voltage (i.e. 9 V) was used. 'Ch 2' and 'Ch 3' show the two almost identical outputs of the E1 TENS. 'Ch 1' shows the signal from the IR detector. b) A close up view of the signals shown in part a.

The TENS devices (i.e. both E1 and E1.2) were tested under a full battery voltage condition at a distance of 0 cm, 5 cm, 10 cm, 15 cm, and 2 m from the front panel of the UPS. Comparison of the output signals of the E1 TENS at 0 cm from the UPS, and at 2 m from the UPS (i.e. baseline) are shown in figure L.3. The types and numbers of pulses did not change in figure L.3. However, the pulse width of the underlying modulating signal which gates the CW output of the E1 TENS showed a miniscule increase (i.e. < 1 %) due to a subtle EMI that is reminiscent of the results shown in figure L.1, when the low battery voltage was used. This effect was mainly seen as a subtle increase in the width of the narrow pulses shown in figure L.3. E1 showed this effect only at 0 cm from the UPS. However, this result could not be reproduced using the E1.2 TENS. The E1.2 TENS did not show evidence of EMI when it was tested under full battery voltage conditions at all distances from the UPS front panel.

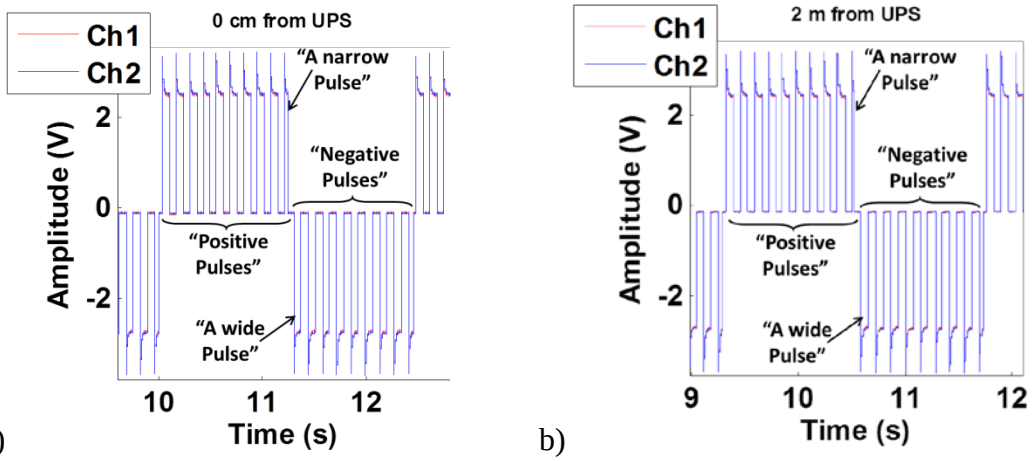

a) b)

Figure L.3: Example of comparison of E1's two output signals (i.e. Ch1 and Ch2) measured when the E1 TENS was at: a) 0 cm from the front panel of the UPS, and b) 2 m from the front panel of the UPS (i.e. baseline).

L.3 Summary

Table L.1 summarizes the additional experiments performed with E1 and E1.2 TENS around the front panel of the UPS of the AIT-2 and discussed in this appendix.

TENS Device	Battery condition	Location and Height	Test Mode	Orientation	Observed Reaction
E1	Low battery voltage (i.e. < 6 V)	Touching the UPS front panel, 0.75 m	Normal	Horizontal / Vertical	The EMI changed the number of pulses by a factor of 5/3. Please see figure L.1.

TENS Device	Battery condition	Location and Height	Test Mode	Orientation	Observed Reaction
	Full battery voltage (i.e. 9 V)	Touching the UPS front panel, 0.75 m	Normal	Horizontal / Vertical	The pulse width of the signal modulating the CW output of the TENS showed a miniscule (i.e. < 1 %) increase. The subtle EMI effect did not change the number or type of pulses. Please see figure L.3.
E1.2	Low battery voltage (i.e. < 6 V)	Touching the UPS front panel, 0.75 m	Normal	Horizontal / Vertical	The EMI changed the number of pulses by a factor of 5/3. Please see figure L.1.
	Full battery voltage (i.e. 9 V)	Touching the UPS front panel, 0.75 m	Normal	Horizontal / Vertical	None.

Table L.1: Summary of the additional TENS testing to look for the effect of EMI when E1 and E1.2 TENS were placed next to the UPS spurious emission hot spot. E1.2 is a newer TENS unit with the same model name as E1 but with different serial number. Please see appendix H for the general procedure used to test TENS devices around the AIT-2.

The EMI can affect the output of the TENS (i.e. both E1 and E1.2) when the following three circumstances happen simultaneously: i) the TENS device is operating under a low battery voltage that is not recommended for use by the manufacturer's labeling; ii) the user does not stop using the TENS device according to the instructions in the manual, when the on and yellow light become dim because of the low battery voltage conditions; iii) the user puts the TENS device within 2 cm of the front panel of AIT-2's UPS, almost touching the surface of the UPS. The simultaneous occurrence of these three circumstances can lead to a hazardous situation involving EMI induced change in the output signal of the TENS device. According to annex E of [3], the underlying hazards that lead to this hazardous situation can be classified as a use error operational hazard (which leads to circumstances i & ii above) and an electromagnetic energy hazard (which leads to circumstance iii). The probability of occurrence of each of the three circumstances is relatively low. Therefore, the probability of simultaneous occurrence of all of the three statistically independent circumstances (which can lead to EMI induced change in the output signal of the TENS) is very low.

When only condition iii occurred (i.e. without simultaneous occurrence of conditions i and ii), the EMI subtly affected the E1 TENS but not the E1.2 TENS. Once again, the probability of

occurrence of condition iii (which can lead to sporadic EMI induced change in the output signal of the TENS) itself is relatively low.

If the EMI induced change in the output signal of the TENS device is harmful, the probability of the occurrence of such harm is very low. Moreover, TENS devices are not life sustaining, and the severity of the harm (i.e. over or under stimulation) by EMI induced change in the output signal of the TENS device is generally expected to be low. Based on the assessment of the probability of the harm and the severity of the harm, the risk associated with the use of the TENS (i.e. both E1 and E1.2) around the AIT-2 is low to very low [3].

Appendix M

AIT-2 mmW simulator

M.1 Overview of mmW AIT-2 simulator

CDRH designed a hardware system to emulate the millimeter wave (mmW) emissions from the AIT-2. This was based on background information received about the AIT-2, and in-band emission measurements at CDRH. Please see appendix B, D, and E for detailed information about the operation and in-band emission characteristics of the AIT-2. The exposure times and field strength levels of the mmW emission from the AIT-2 are characterized for the particular AIT-2 unit studied by the CDRH. However, it is plausible that there may be slight variations across different AIT-2 units. The mmW simulator provides a mechanism to test PMEDs under higher field strength levels and prolonged exposure times than the AIT-2 unit investigated by the CDRH. In other words, the mmW AIT-2 simulator provides an opportunity to explore the worst case scenario that PMEDs may encounter due to mmW emissions from the AIT-2. This appendix discusses the design, operation, and characterization of the mmW simulator; whereas appendix N presents the protocol used to test PMEDs in the mmW simulator.

The mmW simulator shown in figure M.1 consisted of the Quanta Electronics Voltage Controlled Oscillator (VCO) that produced the fundamental signal from 12.125 GHz – 15 GHz. Amplitude and frequency modulation of the VCO was controlled by the two channels from the Agilent Arbitrary Waveform Generator (AWG). The VCO was connected to a Space Labs frequency multiplier which doubled the fundamental frequency to obtain the desired 24.5 GHz - 30 GHz. The waveform of the signal including the frequencies and duty cycles were simulating the signal to which a PMED would be exposed to inside the AIT-2. The output of the frequency multiplier then fed through a set of fixed attenuators. The fixed attenuators were specifically chosen to approximately tune the output power to one of the four desired power levels used during PMED testing. Appendix N discusses how these four power levels are used as part of the PMED testing procedure. Following the fixed attenuators, a 10 dB directional coupler was connected, where a power meter measured the forward and reflected power. The output of the directional coupler was fed to the horn antenna through a WR34 standard waveguide with a 90 degree bend section. The PMED was placed 0.47 m away from the aperture of the horn antenna.

M.2 Components of mmW AIT-2 Simulator

The components of the mmW simulator are shown in figure M.1 below and listed in table M.1 that follows.

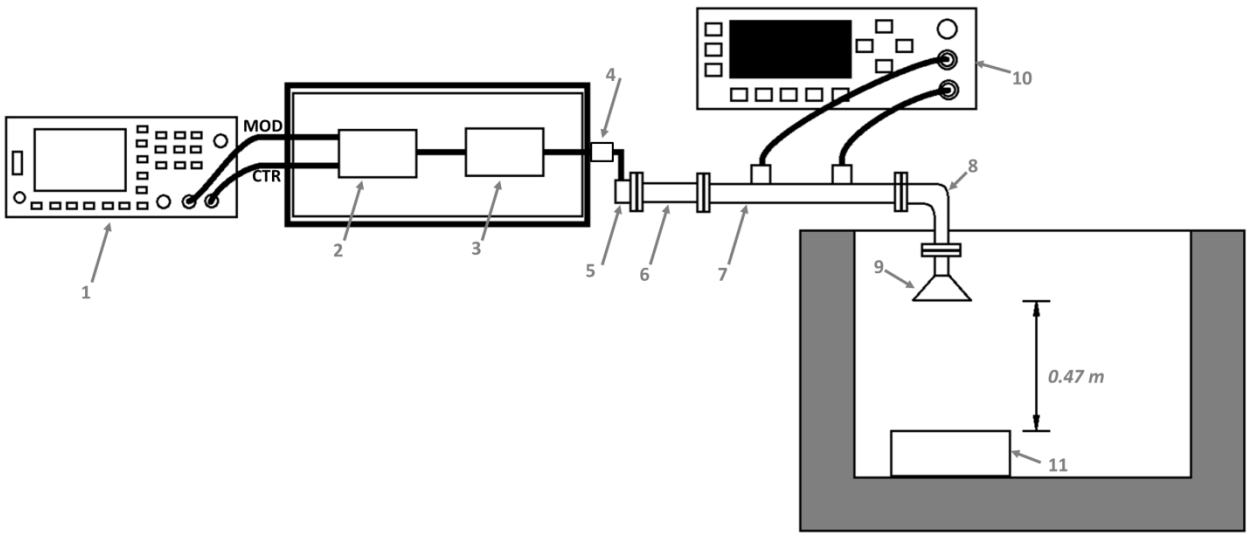

Figure M.1: Illustration of the mmW AIT-2 Simulator System. Please see table M.1 for description, picture, and settings of the components labeled 1 to 11 in this schematic.

	Description	Picture	Details / Setting
1	Agilent 33522A Arbitrary Waveform Generator (AWG)		The AWG controlled the voltage controlled oscillator (VCO) using two channels: channel 1 and channel 2. Channel 1 of the AWG outputted a ramp function to control the carrier frequency sweep of the VCO. Channel 2 controlled the on/off switching of the VCO that allows for the appropriate modulation of the carrier. In our tests, the frequencies that needed to be swept were between 12.125 GHz – 15 GHz, which corresponds to a ramp from 1.9 V – 4 V delivered by channel 1 of the AWG.
2	Quanta Electronics Voltage Controlled Oscillator (VCO) 12-18GHz		The VCO has two input ports: MOD and CTL ports. The MOD port took an input from channel 1 of the AWG. The CTL port was connected to channel 2 of the AWG which switches between 0 V and 5 V for on/off modulations. The VCO had an RF out port which can output frequencies between 12 GHz and 18 GHz. The VCO needs a +12 V / -12 V / GND power supply.

	Description	Picture	Details / Setting
3	Spacek Labs A276-2X-23 Frequency Multiplier (FM)		The FM took input from the RF out port of the VCO and doubled the frequency. The FM requires a +12V voltage supply.
4	Pasternack 2W Fixed Attenuators		There were 2-4 attenuators for each of the following attenuation values: 1dB, 3dB, 10dB, and 20dB.
5	Pasternack PE9827 WR34 K/Waveguide Adapter	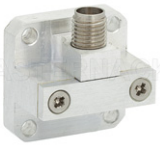	This waveguide adapter took its input from the frequency multiplier and fed the WR34 waveguide.
6	Antenna Systems and Solutions Waveguide	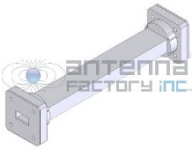	This is a WR34 waveguide.
7	ATM PNR 24-310A		This is a 10dB directional coupler; it is WR34 (22.0GHz – 33.0 GHz)
8	Antenna Systems and Solutions 90deg Bend		This is a WR34 90 degree bend to feed the horn antenna.
9	Pasternack PE9851-20 Horn		This is a WR34 horn antenna that was fed from the 90 deg bend to radiate the field towards the PMED under test.

	Description	Picture	Details / Setting
10	Agilent E4419B		This is a power meter to measure the power delivered to the horn antenna and the power reflected from the antenna.
11	DUT		This can be any of the PMEDs (i.e. pacemaker, ICD, neuro-stimulator, insulin pump, or TENS) tested according to the protocol in appendix I.

Table M.1: List of components of the mmW AIT-2 Simulator

M.3 Operating the mmW Simulator

M.3.i Defining Waveform Parameters

Once all the active components are powered, the parameters of the mmW simulator were set by the arbitrary waveform generator (AWG). The AWG has two output channels. Channel 1 controlled the output frequency of the VCO. Channel 2 toggled the output power on and off. In order to obtain the mmW waveform profile of the AIT-2, we needed to set the output of the two channels of the AWG as shown in figure M.2.

If the two channels of AWG are set as such, the output of the mmW simulator will chirp in frequency from 24.25 GHz to 30 GHz in 5.59 μs, turn the power off for 2.49 μs, and repeat. This results in a pulse with period of 8.08 μs. The 192 AIT-2 antennas emit these pulses successively in a top to bottom fashion (please see appendix D and E for more details about the characteristics of the mmW emissions from the AIT-2). One full cycle emission from the 192 antennas is called a vertical scan line. A single vertical scan line takes about 3.1 ms. Due to the limited beam width of the AIT-2 antennas, a PMED placed at the center of the AIT-2 is exposed to a longer duration of the 3.1 ms long vertical scan line than a PMED at the inner wall of the AIT-2. The vertical exposure time is defined as the amount of time that the PMED gets exposed to emission from a single vertical scan line in the AIT-2. The mmW simulator is designed to emulate the vertical exposure time that a typical PMED would face inside a particular location in the AIT-2. The vertical exposure time is specified using the t_{et} parameter in figure M.2. The mmW simulator is typically operated to emulate conditions at the center of the AIT-2 (location 1) or at the inner wall of the AIT-2 (location 2). Based on the geometric discussions in appendix D, a typical PMED at location 1 is irradiated by at most 92 antennas, and a typical PMED at location 2 is irradiated by at most 14 antennas (see table D.1). Therefore, the vertical exposure time (t_{et}) is 92 x 2 x 8.08 μs = 1.49 ms for location 1 and 14 x 2 x 8.08 μs = 0.22 ms for location 2, for a typical PMED. These

parameters of the AWG were set remotely using GPIB interface and were programmed using MATLAB's instrument control toolbox.

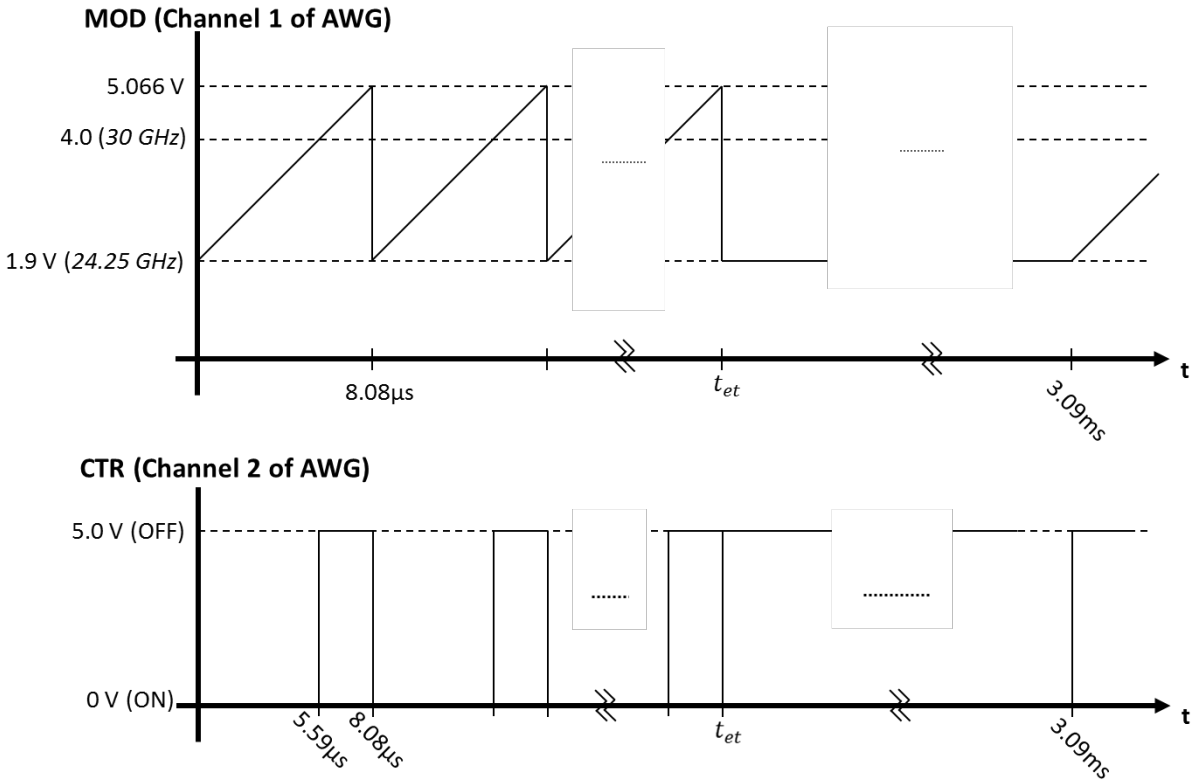

Figure M.2: The mmW simulator uses the following waveforms to simulate the in-band emission from the AIT-2. The vertical exposure time (t_{et}) was chosen appropriately to emulate waveforms at the center of the AIT-2 (location 1) or at the inner wall of the AIT-2 (location 2).

M.3.ii Tuning the power

The power fed to the horn antenna (i.e. transmitted power, P_t) was held fixed at 22 dBm ± 0.25 dB at 27.125 GHz, when there are no fixed attenuators. This determined the electric field strength that can be attained at the location of the DUT in figure M.1. However, fixed attenuators (component 4 in figure M.1) can be inserted between components 3 and 5 of figure M.1 in order to control the electric field strength at the DUT (i.e. the PMED being tested in the mmW simulator).

$$E = \sqrt{120\pi * P_d}$$

Equation M.1: Relationship between the electric field (E) and power density (P_d) in free space.

The electric field and the power density at the location of the PMED can be related using equation M.1. In turn, equation M.2 expresses the power density at the PMED in terms of: the linear gain of the transmitting horn antenna (G), the power transmitted by the horn antenna (P_t),

and the on axis distance (R) between the horn antenna and the PMED. For the mmW simulator, G=100 (or 20 dBi) and R=0.47 m.

$$P_d = \frac{P_t G}{4\pi R^2}$$

Equation M.2: The power density at a distance R from the transmitting antenna with gain G.

There are four desired electric field strengths that are used during PMED testing in the mmW simulator. These are: (i) the electric field at the center of the AIT-2 (i.e. location 1), (ii) 10 times the electric field at the center of the AIT-2, (iii) the electric field at the inner wall of the AIT-2 (i.e. location 2), and (iv) 10 times the electric field at the inner wall of the AIT-2. Appendix N discusses how these four conditions are used as part of the PMED testing procedure in the mmW simulator. Table M.2 shows the values of the fixed attenuators that were used to achieve electric field strengths that are at least as strong as the four conditions mentioned here. Due to the limited number of fixed attenuators available, the precision of the electric field generated at the PMED was limited. However, the electric field at the PMED was always at least as strong as the desired electric field strength that had to be simulated.

Fixed Attenuators	Transmitted Power (P_t)	Electric Field at the PMED	Condition Simulated (and desired Electric Field)	Vertical Exposure Time (t_{et})
54 dB	-32 dBm	0.092 V/m	The E-field at the center of the AIT-2 (i.e. 0.075 V/m)	1.49 ms for location 1
34 dB	-12 dBm	0.92 V/m	~10 times the E-field at the center of the AIT-2 (0.75 V/m)	1.49 ms for location 1
28 dB	-6 dBm	1.85 V/m	The E-field at the inner wall of the AIT-2 (i.e. 1.5 V/m)	0.22 ms for location 2
8 dB	14 dBm	18.5 V/m	~10 times the E-field at the inner wall of the AIT-2 (i.e. 15 V/m)	0.22 ms for location 2

Table M.2: These are the set of available attenuators used and the corresponding electric fields generated at the PMED for each of the conditions that are desired to be simulated.

M.4 Field mapping in mmW simulator

The electric field within the boresight of the transmitting antenna can be predicted using equation M.1 and equation M.2. The center of the PMED is normally situated within the boresight of the

transmitting antenna of the mmW simulator at a distance of 0.47 m. However, parts of the PMED may be outside the boresight. Therefore, it is useful to understand the planar profile of the electric field on the plane that is at a distance of 0.47 m.

The electric field strength at the plane of the PMED was measured as follows. The plane of the measurement was located 0.47 m below the transmitting horn antenna, and the plane was approximately parallel to the aperture of the horn. The measurement locations on the plane are depicted by dots in figure M.4, which shows a 10 x 11 grid of points with two adjacent points separated by 2 cm in both x and y directions. The receiving antenna, which is a WR28 open ended waveguide, is also shown to scale in figure M.4.

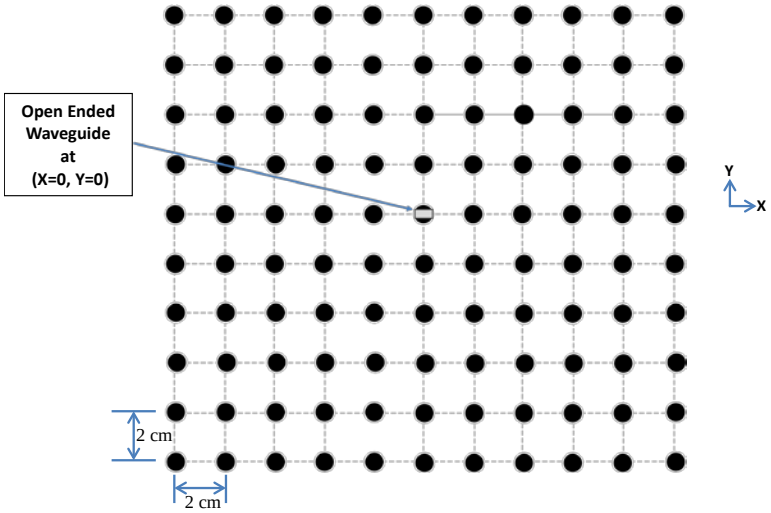

Figure M.4: Locations for field mapping measurement

Equipment	Description
Open Ended Waveguide	5.6 dBi Gain at 27.125 GHz, WR28
Agilent E4419B	Power Meter
Agilent N8485A	Thermocouple Power Sensors, 10 MHz-33 GHz, -35 dBm to +20 dBm

Table M.3: List of equipment to map the field

The field mapping measurement equipment is listed in table M.3. The power received (P_r) by the open ended waveguide was measured by the thermocouple power sensor and was displayed on the power meter. The electric field was obtained from the power density (P_d) using equation M.1. The power density was calculated from the power measured by the power sensor (P_r) using equation M.3. The gain (G) of the open ended waveguide is about 5.6 dBi (3.63) at 27.125 GHz.

The planar mapping of the electric field was done using a continuous wave at a frequency of 27.125 GHz.

$$P_d = \frac{P_r 4\pi}{G\lambda^2}$$

Equation M.3: Power density (P_d) at an aperture of antenna (with gain G) as a function of the power received by the antenna (P_r) and the wavelength (λ).

Figure M.5 shows the experimental set up used to perform the planar mapping of the electric field. The open ended waveguide is used to make measurements at 10 x 11=110 points on the plane that is 0.47 m away from the aperture of the transmitting horn antenna. These measurement points are schematically shown in figure M.4. The measured electric field is presented in figure M.6 as a function of the (x,y) coordinates of the measurement plane. The PMED is typically placed on this plane during testing. The transmitted power (P_t) is 22.0 (± 0.25) dBm for this planar mapping measurement, which means that there were no fixed attenuators used (between components 3 and 5 of figure M.1) during the planar mapping measurement.

Figure M.5: This is the experimental setup for the field mapping measurement. The open ended waveguide was used to measure the electric field strength at 110 points on the plane where the PMEDs were eventually placed for testing.

The result shown in figure M.6 was used as a guide when placing PMEDs in the mmW simulator for testing. The PMEDs were placed to maximize their exposure to the electric field generated by the mmW simulator. The components of the mmW simulator are linear. Therefore, the fixed

attenuators, which are mentioned in table M.2, do not alter the profile of the electric field distribution mapped out in figure M.6.

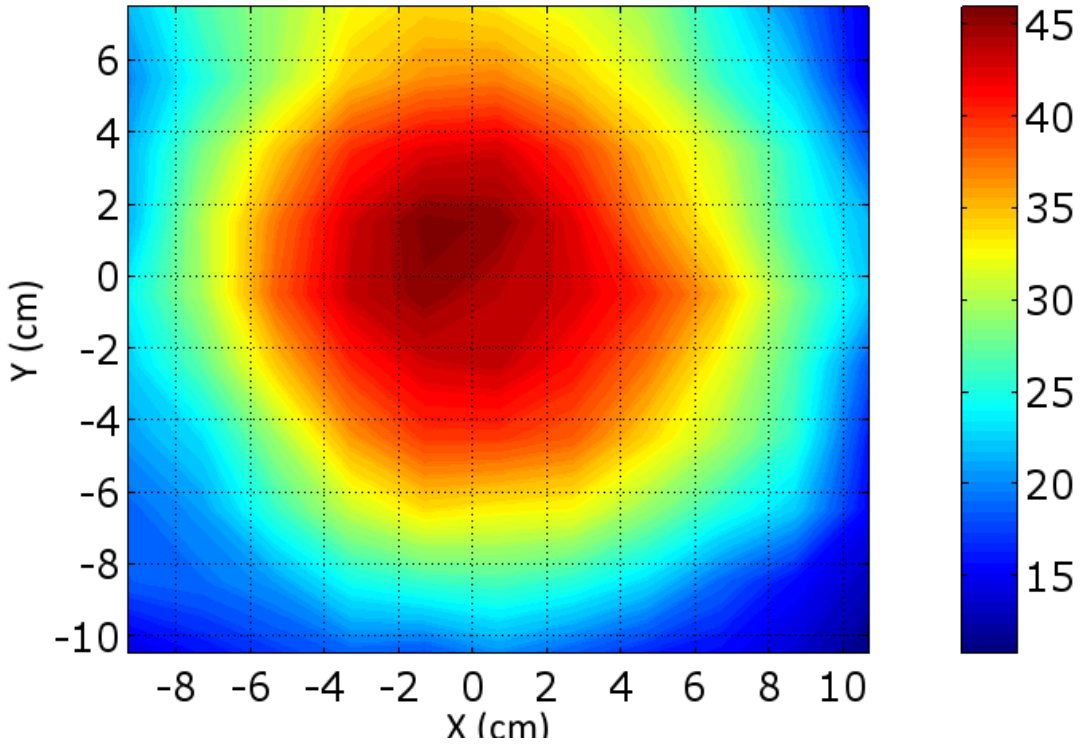

Figure M.6: Measured Electric Field (in V/m) on a plane that is approximately parallel to and 0.47 m away from the aperture of the transmitting horn antenna of the mmW simulator.

M.5 Summary

The mmW simulator can be configured to emit waveforms that would be detected at the center of the AIT-2 (location 1) and inner wall of the AIT-2 (location 2) by specifying the appropriate vertical exposure time (t_{et}). The mmW simulator outputs a continuous burst of signals that contain the appropriate portion of the vertical scan line (which is 3.1 ms long). Therefore, the mmW simulator can be considered as the simulation of the fixed mast emission mode of the AIT-2. In fixed mast mode, the AIT-2 continuously emits vertical scan lines from its mast, which is fixed at the mid-point of the 120^0 arc. This facilitates a prolonged exposure time for the PMEDs in the mmW simulator compared to the limited PMED exposure time achievable in the AIT-2 during a scan that lasts for less than 1.5 s. Please see appendix E for more discussions about the fixed mast mode.

The electric field strength of the emissions can be controlled using a set of fixed attenuators that can be inserted in the mmW simulator. The four conditions that are typically simulated by the mmW simulator are shown in table M.2. The appropriate pair of vertical exposure time and field strengths were used to simulate conditions at location 1 and location 2 of the AIT-2.

Appendix N

Procedures for testing PMEDs with AIT-2 mmW simulator

N.1 Procedure for Testing Implantable Cardiac Pacemakers for Exposure in the AIT-2 mmW Simulator

Setup Monitoring System and Torso Simulator

25. Prepare the torso simulator for pacemaker testing as described in appendix I, and verify the appropriate conductivity of the saline (i.e. 0.27 S/m).
26. Mount the device under test (DUT) on the torso simulator as shown in figure N.1. The DUT consists of the Implantable Pulse Generator (IPG) of the pacemaker and its monitoring or pacing leads. The leads should be secured on a predetermined curve drawn on the grid, which makes the required 225 cm^2 closed loop based on the testing standards [11]. There is a microwave absorber between the IPG (which is in air) and the saline. So, connect the IPG to the saline using a wire to complete the conduction loop.

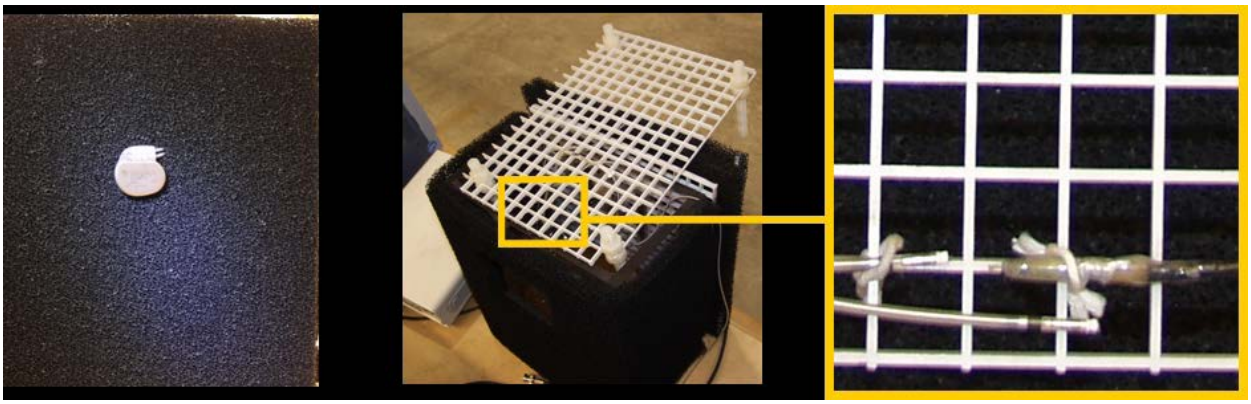

Figure N.1: This shows the installation of the DUT (pacemaker) on the torso simulator.

27. Connect DUT monitoring cable leading out of the torso simulator to a digital oscilloscope through a pre amplifier.
28. Connect DUT monitoring cable (with a BNC-T) to A/D converter which is linked with the controlling PC. Besides, connect the low frequency envelope for the output of the mmW simulator to the A/D converter.
29. Connect the external simulated cardiac signal generator to the torso simulator. The simulated cardiac signal is generated according to the specifications in [11].
30. Set up the data acquisition software on the PC connected to the A/D converter.
31. Check torso simulator and cables on the oscilloscope to verify minimum noise from the exposure.
32. Program DUT according to the operating modes, and lead configurations in appendix J, and perform steps 9-10 for each of the lead configurations (i.e. unipolar and bipolar). If the DUT allows RF telemetry, set up the programmer to remotely monitor the activity of the DUT during the test; this provides an additional monitoring mechanism.
33. Start the external simulated cardiac signal generator. Determine the minimum voltage level needed to be applied to inhibit pacing. Double the minimum voltage level to find the

voltage level that needs to be applied for injected simulated heart signal test, at the current device settings. Once this is determined, turn the cardiac injected signal off.

34. To verify DUT operation, run a baseline test recording signals from the device while the mmW simulator is still off. Do the baseline test with and without the simulated cardiac signal.

Test the DUT in the mmW simulator

35. Set up the torso simulator at the center of the mmW simulator at a height of 0.47 meters from the horn antenna as shown in figure N.2. DUT monitoring and cardiac signal injection cables are fed in and out of the mmW simulator. The cables are oriented perpendicular to the radiated electric field and wrapped with a millimeter wave absorber, while they are within the field of view of the horn antenna.
36. Command the mmW simulator to start simulating condition i) mentioned in step 14.
37. Record the DUT's orientation, operating mode, lead configurations, settings, and status (i.e. on or off) of the simulated cardiac signal on the data acquisition software.
38. Record the name of the condition simulated by the mmW simulator on the data acquisition software. There are four conditions simulated at the location where the DUT is situated. These are: i) the electric field pattern that is measured at location 1 of the AIT-2,
    ii) ten times the electric field pattern that is measured at location 1 the AIT-2,
    iii) the electric field pattern that is measured at location 2 of the AIT-2, and
    iv) ten times the electric field pattern that is measured at location 2 of the AIT-2.

Figure N.2: This shows the installation of the DUT (pacemaker) on the torso simulator inside the AIT-2 simulator.

39. Run the data acquisition software to start the 30 seconds long recording.
40. During the 30 seconds recording, observe the DUT’s output signal on the oscilloscope, which is shown in figure N.3. At the same time, observe the screen of the programmer if the DUT is connected to the programmer using RF telemetry.

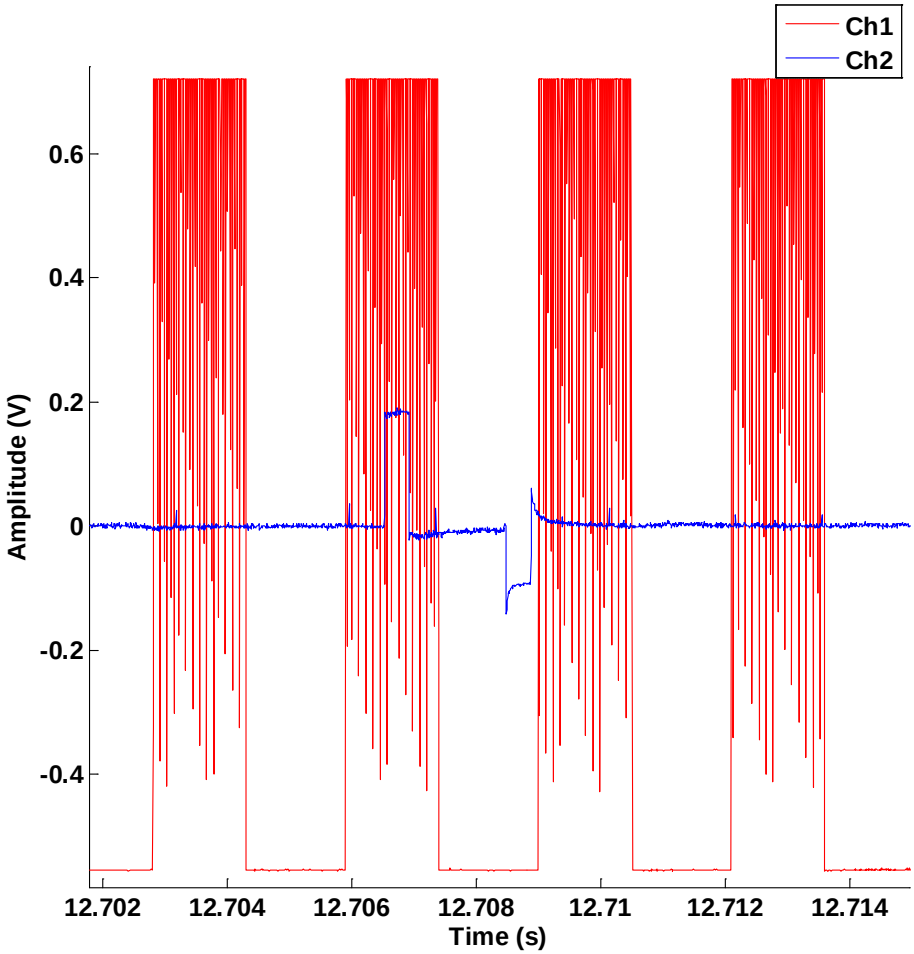

Figure N.3: Channel 2 shows the output of a pacemaker. Channel 1 shows the envelope of the mmW emission from the mmW simulator. The mmW simulator is simulating the vertical exposure time at location 1 of the AIT-2, which is 1.49ms.

41. Repeat steps 13-16 with the simulated cardiac signal on.
42. Rotate the DUT by 90 degrees to a new orientation as shown in figure I.4 and repeat steps 13 - 17.
43. Change the operating mode from unipolar to bipolar and repeat steps 13 – 18.

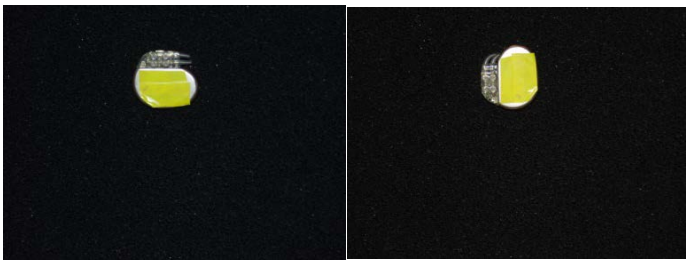

Figure N.4: The first figure shows the DUT in horizontal orientation, the second shows the DUT in vertical orientation.

44. Command the mmW simulator to start simulating condition ii) mentioned in step 14, and repeat steps 13-19.

45. Command the mmW simulator to start simulating condition iii) mentioned in step 14, and repeat steps 13-19.
46. Command the mmW simulator to start simulating condition iv) mentioned in step 14, and repeat steps 13-19.
47. Retrieve any relevant files saved by the device programmer, and save them along with the data that is automatically saved by the data acquisition software.
48. Finally, program the device to a mode that saves its battery life.

N.2 Procedure for Testing ICDs for Exposure in the AIT-2 mmW Simulator

Setup Monitoring System and Torso Simulator

29. Prepare the torso simulator for ICD testing as described in appendix I, and verify the appropriate conductivity of the saline (i.e. 0.27 S/m).
30. For safety reasons, check that the ICD therapy functionality is turned OFF using the programmer, before touching it. The ICD therapy functionality needs to be turned on with minimum energy levels only during the actual test.
31. Mount the device under test (DUT) on the torso simulator. The DUT consists of the ICD's Implantable Pulse Generator (IPG) and its monitoring or pacing leads shown in figure N.5. The leads should be secured on a predetermined curve drawn on the grid, which makes the required 225 cm^2 closed loop based on the testing standards [11]. There is a microwave absorber between the IPG (which is in air) and the saline. So, connect the IPG to the saline using a wire to complete the conduction loop.

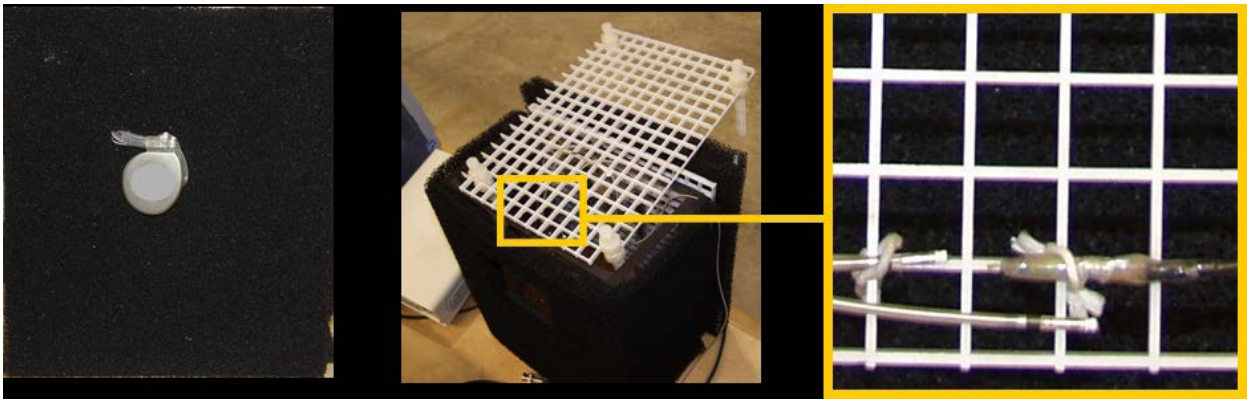

Figure N.5: This shows the installation of the DUT (ICD) on the torso simulator.

32. Connect DUT monitoring cable leading out of the torso simulator to a digital oscilloscope through a pre amplifier.
33. Connect DUT monitoring cable (with a BNC-T) to A/D converter which is linked with the controlling PC. Besides, connect the low frequency envelope for the output of the mmW simulator to the A/D converter.
34. Connect the external simulated cardiac signal generator to the torso simulator. The simulated cardiac signal is generated according to the specifications in [11].
35. Set up the data acquisition software on the PC connected to the A/D converter.
36. As a safety measure, make sure that voltage protection circuits are present on all cables coming out of the torso simulator.

37. Check torso simulator and cables on the oscilloscope to verify minimum noise from the exposure.
38. As a safety measure, program the ICD to set the shock therapy levels to minimum energy levels, without touching the ICD. Once this is done, recognize the risk of shocking during steps 11-13, and avoid touching the ICD without protective gloves. If signs of ICD shock therapy sequence are seen during steps 11-13, be prepared to safely unplug the measurement equipment, and program the ICD shock therapy off.
39. Program DUT according to device operating modes, and settings in appendix J, and perform steps 12-13. If the DUT allows RF telemetry, set up the programmer to remotely monitor the activity of the DUT during the test. This provides an additional monitoring mechanism.
40. Start the external simulated cardiac signal generator. Determine the minimum voltage level needed to be applied to inhibit pacing. Double the minimum voltage level to find the voltage level that needs to be applied for injected simulated heart signal test. Once this is determined, turn the cardiac injected signal off.
41. To verify DUT operation, run a baseline test recording signals from the device while the mmW simulator is off. Do the baseline test with and without the simulated cardiac signal.
42. As a safety measure, program the ICD to make sure that its shock therapy functionality is OFF while it is still situated on the torso, without touching it.

<u>Test the DUT in the mmW simulator</u>

43. Set up the torso simulator at the center of the mmW simulator at a height of 0.47 meters from the horn antenna as shown in figure N.6. DUT monitoring and cardiac signal injection cables are fed in and out of the mmW simulator. The cables are oriented perpendicular to the radiated electric field and wrapped with a millimeter wave absorber, while they are within the field of view of the horn antenna.

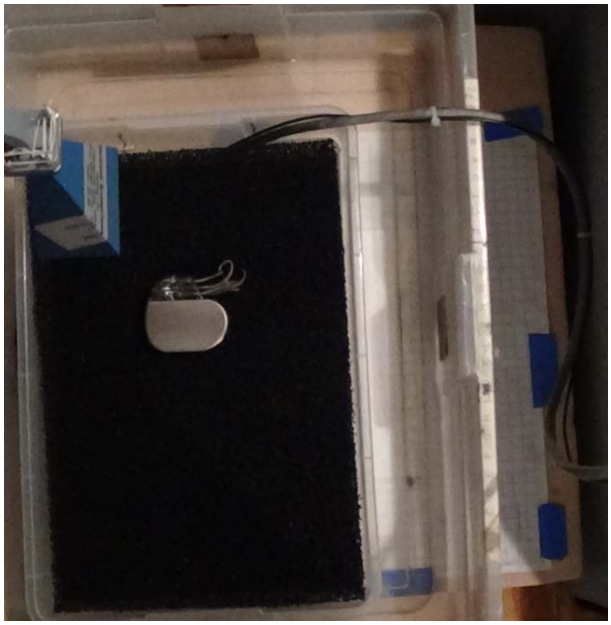

Figure N.6: This shows the installation of the DUT (ICD) on the torso simulator inside the AIT-2 simulator.

44. As a safety measure, program the ICD to set the shock therapy to minimum energy levels, without touching the ICD. Once this is done, recognize the risk of shocking during steps 17

to 27, and avoid touching the ICD without protective gloves. If signs of ICD shock therapy sequence are seen during steps 17 to 27, be prepared to safely unplug the measurement equipment, turn off the mmW simulator, and program the ICD shock therapy off.

45. Command the mmW simulator to start simulating condition i) mentioned in step 19.
46. Record the DUT's orientation, operating mode, settings, and status (on or off) of the simulated cardiac signal on the data acquisition software.
47. Record the name of the condition simulated by the mmW simulator on the data acquisition software. There are four conditions simulated at the location where the DUT is situated. These are: i) the electric field pattern that is measured at location 1 of the AIT-2,
    ii) ten times the electric field pattern that is measured at location 1 the AIT-2,
    iii) the electric field pattern that is measured at location 2 of the AIT-2, and
    iv) ten times the electric field pattern that is measured at location 2 of the AIT-2.
48. Run the data acquisition software to start the 30 seconds long recording.
49. During the 30 seconds recording, observe the DUT's output signal on the oscilloscope. At the same time, observe the screen of the programmer if the DUT is connected to the programmer using RF telemetry.

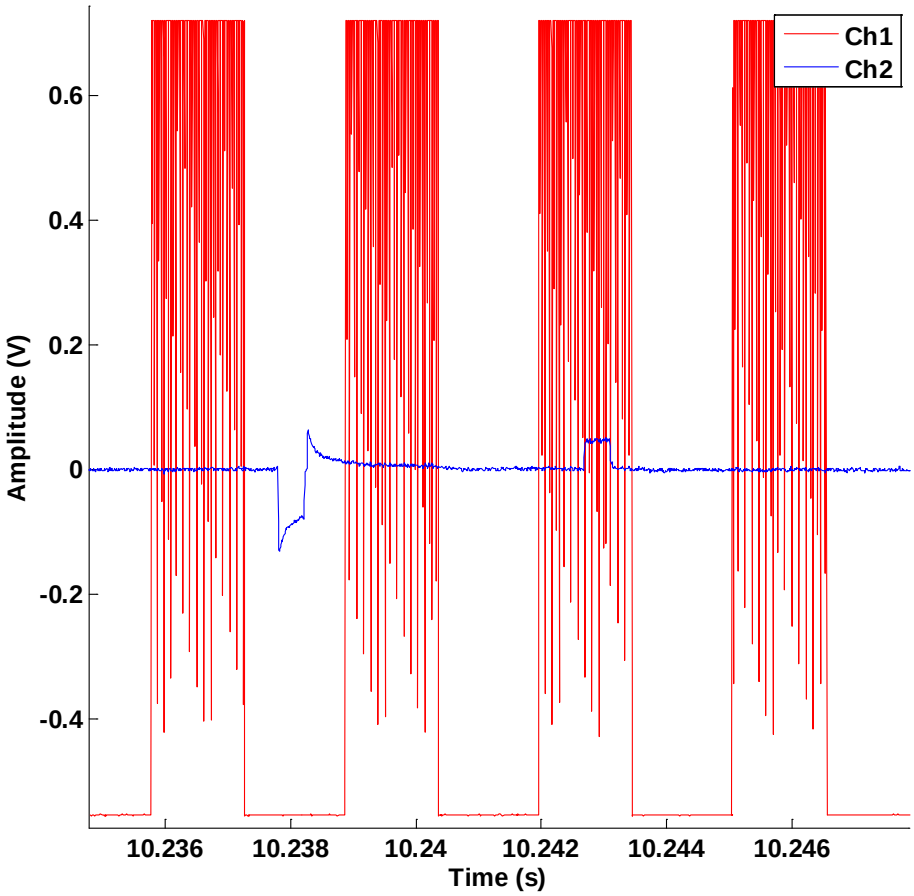

Figure N.7: Channel 2 shows the output of an ICD. Channel 1 shows the envelope of the mmW emission from the mmW simulator. The mmW simulator is simulating the vertical exposure time at location 1 of the AIT-2, which is 1.49ms.

50. Repeat steps 18 to 21 with the simulated cardiac signal on.

51. Rotate the IPG of the DUT by 90 degrees to a new orientation as shown in figure N.8 and repeat steps 18 to 22.

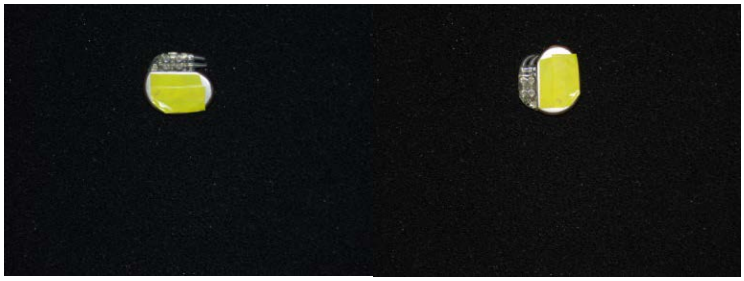

Figure N.8: The first figure shows the DUT in horizontal orientation, the second shows the DUT in vertical orientation.

52. Command the mmW simulator to start simulating condition ii) mentioned in step 19, and repeat steps 18-23.
53. Command the mmW simulator to start simulating condition iii) mentioned in step 19, and repeat steps 18-23.
54. Command the mmW simulator to start simulating condition iv) mentioned in step 19, and repeat steps 18-23.
55. Retrieve any relevant files saved by the device programmer, and save them along with the data that is automatically saved by the data acquisition software.
56. Finally, program the ICD to make sure that its shock therapy functionality is OFF while it is still situated on the torso, without touching it. Besides, program the device to save its battery life.

N.3 Procedure for Testing Neuro-stimulators for Exposure in the AIT-2 mmW Simulator

Setup Monitoring System and Torso Simulator

22. Prepare the torso simulator for neuro-stimulator testing as described in appendix I, and verify the appropriate conductivity of the saline (i.e. 0.27 S/m).
23. Mount the device under test (DUT) on the torso simulator. The DUT consists of the neuro-stimulator's Implantable Pulse Generator (IPG) and its leads shown in figure N.9. There is a millimeter-wave absorber between the IPG (which is in air) and the saline. So, connect the IPG to the saline using a wire to complete the conduction loop.

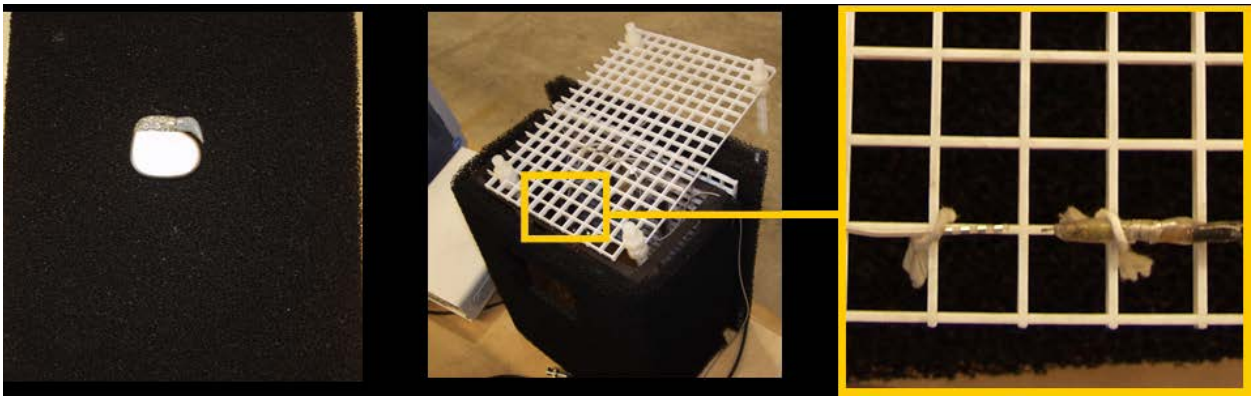

Figure N.9: This shows the installation of the DUT (neuro-stimulator) on the torso simulator.

24. Connect DUT monitoring cable leading out of the torso simulator to a digital oscilloscope through a pre amplifier.
25. Connect DUT monitoring cable (with a BNC-T) to A/D converter which is linked with the controlling PC. Besides, connect the low frequency envelope for the output of the mmW simulator to the A/D converter.
26. Set up the data acquisition software on the PC connected to the A/D converter.
27. Check torso simulator and cables on the oscilloscope to verify minimum noise from the exposure.
28. Program DUT according to the device operating modes, and settings in appendix J and perform step 8 for each of the settings. If the DUT allows RF telemetry, set up the programmer to remotely monitor the activity of the DUT during the test. This provides an additional monitoring mechanism.
29. To verify DUT operation, run a baseline test recording signals from the device while the mmW simulator is off.

<u>Test the DUT in the mmW simulator</u>

30. Set up the torso simulator at the center of the mmW simulator at a height of 0.47 meters from the horn antenna. DUT monitoring cables are fed in and out of the mmW simulator. The cables are oriented perpendicular to the radiated electric field and wrapped with a millimeter wave absorber, while they are within the field of view of the horn antenna.
31. Command the mmW simulator to start simulating condition i) mentioned in step 12.
32. Record the DUT's orientation, operating mode and settings on the data acquisition software.
33. Record the name of the condition simulated by the mmW simulator on the data acquisition software. There are four conditions simulated at the location where the DUT is situated. These are: i) the electric field pattern that is measured at location 1 of the AIT-2,
    ii) ten times the electric field pattern that is measured at location 1 the AIT-2,
    iii) the electric field pattern that is measured at location 2 of the AIT-2, and
    iv) ten times the electric field pattern that is measured at location 2 of the AIT-2.
34. Run the data acquisition software to start the 30 seconds long recording.
35. During the 30 seconds recording, observe the DUT’s output signal on the oscilloscope. Figure N.10 below is an example of DUT’s output. At the same time, observe the screen of the programmer if the DUT is connected to the programmer using RF telemetry.

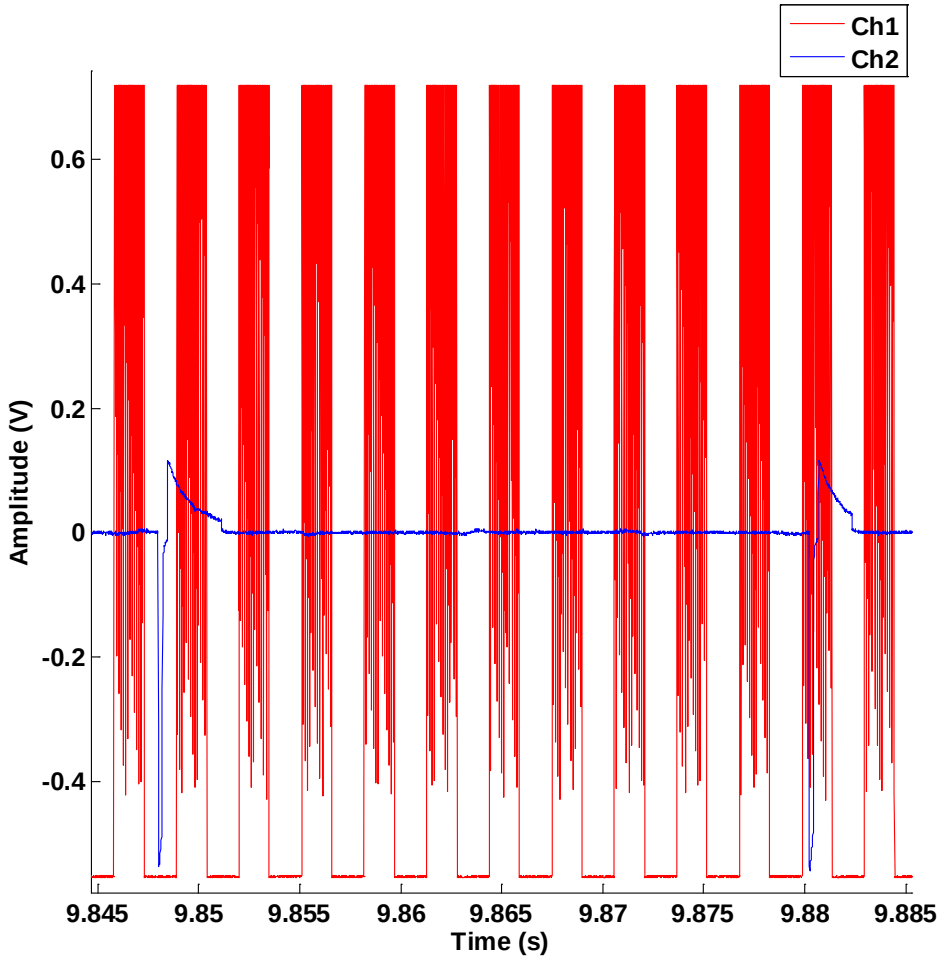

Figure N.10: Channel 2 shows the output of a neuro-stimulator. Channel 1 shows the envelope of the mmW emission from the mmW simulator. The mmW simulator is simulating the vertical exposure time at location 1 of the AIT-2, which is 1.49 ms.

36. Rotate the IPG of the DUT by 90 degrees to a new orientation as shown in figure N.11 and repeat steps 11 to 14.
37. If the device has a magnet mode, switch from continuous (cycling) mode to the magnet mode and repeat steps 11 to 15. This is done by moving the magnet across the device.

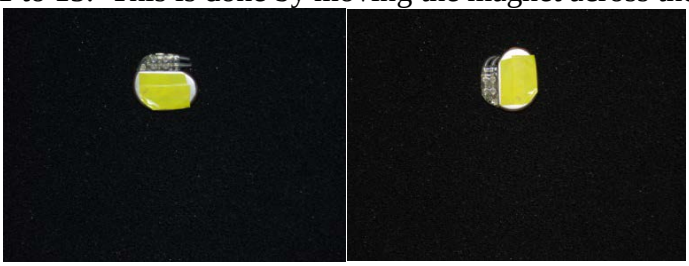

Figure N.11: The first figure shows the DUT in horizontal orientation, the second shows the DUT in vertical orientation.

38. Command the mmW simulator to start simulating condition ii) mentioned in step 12, and repeat steps 11-16.

39. Command the mmW simulator to start simulating condition iii) mentioned in step 12, and repeat steps 11-16.
40. Command the mmW simulator to start simulating condition iv) mentioned in step 12, and repeat steps 11-16.
41. Retrieve any relevant files saved by the device programmer, and save them along with the data that is automatically saved by the data acquisition software.
42. Finally, program the device to a mode that saves its battery life.

N.4 Procedure for Testing Insulin Pumps for Exposure in the AIT-2 mmW Simulator

Setup Monitoring System and Torso Simulator

22. Prepare the torso simulator for insulin pump testing as described in appendix I.
23. Mount the devices under test (DUT) on the torso simulator. The DUT consists of an insulin pump, a glucose sensor transmitter (GST), a smart phone (iPhone), and a translator which enables communication of the insulin pump with the smart phone. The GST is attached to a load that simulates a human body with constant glucose levels. The DUT should be mounted on the outside of the torso simulator as shown in figure N.12 a. Figure N.12 b shows a 10 turn, 5 cm diameter, loop antenna that is mounted behind the millimeter-wave absorber of the torso simulator. The loop antenna is intended to monitor activations of the insulin pump motor which displaces the cylinder delivering insulin. The loop antenna may also record other communication signals from the insulin pump, and hence the loop antenna signal needs to be interpreted carefully. Since the signal from the loop antenna can be noisy, a complementary method was developed to measure the displacement of the insulin pump cylinder. This is done by using a high precision digital displacement meter. This digital displacement meter is used to measure the location of the insulin pump cylinder before and after exposure to the potential source of electromagnetic interference. The difference between the two displacement readings is compared with the expected result considering the experimental uncertainties of the measurement.

b)  b)  c) 

Figure N.12: a) This shows the installation of three components of the DUT on the exterior surface of the torso simulator. These are: the translator, the insulin pump, and the Glucose Sensor Transmitter (GST). b) The 10 turn, 5 cm diameter loop antenna was mounted inside the torso simulator behind the insulin pump. c) The smart phone that communicates with the insulin pump through the translator was also installed on the other side of the torso simulator.

24. Connect DUT monitoring cable leading out of the torso simulator to a digital oscilloscope through a pre amplifier. The DUT monitoring cable transmits signals from the loop antenna which is designed to monitor activations of the insulin pump motor as it pushes the cylinder delivering insulin.

25. Connect the above DUT monitoring cable (with a BNC-T) to A/D converter which is linked with the controlling PC. Besides, connect the low frequency envelope for the output of the mmW simulator to the A/D converter.
26. Set up a data acquisition software (MATLAB based) on the PC connected to the A/D converter.
27. Check the torso simulator and cables on the oscilloscope to verify minimum noise from the exposure.
28. Set up the DUT according to each of the three device test modes specified in appendix J (i.e. idle mode, alarm mode, and bolus delivery mode) and perform step 8 for each of the modes. These test modes are chosen in accordance with [15].
29. To verify DUT operation, run a baseline test recording signals from the device while the mmW simulator is off.

Test the DUT in the mmW simulator

30. Set up the torso simulator at the center of the mmW simulator at a height of 0.47 meters from the horn antenna. DUT monitoring cables are fed in and out of the mmW simulator. The cables are oriented perpendicular to the radiated electric field and wrapped with a millimeter wave absorber, while they are within the field of view of the horn antenna.
31. Command the mmW simulator to start simulating condition i) mentioned in step 11.
32. Record the DUT's orientation, operating mode and settings in the data acquisition software. Use the high precision displacement meter to measure the position of the insulin pump cylinder before exposure.
33. Record the name of the condition simulated by the mmW simulator on the data acquisition software. There are four conditions simulated at the location where the DUT is situated. These are: i) the electric field pattern that is measured at location 1 of the AIT-2,
    ii) ten times the electric field pattern that is measured at location 1 the AIT-2,
    iii) the electric field pattern that is measured at location 2 of the AIT-2, and
    iv) ten times the electric field pattern that is measured at location 2 of the AIT-2.
34. Run the data acquisition software to start the 30 seconds long recording.
35. During the 30 seconds recording, use the oscilloscope to observe the signal from the loop antenna, which monitors the activations of the insulin pump motor. Figure N.13 below shows an example of signal from the loop antenna monitoring the insulin pump. Scrutinize any effects or spurious data within the 30 seconds long recording.

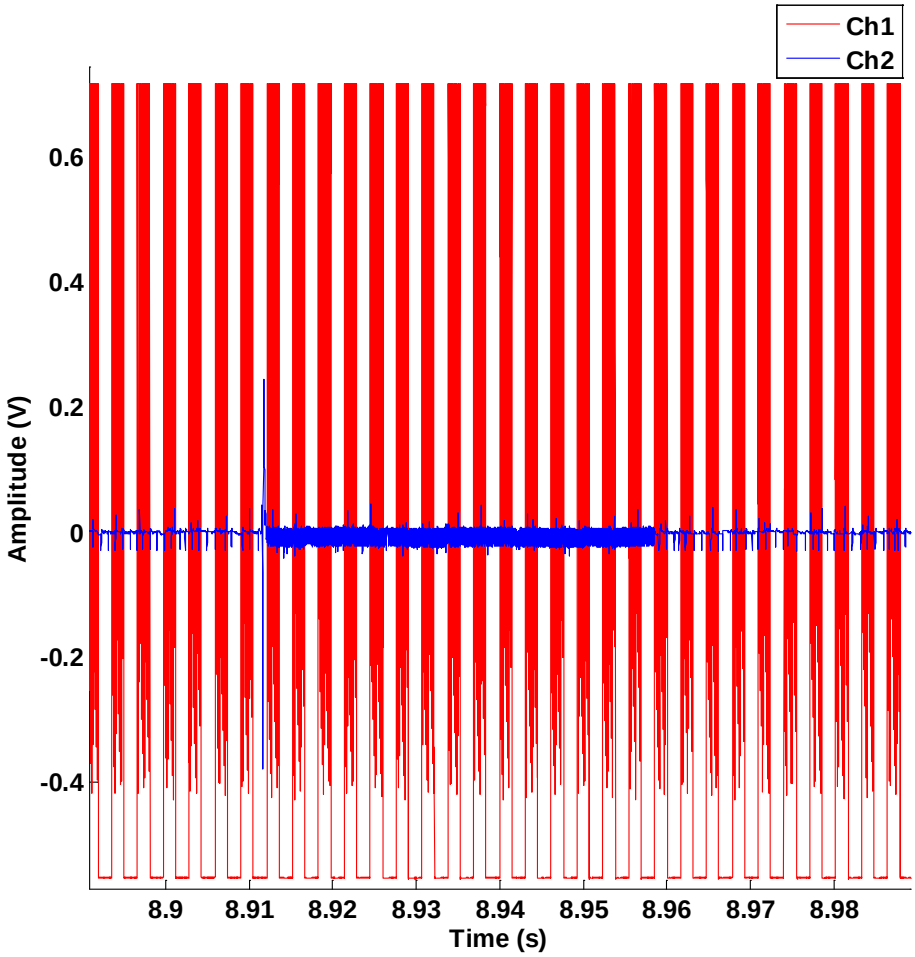

Figure N.13: Channel 2 shows the output of the loop antenna monitoring the activations of the cylinder of an insulin pump. Channel 1 shows the envelope of the mmW emission from the mmW simulator. The mmW simulator is simulating the vertical exposure time at location 1 of the AIT-2, which is 1.49 ms.

36. Physically measure any net displacement of the cylinder of the insulin pump after the 30 seconds exposure using the high precision displacement meter. Finally, use the smart phone, which communicates with the insulin pump using a translator device, to look for any abnormalities that may happen after the exposure. If the insulin pump is designed to test the communication to the glucose sensor transmitter (GST), check if any of the test packets that are sent every 0.5s are lost or corrupted due to potential electromagnetic interference; typical insulin pumps communicate with the glucose sensor transmitter (GST) once every 5 minutes.
37. Rotate the insulin pump by 90 degrees to a new orientation as shown in figure N.14 and repeat steps 11 to 15.
38. Change the mode of the DUT to the rest of the three device test modes specified in appendix J (i.e. idle mode, alarm mode, and bolus delivery mode) and repeat steps 11 to 16.
39. Command the mmW simulator to start simulating condition iii) mentioned in step 12, and repeat steps 11-17.
40. Command the mmW simulator to start simulating condition iii) mentioned in step 12, and repeat steps 11-17.
41. Command the mmW simulator to start simulating condition iii) mentioned in step 12, and repeat steps 11-17.

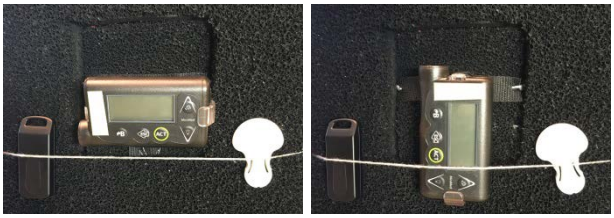

Figure N.14: The first figure shows the insulin pump in horizontal orientation, the second shows the insulin pump in vertical orientation.

42. Retrieve any relevant files saved by the device, and save them along with the data that is automatically saved by the data acquisition software.
43. Finally, turn off the devices and remove their batteries, as appropriate, before storing them.

N.5 Procedure for Testing TENS for Exposure in the mmW Simulator

Setup Monitoring System and Torso Simulator

20. Prepare the torso simulator for TENS testing as described in appendix I.
21. Mount the device under test (DUT) on the torso simulator. The DUT consists of a TENS device that is connected to a loop of the TENS leads as shown in Figure N.15. The DUT is placed on the millimeter-wave absorber material of the torso simulator. The leads of the TENS are terminated by a 500 Ω resistor, which is connected to a coaxial cable, based on the testing standard in [16].

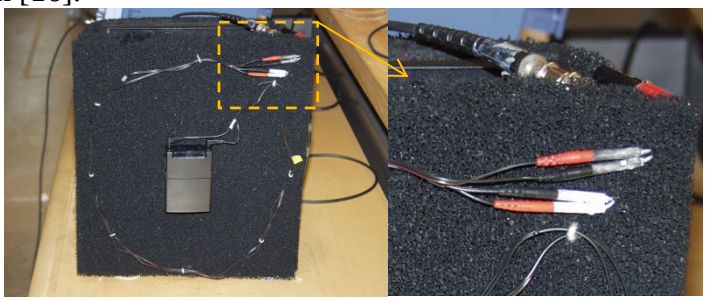

Figure N.15: This shows the installation of the DUT (TENS device) on the torso simulator.

22. Connect DUT monitoring coaxial cable leading out of the torso simulator to a digital oscilloscope through a pre amplifier.
23. Connect DUT monitoring cable (with a BNC-T) to A/D converter which is linked with the controlling PC. Besides, connect the low frequency envelope for the output of the mmW simulator to the A/D converter.
24. Set up a data acquisition software (MATLAB based) on the PC connected to the A/D converter.
25. Check the torso simulator and cables on the oscilloscope to verify minimum noise from the exposure.
26. Program DUT according to each of the device settings, and operating modes specified in appendix J (i.e. normal mode, modulated mode, and burst mode) and perform step 8 for each of the settings.

27. To verify DUT operation, run a baseline test recording signals from the device while the mmW simulator is off.

Test the DUT in the mmW simulator

28. Power the AIT-2, log on, and calibrate the system.
29. Set up the torso simulator at the center of the mmW simulator at a height of 0.47 meters from the horn antenna. DUT monitoring and cardiac signal injection cables are fed in and out of the mmW simulator. The cables are oriented perpendicular to the radiated electric field and wrapped with a millimeter wave absorber, while they are within the field of view of the horn antenna.
30. Command the mmW simulator to start simulating condition i) mentioned in step 13.
31. Record the DUT's orientation, operating mode and settings on the data acquisition software.
32. Record the name of the condition simulated by the mmW simulator on the data acquisition software. There are four conditions simulated at the location where the DUT is situated. These are: i) the electric field pattern that is measured at location 1 of the AIT-2,
    ii) ten times the electric field pattern that is measured at location 1 the AIT-2,
    iii) the electric field pattern that is measured at location 2 of the AIT-2, and
    iv) ten times the electric field pattern that is measured at location 2 of the AIT-2.
33. Run the data acquisition software to start the 30 seconds long recording.
34. During the 30 seconds recording, observe the DUT's output signal on the oscilloscope. Figure N.16 below is an example of DUT's output.

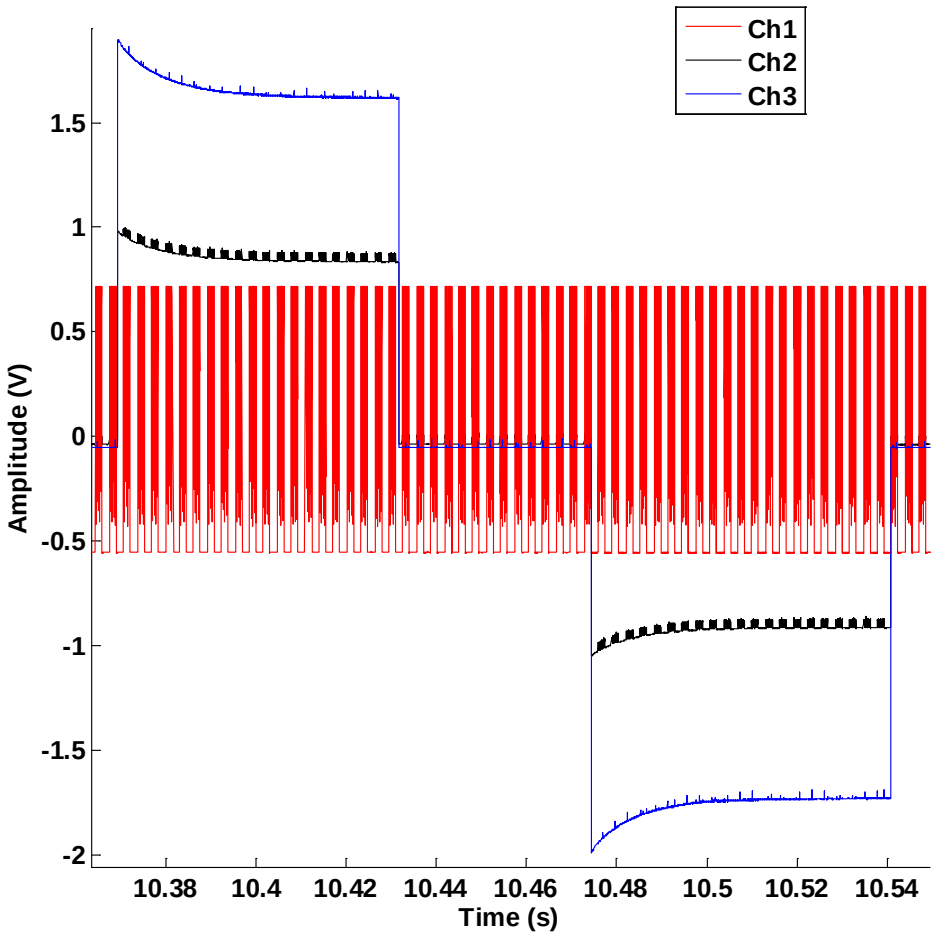

Figure N.16: Channel 2 and 3 show the outputs of a TENS device. Channel 1 shows the envelope of the mmW emission from the mmW simulator. The mmW simulator is simulating the vertical exposure time at location 1 of the AIT-2, which is 1.49 ms.

35. Rotate the TENS device by 90 degrees to a new orientation as shown in figure N.17 and repeat steps 12 to 15.

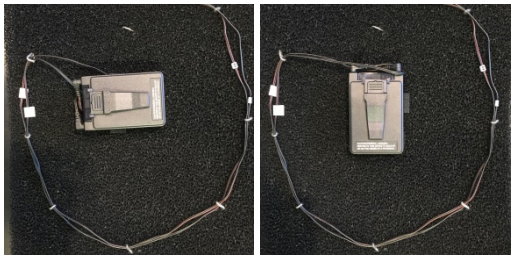

Figure N.17: The first figure shows the TENS in horizontal orientation, the second shows the TENS in vertical orientation.

36. Command the mmW simulator to start simulating condition ii) mentioned in step 13, and repeat steps 12 to 16.
37. Command the mmW simulator to start simulating condition iii) mentioned in step 13, and repeat steps 12 to 16.

38. Command the mmW simulator to start simulating condition iv) mentioned in step 13, and repeat steps 12 to 16.
39. Finally, turn off the devices and remove their batteries, as appropriate, before storing them.

Appendix O

Findings for PMED testing in the AIT-2 mmW simulator

The results of PMED test in the AIT-2 mmW simulator are presented in this appendix. The general PMED setting and explanation about the test modes are in appendix J.

Device	Condition Simulated	Test Mode	Lead Configuration	Cardiac Signal	Orientation	Observed Reaction
A1	Electric field at location 1	DDD	Unipolar	On	Horizontal	None
					Vertical	None
				Off	Horizontal	None
					Vertical	None
			Bipolar	On	Horizontal	None
					Vertical	None
				Off	Horizontal	None
					Vertical	None
	10 times the electric field at location 1	DDD	Unipolar	On	Horizontal	None
					Vertical	None
				Off	Horizontal	None
					Vertical	None
			Bipolar	On	Horizontal	None
					Vertical	None
				Off	Horizontal	None
					Vertical	None
	Electric field at location 2	DDD	Unipolar	On	Horizontal	None
					Vertical	None
				Off	Horizontal	None
					Vertical	None
			Bipolar	On	Horizontal	None
					Vertical	None
				Off	Horizontal	None
					Vertical	None
	10 times the electric field at location 2	DDD	Unipolar	On	Horizontal	None
					Vertical	None
				Off	Horizontal	None
					Vertical	None
			Bipolar	On	Horizontal	None
					Vertical	None
				Off	Horizontal	None
					Vertical	None
A2	Electric field at location 1	DDD	Unipolar	On	Horizontal	None
					Vertical	None
				Off	Horizontal	None
					Vertical	None

Device	Condition Simulated	Test Mode	Lead Configuration	Cardiac Signal	Orientation	Observed Reaction
			Bipolar	On	Horizontal	None
					Vertical	None
				Off	Horizontal	None
					Vertical	None
	10 times the electric field at location 1	DDD	Unipolar	On	Horizontal	None
					Vertical	None
				Off	Horizontal	None
					Vertical	None
			Bipolar	On	Horizontal	None
					Vertical	None
				Off	Horizontal	None
					Vertical	None
	Electric field at location 2	DDD	Unipolar	On	Horizontal	None
					Vertical	None
				Off	Horizontal	None
					Vertical	None
			Bipolar	On	Horizontal	None
					Vertical	None
				Off	Horizontal	None
					Vertical	None
	10 times the electric field at location 2	DDD	Unipolar	On	Horizontal	None
					Vertical	None
				Off	Horizontal	None
					Vertical	None
			Bipolar	On	Horizontal	None
					Vertical	None
				Off	Horizontal	None
					Vertical	None
A3	Electric field at location 1	DDD	Unipolar	On	Horizontal	None
					Vertical	None
				Off	Horizontal	None
					Vertical	None
			Bipolar	On	Horizontal	None
					Vertical	None
				Off	Horizontal	None
					Vertical	None
	10 times the electric field at location 1	DDD	Unipolar	On	Horizontal	None
					Vertical	None
				Off	Horizontal	None
					Vertical	None
			Bipolar	On	Horizontal	None
					Vertical	None
				Off	Horizontal	None

Device	Condition Simulated	Test Mode	Lead Configuration	Cardiac Signal	Orientation	Observed Reaction
					Vertical	None
	Electric field at location 2	DDD	Unipolar	On	Horizontal	None
					Vertical	None
				Off	Horizontal	None
					Vertical	None
			Bipolar	On	Horizontal	None
					Vertical	None
				Off	Horizontal	None
					Vertical	None
	10 times the electric field at location 2	DDD	Unipolar	On	Horizontal	None
					Vertical	None
				Off	Horizontal	None
					Vertical	None
			Bipolar	On	Horizontal	None
					Vertical	None
				Off	Horizontal	None
					Vertical	None
A4	Electric field at location 1	DDD	Unipolar	On	Horizontal	None
					Vertical	None
				Off	Horizontal	None
					Vertical	None
			Bipolar	On	Horizontal	None
					Vertical	None
				Off	Horizontal	None
					Vertical	None
	10 times the electric field at location 1	DDD	Unipolar	On	Horizontal	None
					Vertical	None
				Off	Horizontal	None
					Vertical	None
			Bipolar	On	Horizontal	None
					Vertical	None
				Off	Horizontal	None
					Vertical	None
	Electric field at location 2	DDD	Unipolar	On	Horizontal	None
					Vertical	None
				Off	Horizontal	None
					Vertical	None
			Bipolar	On	Horizontal	None
					Vertical	None
				Off	Horizontal	None
					Vertical	None
		DDD	Unipolar	On	Horizontal	None
					Vertical	None

Device	Condition Simulated	Test Mode	Lead Configuration	Cardiac Signal	Orientation	Observed Reaction
	10 times the electric field at location 2			Off	Horizontal	None
					Vertical	None
			Bipolar	On	Horizontal	None
					Vertical	None
				Off	Horizontal	None
					Vertical	None
A5	Electric field at location 1	DDD	Unipolar	On	Horizontal	None
					Vertical	None
				Off	Horizontal	None
					Vertical	None
			Bipolar	On	Horizontal	None
					Vertical	None
				Off	Horizontal	None
					Vertical	None
	10 times the electric field at location 1	DDD	Unipolar	On	Horizontal	None
					Vertical	None
				Off	Horizontal	None
					Vertical	None
			Bipolar	On	Horizontal	None
					Vertical	None
				Off	Horizontal	None
					Vertical	None
	Electric field at location 2	DDD	Unipolar	On	Horizontal	None
					Vertical	None
				Off	Horizontal	None
					Vertical	None
			Bipolar	On	Horizontal	None
					Vertical	None
				Off	Horizontal	None
					Vertical	None
	10 times the electric field at location 2	DDD	Unipolar	On	Horizontal	None
					Vertical	None
				Off	Horizontal	None
					Vertical	None
			Bipolar	On	Horizontal	None
					Vertical	None
				Off	Horizontal	None
					Vertical	None

Table O.6: Test data of sample Implantable Pacemakers tested in the mmW simulator.

Device	Location	Test Mode	Lead Configuration	Cardiac Signal	Orientation	Observed Reaction
B1	Electric field at location 1	DDD	Bipolar	On	Horizontal	None
					Vertical	None
				Off	Horizontal	None
					Vertical	None
	10 times the electric field at location 1	DDD	Bipolar	On	Horizontal	None
					Vertical	None
				Off	Horizontal	None
					Vertical	None
	Electric field at location 2	DDD	Bipolar	On	Horizontal	None
					Vertical	None
				Off	Horizontal	None
					Vertical	None
	10 times the electric field at location 2	DDD	Bipolar	On	Horizontal	None
					Vertical	None
				Off	Horizontal	None
					Vertical	None
B2	Electric field at location 1	DDD	Bipolar	On	Horizontal	None
					Vertical	None
				Off	Horizontal	None
					Vertical	None
	10 times the electric field at location 1	DDD	Bipolar	On	Horizontal	None
					Vertical	None
				Off	Horizontal	None
					Vertical	None
	Electric field at location 2	DDD	Bipolar	On	Horizontal	None
					Vertical	None
				Off	Horizontal	None
					Vertical	None
	10 times the electric field at location 2	DDD	Bipolar	On	Horizontal	None
					Vertical	None
				Off	Horizontal	None
					Vertical	None
B3	Electric field at location 1	DDD	Bipolar	On	Horizontal	None
					Vertical	None
				Off	Horizontal	None
					Vertical	None

Device	Location	Test Mode	Lead Configuration	Cardiac Signal	Orientation	Observed Reaction
	10 times the electric field at location 1	DDD	Bipolar	On	Horizontal	None
					Vertical	None
				Off	Horizontal	None
					Vertical	None
	Electric field at location 2	DDD	Bipolar	On	Horizontal	None
					Vertical	None
				Off	Horizontal	None
					Vertical	None
	10 times the electric field at location 2	DDD	Bipolar	On	Horizontal	None
					Vertical	None
				Off	Horizontal	None
					Vertical	None
B4	Electric field at location 1	VVI	Bipolar	On	Horizontal	None
					Vertical	None
				Off	Horizontal	None
					Vertical	None
	10 times the electric field at location 1	VVI	Bipolar	On	Horizontal	None
					Vertical	None
				Off	Horizontal	None
					Vertical	None
	Electric field at location 2	VVI	Bipolar	On	Horizontal	None
					Vertical	None
				Off	Horizontal	None
					Vertical	None
	10 times the electric field at location 2	VVI	Bipolar	On	Horizontal	None
					Vertical	None
				Off	Horizontal	None
					Vertical	None

Table O.7: Test data of sample Implantable Cardioverter Defibrillators tested in the mmW simulator.

Device	Location	Test Mode	Orientation	Observed Reaction
C1	Electric field at location 1	Normal	Horizontal	None
			Vertical	None
		Magnet	Horizontal	None
			Vertical	None
	10 times the electric field at location 1	Normal	Horizontal	None
			Vertical	None
		Magnet	Horizontal	None
			Vertical	None
	Electric field at location 2	Normal	Horizontal	None
			Vertical	None
		Magnet	Horizontal	None

Device	Location	Test Mode	Orientation	Observed Reaction
			Vertical	None
	10 times the electric field at location 2	Normal	Horizontal	None
			Vertical	None
		Magnet	Horizontal	None
			Vertical	None
C2	Electric field at location 1	Normal	Horizontal	None
			Vertical	None
		Magnet	Horizontal	None
			Vertical	None
	10 times the electric field at location 1	Normal	Horizontal	None
			Vertical	None
		Magnet	Horizontal	None
			Vertical	None
	Electric field at location 2	Normal	Horizontal	None
			Vertical	None
		Magnet	Horizontal	None
			Vertical	None
	10 times the electric field at location 2	Normal	Horizontal	None
			Vertical	None
		Magnet	Horizontal	None
			Vertical	None

Table O.8: Test data of sample Implantable Neuro-stimulators tested in the mmW simulator.

Device	Location	Test Mode	Orientation	Observed Reaction
D1	Electric field at location 1	1U Bolus	Horizontal	None
			Vertical	None
		Alarm	Horizontal	None
			Vertical	None
		Idle	Horizontal	None
			Vertical	None
	10 times the electric field at location 1	1U Bolus	Horizontal	None
			Vertical	None
		Alarm	Horizontal	None
			Vertical	None
		Idle	Horizontal	None
			Vertical	None
	Electric field at location 2	1U Bolus	Horizontal	None
			Vertical	None
		Alarm	Horizontal	None
			Vertical	None
		Idle	Horizontal	None
			Vertical	None

Device	Location	Test Mode	Orientation	Observed Reaction
	10 times the electric field at location 2	1U Bolus	Horizontal	None
			Vertical	None
		Alarm	Horizontal	None
			Vertical	None
		Idle	Horizontal	None
			Vertical	None
D2	Electric field at location 1	PING at 2Hz	Horizontal	None
			Vertical	None
	10 times the electric field at location 1	PING at 2Hz	Horizontal	None
			Vertical	None
	Electric field at location 2	PING at 2Hz	Horizontal	None
			Vertical	None
	10 times the electric field at location 2	PING at 2Hz	Horizontal	None
			Vertical	None
D3	Electric field at location 1	16U Bolus	Horizontal	None
			Vertical	None
		Alarm	Horizontal	None
			Vertical	None
		Idle	Horizontal	None
			Vertical	None
	10 times the electric field at location 1	16U Bolus	Horizontal	None
			Vertical	None
		Alarm	Horizontal	None
			Vertical	None
		Idle	Horizontal	None
			Vertical	None
	Electric field at location 2	16U Bolus	Horizontal	None
			Vertical	None
		Alarm	Horizontal	None
			Vertical	None
		Idle	Horizontal	None
			Vertical	None
	10 times the electric field at location 2	16U Bolus	Horizontal	None
			Vertical	None
		Alarm	Horizontal	None
			Vertical	None
		Idle	Horizontal	None
			Vertical	None

Table O.9: Test data of sample Insulin Pumps tested in the mmW simulator.

Device	Location	Test Mode	Orientation	Observed Reaction
E1	Electric field at location 1	Normal	Horizontal	None

Device	Location	Test Mode	Orientation	Observed Reaction
			Vertical	None
	10 times the electric field at location 1	Normal	Horizontal	None
			Vertical	None
	Electric field at location 2	Normal	Horizontal	None
			Vertical	None
	10 times the electric field at location 2	Normal	Horizontal	None
			Vertical	None

Table O.10: Test data of sample Transcutaneous Electrical Nerve Stimulators (TENS) tested in the mmW simulator.